Characterization of extraction chromatographic resins and method development for the separation and determination of Pd / Pt and ^{36}Cl / ^{129}I

Dissertation

zur

Erlangung des Doktorgrades

der Naturwissenschaften

(Dr. rer. nat.)

dem

Fachbereich Chemie der Philipps-Universität Marburg

vorgelegt von

Alexander Zulauf

aus Datschnyj / Kirgisistan

Marburg / Lahn 2010

Vom Fachbereich Chemie der Philipps-Universität Marburg
am _____ angenommen.

Erstgutachter: Prof. Dr. H. Jungclas
Zweitgutachter: Prof. Dr. W. Ensinger

Tag der mündlichen Prüfung: 10. Dezember 2010

Dedicated to my wife Anna

and my daughters

Xenia, Klara and Kristina

Table of contents

Abstract

The topic of the present work is the characterization of extraction chromatographic resins and method developments for the preconcentration, separation and detection of Pd and Pt and for ^{36}Cl and ^{129}I.

Possible applications of both methods are described in detail in chapter 1. It is, for the Pd / Pt-method, the determination of these elements in road dust and automotive exhaust catalysts by ICP-MS. For the ^{36}Cl / ^{129}I-method the determination of these isotopes in environmental and decommissioning samples by LSC.

Two newly developed resins (FClA and F49A, both TrisKem International) were at first characterized and compared with respect to the uptake of an elevated number of metal cations. Characterization studies were performed in batch experiments and included the determination of maximum uptakes, weight distribution ratios (D_w) and the influence of interferences on the uptake of the cations. Maximum uptakes were determined for Pd, Pt and Ag for varying acids at a fixed acid concetration. Weight distribution ratios were determined for several metal cations in different acids and acid concentrations with a main focus on Pd, Pt and Ag. The interferences caused upon the uptake of Pd and Pt was evaluated for an elevated number of cations and anions.

High maximum uptakes were found for Pd, Pt and Ag, indicating, both resins are suitable for the foreseen applications. However maximum uptakes of the FClA resin were greater than for the F49A resin by a factor of up to 2.

Weight distribution ratios were found to be high for Pd, Pt and Ag. No significant difference was observed between both resins. For Pd and Ag weight distribution ratios decrease with increasing pH value of the respective acid but remain higher than 100 (D_w values greater than 100 indicate good retention conditions for the resin). Weight distribution ratios for Pt decrease with decreasing pH value. Especially in the case of FClA resin a D_w value of less than 10 was determined for Pt in 3M nitric acid (D_w values lower than 10 indicate good eluting conditions).

Also no differences between both resins were found with respect to the influence of interferences. Cationic interferences were found to have negligible impact on Pd and Pt uptake, only high iron concentrations lead to decreasing D_w values. Anions such as phosphate, oxalate and EDTA show high interference, resulting in D_w values lower than 10. This is not surprising since all of them are strong chelating agents.

Based on the results of the characterization studies a scheme for a method for the preconcentration and separation of Pd and Pt was developed. From the characterization studies it was deduced that using FClA resin and loading from 3M nitric acid should lead to the desired separation of Pd and Pt (Fig. 53). Under these conditions Pt should be eluted during the column loading and Pd should remain on

the resin. Some anions, especially phosphate, were very promising agents for the elution of Pd.

Conditions seemingly best suited to obtain the desired separation were found in the characterization study. These conditions were applied to separation experiments in column geometry and further optimized mainly by means of elution studies. During the optimization procedure $SnCl_2$ was found to have a key function for the separation and quantitative elution of Pd and Pt.

The optimized method (Fig. 72) for the preconcentration and separation of Pd and Pt implies loading of both elements from 10ml 5M HNO_3/0.01M $SnCl_2$ solution, rinsing with an additional 5ml of 5M HNO_3/0.01M $SnCl_2$ solution and finally eluting Pd with 10ml 9M NH_3.

Pt is eluted during the loading and rinsing procedures. In these steps elements causing isobaric interferences for the determination of Pd by ICP-MS are equally eliminated, thus allowing an interference-free determination of Pd via ICP-MS. Since Pt has a high mass these interferences do not interfere with the determination of Pt by ICP-MS.

The method has a good selectivity and sensitivity (see method validation, section 4.2.1). Unfortunately further method validation studies (especially for linearity, precision, recovery and ruggedness) could not be performed due to inconsistencies of the performances and elution characteristics of newer resin lots received.

For the preconcentration, separation and determination of ^{36}Cl and ^{129}I a new resin was prepared by loading FClA resin with silver ions (“silver loaded FClA resin”). The resin was also characterized by the determination of weight distribution ratios for chloride and iodide using ^{36}Cl and ^{129}I. Retention of both isotopes was tested in 1M H_2SO_4, elution conditions for chloride were tested using 0.01-0.2M KSCN solution and for iodide using 0.04-0.35M Na_2S solution. High D_w values were found for chloride and iodide in 1M H_2SO_4 indicating quantitative uptakes. Chloride can be eluted with SCN^- at any concentration (D_w values < 1) whereas iodide remains on the resin ($D_w \geq 4000$). Iodide is then eluted at elevated Na_2S concentrations.

The silver loaded resin also shows high maximum uptakes for chloride and iodide. However, the maximum uptake strongly depends on the amount of silver previously loaded onto the resin.

Retention and elution conditions identified during the characterization studies were transferred to column geometry and further optimized. It was found that an additional wash step after the loading of the analytes is necessary to eliminate potential interferences and an additional rinsing step in upfront to iodide elution is necessary to achieve a quantitative elution.

Fig. 95 summarizes the optimized procedure for preconcentration, separation and determination of ^{36}Cl and ^{129}I. The method was validated with respect to its selectivity, linearity, trueness, precision, recovery and ruggedness (section 4.3.5). The method was also validated for different matrices (water, soil, filter and concrete).

The results of the validation study show that the developed method is fit for its purpose.

Zusammenfassung

Die vorliegende Arbeit befasst sich mit der Charakterisierung von extraktionschromatographischen Harzen und mit der Entwicklung von Methoden zur Aufkonzentrierung, Trennung und Nachweis von Pd und Pt sowie von ^{36}Cl und ^{129}I.

Mögliche Anwendungsgebiete beider Methoden sind in Kapitel 1 beschrieben. Für die Pd / Pt-Methode liegt die Anwendung im Nachweis beider Elemente im Straßenstaub und Autokatalysatoren mittels ICP-MS. Die ^{36}Cl / ^{129}I – Methode soll für die Analytik von Umweltproben sowie für Proben aus der Stilllegung und Entsorgung kerntechnischer Anlagen mittels LSC eingesetzt werden.

Zwei neu entwickelte Harze (FClA und F49A, TrisKem International) wurden zunächst in Hinblick auf ihr Extraktionsverhalten bezüglich einer Vielzahl von Schwermetallkationen charakterisiert und miteinander verglichen. Studien zur Charakterisierung wurden in Batch-Experimenten durchgeführten, in welchen die maximale Aufnahme, Verteilungskoeffizienten D_w und der Einfluss verschiedener Interferenzen auf die Extraktionseigenschaften bestimmt wurden. Maximale Aufnahmen wurden für Pd, Pt und Ag für unterschiedliche Säuren bei einer festen Säurekonzentration bestimmt. Verteilungskoeffizienten D_w wurden für eine Vielzahl von Schwermetallen in verschiedenen Säuren und Säurekonzentrationen bestimmt, wobei das Hauptaugenmerk auf den Elementen Pd, Pt und Ag lag. Es wurde weiterhin der Einfluss verschiedener kationischer und anionischer Interferenzen auf die Pd und Pt Extraktion untersucht.

Es wurden hohe Aufnahmen von Pd, Pt und Ag gefunden, was darauf hindeutet, dass beide Harze für die vorgesehenen Anwendungen geeignet sind. Für das FClA Harz sind die maximalen Aufnahmen jedoch bis zu einem Faktor 2 größer als die des F49A Harzes. Es wurden darüberhinaus hohe Verteilungskoeffizienten für Pd, Pt und Ag gefunden, wobei hier keine ausschlaggebenden Unterschiede zwischen den beiden Harzen festgestellt werden konnten. Die Verteilungskoeffizienten für Pd und Ag nehmen mit steigendem pH-Wert der jeweilig untersuchten Säure ab, bleiben jedoch oberhalb von 100 (D_w-Werte, welche größer als 100 sind, weisen auf gute Retentionseigenschaften des Harzes hin). Verteilungskoeffizienten für Pt nehmen mit abnehmendem pH-Wert ab. Insbesondere im Falle des FClA Harzes wurde für Pt ein D_w-Wert in 3M Salpetersäure gefunden welcher kleiner 10 ist (D_w-Werte, die kleiner 10 sind, weisen auf gute Eigenschaften des Harzes bezüglich des Elutionsvermögens).

Auch bezüglich der Interferenzen wurden keine signifikanten Unterschiede festgestellt. Kationische Interferenzen, die das Rückhaltevermögen des Harzes bezüglich der Pd und Pt Retention stören könnten, sind vernachlässigbar klein. Einzig hohe Eisenkonzentrationen führen zu einer Abnahme der D_w-Werte. Anionen wie z.B. Phosphate, Oxalate und EDTA zeigen starke Interferenzen, welche sich in

D_w-Werten kleiner 10 äußern. Dies ist aber nicht weiter verwunderlich, da diese Anionen starke Komplexbildner sind.

Ausgehend von den Ergebnissen der Charakterisierungsstudien wurde eine Methode zur Aufkonzentrierung und Trennung von Pd und Pt entwickelt. Aus den Charakterisierungsstudien hat sich ergeben, dass die gewünschte Trennung von Pd und Pt erreicht werden kann, wenn diese auf das FClA Harz aus einer 3M Salpetersäure geladen werden (Fig. 53). Unter diesen Bedingungen sollte das Pt während des Beladevorganges eluiert und Pd von dem Harz zurückgehalten werden.

Während der Methodenentwicklung wurden die Extraktionsbedingungen, die in Charakterisierungstudien gefunden wurden, auf Säulengeometrie übertragen und weiter optimiert. In den Optimierungsstudien hat sich gezeigt, dass $SnCl_2$ eine Schlüsselrolle für die Trennung und die quantitative Elution von Pd und Pt spielt.

Die optimierte Methode (Fig. 72) für die Aufkonzentrierung und Trennung von Pd und Pt beinhaltet folgende Schritte: laden beider Elemente aus 10ml 5M HNO_3/0.01M $SnCl_2$-Lösung, gefolgt von einem Spülschritt mit 5ml 5M HNO_3/0.01M $SnCl_2$-Lösung und anschließender Pd-Elution mit 10ml 9M NH_3.

Pt wird während des Ladens und Spülens des Resins eluiert. In diesen beiden Schritten werden auch Elemente, die bei der Bestimmung von Pd mittels ICP-MS isobare Störungen verursachen, eliminiert, Pd kann somit störungsfrei mittels ICP-MS bestimmt werden. Da Pt eine hohe Atommasse besitzt, stören diese Elemente die Bestimmung von Pt mittels ICP-MS nicht.

Die Methode weist eine gute Selektivität und Sensitivität auf (siehe Methodenvalidierung, Abschnitt 4.2.1). Leider konnten weitere Validierungsschritte (insbesondere Linearität, Präzision, Wiederfindung und Robustheit) nicht durchgeführt werden, weil Probleme mit den neuen Lots des Harzes auftraten (veränderte Elutions-Charakteristika).

Für die Aufkonzentrierung, Trennung und Nachweis von ^{36}Cl und ^{129}I wurde ein neues Harz hergestellt, indem das FClA Harz mit Silberionen beladen wurde (silberbeladenes FClA Harz). Dieses Harz wurde ebenfalls charakterisiert, indem Verteilungskoeffizienten für Chlorid und Iodid bestimmt wurden. Die Retention beider Halogenide wurde in 1M Schwefelsäure getestet. Elutionsbedingungen für Chlorid wurden in 0.01-0.2M KSCN und für Iodid in 0.04-0.35M Na_2S getestet. Chlorid und Iodid weisen in 1M H_2SO_4 hohe Verteilungskoeffizienten auf, welche auf eine quantitative Aufnahme der Nuklide durch das Harz hinweisen. Chlorid kann durch SCN^- bei jeder Konzentration eluiert werden (D_w <1) während Iodid auf dem Harz zurückgehalten wird ($D_w \geq 4000$). Iodid wird dann bei höheren Na_2S Konzentrationen eluiert.

Das silberbeladene Harz zeigt auch eine hohe Aufnahme von Chlorid und Iodid. Die Aufnahme hängt jedoch stark von der Silbermenge, mit der das Harz beladen wurde, ab.

Retentions- und Elutionsbedingungen aus den Charakterisierungsstudien wurden dann auf Säulengeometrie übertragen und weiter optimiert. Ein weiterer Waschschritt, welcher sich an den Beladeschritt anschließt, erwies sich als notwendig, um potenzielle Interferenzen zu eliminieren. Ebenfalls wurde ein weiterer Spülschritt vor die Elution des Iodids eingeführt, um eine quantitative Iodidelution zu erreichen.

In Fig. 95 ist die optimierte Methode zur Aufkonzentrierung, Trennung und Nachweis von ^{36}Cl und ^{129}I zusammengefasst. Die Methode wurde bezüglich Selektivität, Linearität, Richtigkeit, Präzision, Wiederfindung und Robustheit validiert (Abschnitt 4.3.5). Die Methode wurde ebenfalls für verschiedene Matrixsubstanzen (Wasser, Boden, Filter und Beton) validiert.

Die Validierungsstudie hat gezeigt, dass die Methode für die gewählte Anwendung geeignet ist.

1 Motivation and Scope

1.1 Palladium and Platinum

Palladium and platinum are mainly used as catalysators in many industrial processes like polymerization of olefins, refining of petroleum, ammonium oxidation, electronic industries, glass and jewellery manufacturing as well as in automotive catalytic converters [1]. They are also used in drugs, e.g. cis-Platin for cancer therapy [2], and in dentistry in dental casting alloys [3].

By the use of Pd and Pt in industry, hospitals and cars there are a lot of potential sources for releasing these metals into the environment. The most important source for the emission of Pd and Pt into the environment is automotive catalytic converters. For example Kümmerer et al. reported a total emission of 187.2 kg of Pt from cars in 1996 in Germany vs. 14.2 kg of Pt from hospital effluents [4].

Before the introduction of exhaust gas catalytic converters airborne samples showed a background level of approx. 2 pg m^{-3} of Pt in Germany and 0.06 pg m^{-3} in California.

In 1976 in California Volvo introduced first the so called three-way catalyst. In Europe in 1986 Swiss was the first country which regulated three-ways catalyst in new cars [5]. Since 1993, European Standards and Directive 94/12/EEC requires all new cars registered in the EU to be fitted with a catalytic converter containing Pt, Pd and Rh [6].

Since the introduction of exhaust gas catalytic converters, the concentration of PGE in environment increased.

In the 1990th first researchers collected data on PGE concentrations in road dust. For example in 1997 Zereini et al. analyzed urban roadside dust samples in Frankfurt and soil samples near the highway A66 (Frankfurt). PGE concentrations were found to be 5 ng g^{-1} for Pd, 7 ng g^{-1} for Rh and 45 ng g^{-1} for Pt [7, 8]. Concern about this high increase in PGE concentrations in traffic-exposed samples led to an international co-operation under CEPLACA project funded by the European Union [9]. From 1997 until 2000 twelve European partners worked on this project. The CEPLACA project dealt with the assessment of the environmental contamination risk by Pt, Rh and Pd from automobile catalysts. Gomez et al. reported that during the time period of the project the PGE concentration in air has increased by more than two orders of magnitude in heavy traffic areas [7].

One main objective of the CEPLACA project was the study of representative diesel and gasoline catalyst behavior from their fresh to spent conditions by measuring the amount of soluble and particulate forms of PGE released along their useful life [9].

It was found that for fresh gasoline catalysts the mean of the total amount released was approx. 100, 250 and 50 ng km^{-1} for Pt, Pd and Rh, respectively. In diesel catalysts the Pt release varied in the range of 400-800 ng km^{-1}. After ageing the catalysts up to 30000 km, the gasoline catalysts released amounts of Pt between 6 and 8 ng km^{-1}, Pd between 12 and 16 ng km^{-1} and Rh between 3 and 12 ng km^{-1}. In diesel catalysts the Pt release varied in the range of 108-150 ng km^{-1}. The soluble portion of PGEs was less than 5% of the total amount for fresh catalysts. For aged catalysts the total amount of soluble PGEs released was similar or slightly higher than for fresh catalysts. The PGEs are released from the catalyst surface mainly by mechanical or thermal erosion. [1]

It is known that the metallic form of PGEs is inert as far as biological reactions are concerned. The acute toxicity of PGEs depends mainly on their solubility. Soluble Pt salts are much more toxic in animal experiments than compounds with low solubility, such as PtO, PtO_2 and $PtCl_2$. Hexachloroplatinate and tetrachloroplatinate complexes are powerful sensitizers. In addition, some platinum complexes bind to nitrogen and sulfur in proteins producing a possible reduction in essential enzymatic activity. Toxicological data on Pd and Rh are scarce. For both $PdCl_2$ and $RhCl_3$, increased tumor incidences were observed in mice studies. Pd and Rh salts are 3- and 30-fold less toxic, respectively, than analogous Pt complexes. [6, 9]

However, up to date only little is known on the biological effects of PGEs emitted from vehicle exhaust catalysts. For humans, the most significant health risk presents the inhalation of PGE-containing dust, mainly the inhalation of platinum particles. Rosner and Merget have performed a calculation of a “guidance value” for the emission of platinum from automotive catalysts. They calculated this upper limit for a “safe concentration” to be between 15 and 150 ng of platinum per m^3. Ambient air concentrations of Pt measured during the CEPLACA project are in the range of 5-100 pg m^{-3} and thus approx. three orders of magnitude below the levels for which adverse health effects might theoretically occur. Therefore, traffic-related PGEs present in airborne particles do not seem to pose any health risk to the general population. [7]

Recent studies have provided evidence that PGEs from automotive catalysts are at least partly bioavailable to plants and animals. Most available studies on bioaccumulation of PGEs are focused on fish, mussels, freshwater isopods and animals. Little is known on the uptake of PGEs emitted from vehicle exhaust catalysts by the terrestrial biosphere except for a few studies showing some uptake by plants [10-12]. Kalbitz et al. studied the effect of PGEs in terrestrial ecosystems on soil microbial processes such as carbon and nitrogen mineralization. They observed no negative effects on microbiological soil processes. [11]

Both elements are typically determined by using ICP-MS. ICP-MS is a very sensitive technique with very low detection limits for Pd and Pt. However, especially for Pd there are many potential interference (Cd, Sr, Zr, Y) which have to be considered and

which may influence the results. Of course, the interferences can be corrected mathematically.

To facilitate the measurement of Pd and Pt with ICP-MS and also to facilitate the calculation of the results it is necessary to eliminate the interferences and at the same time to have a simple sample preparation method.

1.2 ^{36}Cl and ^{129}I

Beside numerous other radionuclides, the long-lived and rather volatile ^{36}Cl (half-life $3.01(3)\times10^5$ years; 98.1% β^- decay to ^{36}Ar, $E_{\beta,max}$: 708.6 keV; 1.9% electron capture to ^{36}S [13]) and ^{129}I (half-life $16.1(7)\times10^6$ years; 100% β^- decay to ^{129}Xe, $E_{\beta,max}$: 190.8 keV [13]) are determined in various sample matrices within the context of the monitoring of nuclear installations, during operation and especially also during decommissioning. ^{36}Cl is, in addition to natural production processes, produced in nuclear installation during the irradiation of nuclear fuel by neutron activation of ^{35}Cl [14]. ^{129}I is a fission product that is, compared to ^{131}I (half-life 8.0233(19) d [13]), produced with a rather low yield, but that has a very long half-life [15]. Both, ^{36}Cl and ^{129}I can be released as gaseous and/or liquid effluents and will be present in radioactive wastes originating from nuclear installations.

Numerous techniques for the determination of ^{36}Cl and ^{129}I are described in literature, ^{36}Cl is frequently determined via AMS [16, 17] or LSC [14, 18, 19], ^{129}I via NAA [20], AMS [21], ICP-MS [22, 23] or ß-spectrometry [24]. LSC measurements have the advantage of availability for a large number of laboratories and are thus interesting especially for routine monitoring. In order to allow the determination of ^{36}Cl and ^{129}I via LSC, and to obtain accurate and precise results, the samples have to pass a number of sample preparation steps; among these steps are the chemical separation and purification of the nuclides and the subsequent preparation of counting samples suitable for LSC. Sample preparation methods frequently employed such as volatilization [14, 18, 24], precipitation and/or ion exchange steps [19] can be rather elaborate.

Therefore, it is attempted to develop a method that allows extraction, and subsequent separation, of Cl and I from pretreated environmental and decommissioning samples and that allows also their determination via LSC.

In both cases, Pd / Pt and ^{36}Cl / ^{129}I, extraction chromatography (EXC) is a technique that is ideally suited for the separation of these elements from a wide range of sample types. This technique combines the selectivity of liquid-liquid extraction with the ease of operation of column chromatography [25].

For this purpose two resins, F49A and FClA, with high selectivity for Pd, Pt and Ag, were developed by TrisKem International.

The scope of this thesis is

- to characterize and compare both resins
- to prepare a silver loaded resin and to characterize the obtained resin
- to develop one method for the preconcentration and separation of Pd and Pt and one method for the preconcentration and separation of ^{36}Cl and ^{129}I
- and finally to validate both methods.

2 State of the art

2.1 Extraction chromatography (EXC)

Extraction chromatography is a particular form of column chromatography. The difference between extraction chromatography and normal partition chromatography lies in the fact that in the process of partition the solute molecules undergo little, if any, chemical change apart from association or proton exchange, while extraction involves the transfer of the initially ionic solute from water into an organic phase, most often accompanied by complex chemical changes involving many interactions and equilibriums. The term extraction chromatography is generally used when the stationary phase is an organic liquid or organic solution, and the mobile phase an aqueous solution. The stationary phase in extraction chromatography most often has complex forming properties.

Extraction chromatography couples the favorable selectivity features of the organic compounds used in liquid-liquid extraction, with the multistage character of a chromatographic process. [26]

2.1.1 Models to the extraction process

Extraction of ions is a complex process involving many interactions and equilibriums. However, the essential steps can be formulated in a simple way.

When a metal ion M^{z+} is extracted from an aqueous phase into an organic phase an equivalent amount of anions A^- is also extracted because of the principle of the electroneutrality of the phases. The overall extraction equation is then:

$$M_{aq}^{z+} + zA_{aq}^{-} \rightleftharpoons MA_{z,org} \qquad \textbf{eq. 1}$$

The species formed, MA_z, can be solvated in the organic phase and can also contain some water molecules. In those cases when the anion (in its acidic form HA) is initially present in the organic phase, its distribution between the two phases has also to be taken into account:

$$HA_{org} \rightleftharpoons HA_{aq} \qquad \textbf{eq. 2}$$

The extraction process of the cation M^{z+} can be described by two models. In both models the extraction is split into two steps but in different way.

In the first model it is assumed that the extractable neutral species is formed in the aqueous phase and then transferred to the organic phase. According to this model, the overall eq. 1 can be split into two equations:

$$M_{aq}^{z+} + zA_{aq}^{-} \rightleftharpoons MA_{z,aq} \qquad \textbf{eq. 3}$$

$$MA_{z,aq} \rightleftharpoons MA_{z,org} \qquad \textbf{eq. 4}$$

In order to obtain an extractable species (and in particular when A^- is an inorganic anion) in many cases the complex MA_Z has to be solvated by organic molecules B having electron donor properties. Equation 3 and eq. 4 then read as follows:

$$M_{aq}^{z+} + zA_{aq}^{-} + yB_{aq} \rightleftharpoons MA_zB_{y,aq} \quad \textbf{eq. 5}$$

$$MA_zB_{y,aq} \rightleftharpoons MA_zB_{y,org} \quad \textbf{eq. 6}$$

In the second model it is assumed that equivalent amounts of cations and anions are first transferred from the aqueous to the organic phase and then associate to form a neutral molecule. These processes can be described as following:

$$M_{aq}^{z+} + zA_{aq}^{-} \rightleftharpoons M_{org}^{z+} + zA_{org}^{-} \quad \textbf{eq. 7}$$

$$M_{org}^{z+} + zA_{org}^{-} \rightleftharpoons MA_{z,org} \quad \textbf{eq. 8}$$

It is that neither model comes near to describing the real course of the extraction process. In the majority of cases the extractable species is formed at the phase boundary, so that complex formation or association proceeds simultaneously with the transfer process. Furthermore, the equilibrium concentrations of the extractable complex and the extractant in the aqueous phase are generally so low as to be devoid of any chemical meaning, as when the extractable complex or the extractant are large hydrophobic molecules.

Nevertheless, this shortcoming of the two models does not impair their usefulness.

Both models are correct from the thermodynamic viewpoint, since thermodynamic functions for the overall process do not depend on the method of dividing the whole process into steps.

They both provide to a simple description and understanding of the basic interactions determining the magnitude of extraction and the differences in the extractability of different cations.

The first model can be profitably applied to describe the extraction of cations of high charge. The second model is suitable for the description of the extraction of ions of low charge and large radius.

However, the second model is improved for praxis since most of the cations of practical interest for extraction have high charge. [26]

2.1.2 Loading of the support material with stationary phase

Column extraction chromatography makes use of the extraction properties of a stationary phase which is more or less permanently fixed on or in the support particles. Extraction properties of the stationary phase can be blurred by adsorption or ion exchange properties of the carrier material. In addition, extractants and diluents generally used are completely or predominantly hydrophobic. This makes it difficult to fix them on hydrophilic materials, hence the support materials have to be hydrophobized or deactivated.

Deactivation of hydrophilic support materials is usually achieved by silanization with dimethyldichlorsilane (DMCS). To prepare support materials for silanization they are first washed with acid or water and dried properly. Dry support particles are then exposed to DMCS by treatment with DMCS vapors or with dilute (~5%) solutions of the reagent in an inert diluents.

After the deactivation process the support material is loaded with the stationary phase.

The amount of stationary phase loaded on support particles is one of the most important parameters in column extraction chromatography. It determines the capacity factor of the column and the diffusion path length in the stationary phase.

Techniques for loading supports should be simple, reproducible and lead to uniformly coated support particles. The solvent evaporation technique is the most widely used loading technique.

In the solvent evaporation technique dry (silanized) support particles are slurred with a known amount of extractant dissolved in a volatile solvent. The solvent is then evaporated by gentle stirring under a stream of air or nitrogen. This technique is simple, leads to uniformly coated particles and can be easily reproduced since the amount of stationary phase can be exactly predetermined. [26]

2.1.3 Stationary phases

2.1.3.1 Main performances

The main performance characteristics of an EXC stationary phase are: retention, selectivity, resolution, capacity, physical and chemical stability, regeneration and repeatability and reproducibility.

2.1.3.1.1 Retention

The retention of a given metal by an extraction column results from its distribution between the stationary phase loaded on the support and the aqueous phase used as the eluent [26].

2.1.3.1.2 Selectivity

Selectivity is the ability of the stationary phase to display suitable distribution coefficients between the two chromatographic phases, so as to allow for the separation of the elements of interest. The selectivity of a column is strictly bound to the nature of the compound used as the stationary phase, and results from a suitable combination of extractant and composition of the aqueous phase used as the eluent. [26]

2.1.3.1.3 Resolution

The resolution ability of a chromatographic column is generally evaluated in terms of theoretical plates. Heights of the theoretical plates (HETP) are useful for simple comparisons among column beds of different dimension. The HETP features of a column depend on several different factors. Two of these factors are strictly bound to the nature of the extraction system, and hence to that of the involved stationary phase. They are the organic phase diffusion coefficient if the extracted complex and the possible slow rate of the chemical reactions involved in the distribution of the element of interest. Both these parameters, on their side, strongly depend on temperature. [26]

2.1.3.1.4 Capacity

A high capacity of a chromatographic resin is important when the more retained elements to be separated are present in macroamounts. The capacity of EXC resin is proportional to the amount of extractant that is present in the column bed, and maximum capacity will depend on the maximum amount of the extractant that can be loaded on the supporting material, without being readily drained away by the eluting solutions. [26]

2.1.3.1.5 Physical stability

Physical stability of a column is the tendency to more or less to lose upon elution the stationary phase originally loaded on the support.

Losses of extractant from the column may derive either from dissolution of it into the eluents, or from drainage by the eluent of undissolved portions of extractant, scarcely retained on the supporting material. They may result in the often undesirable presence of extractant in the eluate, and also in the variation of the characteristics of the column. Although most extractants used as stationary phases are very slightly soluble in aqueous solutions, some of them appreciably dissolve in the eluents. In these cases, the eluent parameters such as pH and electrolyte concentration, are often carefully chosen to keep solubility to a minimum. However, the presence of relatively great amounts of extractant in the eluate is unavoidable, and eluting solutions are generally presaturated with it to maintain the constancy of the column characteristics. [26]

2.1.3.1.6 Chemical stability

The chemical composition of a stationary phase can change either because of reactions with chemical agents occasionally present in the eluting solution, or because of its degradation caused by factors such as light, temperature and nuclear radiation. The extractant fixed on the support can also lead to possible unwanted redox reactions with the element of interest.

Most compounds used in chromatography directly derive from previous liquid-liquid extraction experience and are generally expected to be stable to most eluting solutions. However, compared to liquid-liquid extraction column chromatography requires longer contact times and degradation phenomena can never be excluded.

Most stationary phases are satisfactorily stable to moderately oxidizing and reducing solutions. [26]

2.1.3.1.7 Regeneration

The possibility of regenerating a column, so as to use it for more than one separation cycle, obviously depends on the physical and chemical stability of the stationary phase to the eluents necessary for the separation cycle itself and for the subsequent regeneration steps. The satisfactory chemical and physical stability of most stationary phases usually allows for a reasonable number of reiterate cycles, in general of the order of twenty or thirty. The most common reason for discarding a column is the excessive loss of capacity deriving from continuous small leakage or dissolution of the extractant. [26]

2.1.3.1.8 Repeatability and reproducibility

Repeatability of a column is the degree of accordance among the results obtained in carrying out the same separation procedure several times with the same column.

Reproducibility of a column is the degree of accordance between results obtained when the same separation cycle is applied to different columns prepared in the same way. In contrast with repeatability, reproducibility represents important information only in very particular cases, such as that of remarkably unstable columns that can be used only once. [26]

2.1.3.2 Extractants for stationary phases

Extractants mainly used as stationary phase include acidic extractants, neutral organophosphorous extractants, amines and quaternary ammonium compounds [26], crown-ethers [27] and increasingly also ionic liquids [28, 29].

2.1.3.2.1 Acidic extractants

Acidic extractants are organic compounds that have acid groups in their molecule, and exploit their extraction features mainly by exchanging the hydrogen ions of these groups for cationic forms originally present in the aqueous solution. They are often called “liquid cation exchangers”, since their behavior can be easily related to that exhibited by cation-exchange resins.

Acidic extractants used as column stationary phases include acidic organophosphorous compounds, sulphonic acids and substituted phenols. Among the various types of acidic organophosphorous compounds that have found practical application in liquid-liquid extraction, only monoalkylphosphoric, dialkylphosphoric and alkylarylphosphonic acids have been used in chromatography. Since the nomenclature of such compounds is rather confusing, their general formulae are reported in Fig. 1.

At fixed conditions of the aqueous phase, all acidic extractants exploit distribution coefficients that increase with the charge of the cationic species involved, as in the case of cation-exchange resins. The extent of the difference between the distribution coefficients of cations of different charge varies with the nature of the extractant considered, but in most cases is adequate for good and easy chromatographic separations. In the case of organophosphorous compounds, however, chelate or other complex formation may be superimposed to the simple cation-exchange mechanism. [26]

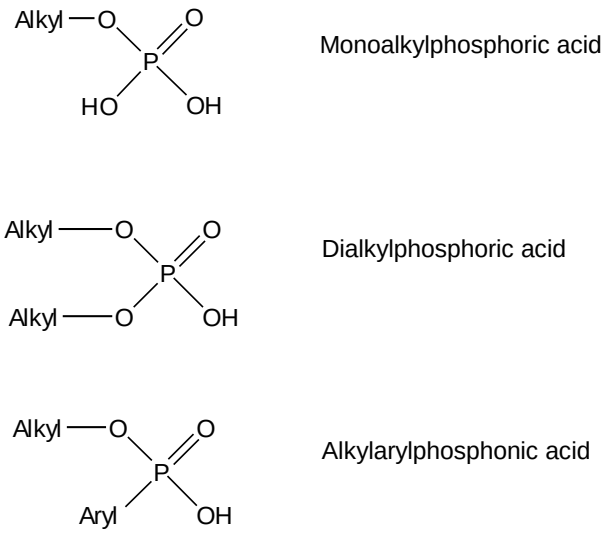

Fig. 1: Acidic organophosphorous compounds used in extraction chromatography

2.1.3.2.2 Neutral organophosphorous extractants

Several classes of neutral organophosphorous compounds were usefully applied to the liquid-liquid extraction of metals. Among them, only trialkyl phosphates and phosphine oxides, e.g. TOPO and TBP found popularity in extraction column chromatography. For example, TBP is used in a very prominent method in nuclear reprocessing for recovery of uranium and plutonium from spent fuel, the so called PUREX [30] process.

Neutral organophosphorous compounds extract by substituting water in solvating neutral species originally present in the aqueous solution. Under certain conditions, extraction by an ion association mechanism may also take place. Extraction of a metal cation normally results from the competition of the extractant, water and the anion in solvating the cation itself. The extracted species is a neutral complex formed from the cation with the anion or the anionic ligand present in the aqueous phase.

The role of water is very important in the overall process, because it competes in solvating the extractable species. High extraction coefficients are obtained only from solutions having high ionic strength, where activity of water is lowered and its competitive effect is therefore depressed. High ionic strength favors also the formation of unionized metal-bearing species essential for extraction: its overall effect is usually referred to as salting-out. [26]

The general formulae of neutral organophosphorous extractants are reported in Fig. 2.

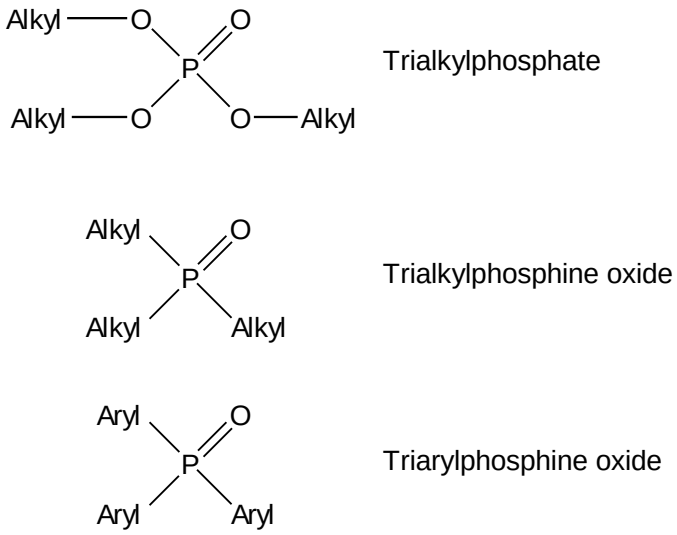

Fig. 2: Neutral organophosphorous compounds used in extraction chromatography

2.1.3.2.3 Amines and quaternary ammonium compounds

High molecular weight organic amines and ammonium salts are often referred to as liquid anion-exchangers, since their behavior in the extraction of metals is noticeably similar to the absorption of metal complexes by anion exchange resins. They found an extensive interest in the field of liquid-liquid extraction, and many of them are produced on an industrial scale, resulting in a mixture of different products usually sold and referred to with trade names hardly understandable from the chemical view-point, but nevertheless thoroughly used also in the scientific literature.

A great number of them has been screened for their behavior towards metals in laminary reversed-phase chromatography. Conversely, a relatively limited number has been applied to column chromatography, namely the secondary amines Amberlite LA-1 and LA-2, the tertiary tri-n-octylamine, tri-i-octylamine and Alamine-336, and the quaternary Aliquat-336 and trilauryl monomethyl ammonium salts. Primary amines as column stationary phases are not reported.

All amines and quaternary ammonium compounds to be used in liquid-liquid extraction fulfill a number of basic requirements such as good extraction power, low solubility in aqueous solutions and sufficient chemical stability. [26]

2.1.3.3 Inert supports in extraction chromatography

2.1.3.3.1 Requirements for supports in EXC

The supports are of great importance in extraction chromatography. Their appointment is to retain the stationary phase distributed as a thin film in order to accelerate the achievement of the equilibrium state between the aqueous and organic phases.

An ideal support has to meet the following requirements:

1. To display good wetability by the stationary phase and its retention in sufficient amounts. The fixed phase must not tear off the support with the flow of the mobile phase.
2. To be chemically inert: it must not dissolve or swell in the stationary phase, nor dissolve or react with the mobile phase; it must not adsorb the components of the mixture to be separated.
3. To consist of particles as identical as possible (spherical ones are the best), which allow the most uniform and reproducible column packing.
4. To have a large enough surface to retain the stationary phase as a thin, even and uniform film. Porous supports generally meet this requirement, but the pore distribution has to be within a narrow range of sizes since the effect of different pore sizes is equivalent to that of different particle diameters. Too narrow pores must not be present, as the equilibrium with the liquid retained

in narrow and deep pores may be very slow, leading to an additional broadening of the chromatographic peaks.

5. To allow for columns having an acceptable pressure drop as regards the mobile phase.
6. To have sufficient mechanical stability; it must not grind during column packing, impregnation of the extractant or regeneration of the support.
7. When applied for routine analyses or for preparative purposes, it must be relatively cheap or permit regeneration.

There is no ideal support for extraction chromatography, so one must choose within a wide range of substances which partially meet the above-mentioned requirements. It can be noted that there is not such a strong demand in connection with the quality of supports in the extraction chromatography of inorganic substances as in the gas-liquid or liquid-liquid extraction chromatography of organic substances. The reason for this is that organic extraction chromatography is usually applied to separate substances with only slightly different distribution coefficients, so that all properties of the support which influence the broadening of the chromatographic peaks (i. e. the plate height), are of great significance in the separation. Conversely, extraction chromatography of inorganic substances only seldom involves the separation of elements with very similar properties.

In most cases, the separation conditions can be selected so that the difference in distribution coefficients is sufficient for separation on the principle of the "sorption filter", where one element passes through the chromatographic column without any absorption while the second is strongly held on the column. For this kind of separation, one can use any support which will hold a sufficient amount of the appropriate extractant. [26]

2.1.3.3.2 Materials used for supports

Various powdered materials are used as the supports for extraction chromatography, being specially produced for other chromatographic techniques (supports and adsorbents for gas, adsorption, gel-permeation chromatography, etc.) or available for completely different purposes (silica gels, powders of polymers).

There are two large groups of supports for extraction chromatography. The first one consists of supports whose surfaces are covered by hydroxyl groups, having high surface energy and being very well wetted by strong polar liquids (e.g. water). It includes kieselguhr, silica gels, glasses, celluloses and aluminas, which find wide application as supports for extraction chromatography when an aqueous solution is the stationary phase.

The second group is supports for EXC includes different organic polymers which have low surface energies, and since they are hydrophobic they are well wetted by various organic solvents. [26]

2.1.3.3.3 Properties of the supports

Chemical resistance

The different supports have different chemical properties which should be considered when choosing a support material.

Polytetraflouroethylene, low pressure and high pressure polyethylene are stable toward acids, alkalies and are partly stable towards oxidants and organic solvents.

Acetylcellulose is not destroyed by diluted acids, but is destroyed by alkalies and concentrated acids.

Cellulose is partially destroyed by concentrated acids and is easily oxidized.

Kieselguhr and silica gels are stable towards acids. [26]

Radiation stability

When using polymers as support, one should take into account that irradiation reduces the resistance of polymers to the action of oxidants and that halogen containing polymers release free halogens and hydrohalic acids.

In general, the radiation stability of organic polymers decreases in the following sequence:

Polyethylene, polyurethane > polymethylsiloxane > polytriflourochlorethylene, acetylcellulose > cellulose > polypropylene > polytetrafluoroethylene.

Supports based on silica have much greater resistance to all kinds of radiation. [26]

Adsorptive properties

Supports based on silica (silica gels, kieselguhrs) are weak cation exchangers. The ion-exchange ability of silica is due to the presence of OH groups on its surface. Metallic ions can substitute the hydrogen of these groups, and this may lead to strong adsorption of some elements, for example Zr. The presence of impurities (Al, Fe) increases the adsorptive properties of silica, because aluminosilicic and ferrosilicic acids are stronger than silicic acid.

When applying silica-based supports, one should take into account that the separated substances may be contaminated by the desorption of elements captured

by silica gel in the process of its production, or contained in kieselguhr. This is important when highly pure substances must be obtained, and when trace amounts of substance must be analyzed.

Cellulose has significant adsorptive properties; many separations on cellulose can be carried out without organic solvents.

Polymers have no groups capable of ion exchange, but nevertheless they adsorb different ions from aqueous solutions (Zr, Cs, Sr, Tl, Ag, Y, Ru). Most sorption studies on polymers involve polyethylene or PTFE, the sorption on PTFE generally being significantly lower than that on polyethylene. [26]

Capacity for the extractant

The ability of supports to be wetted by organic solvents and to hold them satisfactorily depends on several factors, namely: the properties of the support surface (surface energy, and nature of groups which cover the surface), the surface tension of the extractant, and the composition of the aqueous solution.

Supports with OH groups on their surface (silica, cellulose) hold amines without hydrophobization, apparently because of their ability to exchange cations.

The ability of polymer supports to retain the organic phase depends appreciably on their previous treatments: the polymerization powder of Ftoroplast-4 holds $CHCl_3$ well, while the thermally treated material does not.

For different purposes, the column may be loaded with different amounts of extractant.

The amount of loaded extractant is often significantly less than the maximum amount that the support can hold, to decrease the HETP when substances with similar properties have to be separated. [26]

2.2 Inductively coupled plasma – mass spectrometry (ICP-MS)

Inductively coupled plasma mass spectrometry (ICP-MS) is a type of mass spectrometry that is highly sensitive and capable of the determination of a range of metals and several non-metals at concentrations below one part in 10^{12} (part per trillion). It is based on coupling an inductively coupled plasma as a method of producing ions (ionization) with a mass spectrometer as a method of separating and detecting the ions. ICP-MS is also capable of monitoring isotopic speciation for the ions of choice. [31]

An ICP-MS device generally consists of the sample introduction, the plasma source, the interface region, the ion optics and the mass analyzer.

2.2.1 Sample Introduction

The majority of inductively coupled plasma mass spectrometry (ICP-MS) applications involve the analysis of liquid samples. There are many ways of introducing a liquid into an ICP mass spectrometer, but they all basically achieve the same result — they generate a fine aerosol of the sample so it can be efficiently ionized in the plasma discharge. The mechanism of introducing a liquid sample into analytical plasma can be considered as two separate events — aerosol generation using a nebulizer and droplet selection by way of a spray chamber. [32]

2.2.1.1 Nebulizers

The sample is normally pumped at ~1 mL/min via a peristaltic pump into the nebulizer. After the sample enters the nebulizer, the liquid is broken up into a fine aerosol by the pneumatic action of gas flow (~1 L/min) smashing the liquid into tiny droplets. The two commonly used nebulizers are the concentric (Fig. 3) and cross flow (Fig. 4) nebulizers.

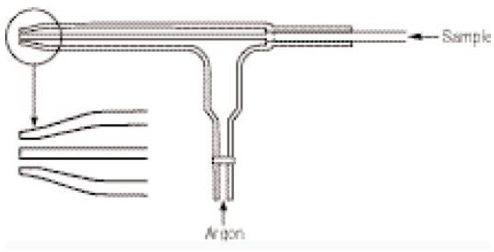

Fig. 3: Concentric nebulizer [32]

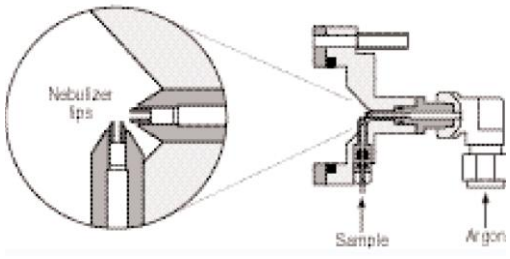

Fig. 4: Cross flow nebulizer [32]

In the concentric nebulizer, the solution is introduced through a capillary tube to a low-pressure region created by a gas flowing rapidly past the end of the capillary. The low pressure and high-speed gas combine to break up the solution into an aerosol, which forms at the open end of the nebulizer tip. This nebulizer is suited for very clean samples.

For samples that contain a heavier matrix or small amounts of undissolved matter, the cross flow design is probably the best option. With this design the argon gas is directed at right angles to the tip of a capillary tube, in contrast to the concentric design, where the gas flow is parallel to the capillary. In either case, contact between the high-speed gas and the liquid stream causes the liquid to break up into an aerosol. Cross flow nebulizers are generally not as efficient as concentric nebulizers at creating the very small droplets needed for ICP-MS analyses. [32]

2.2.1.2 Spray chambers

Because the plasma discharge is inefficient at dissociating large droplets, the spray chamber's function is primarily to allow only the small droplets to enter the plasma. Its secondary purpose is to smooth out pulses that occur during the nebulization process, due mainly to the peristaltic pump. Basically two designs are used in commercial ICP-MS instrumentation — double pass (Fig. 5) and cyclonic (Fig. 6) spray chambers.

In a double-pass spray chamber the aerosol emerges from the nebulizer and is directed into a central tube running the whole length of the chamber. The droplets travel the length of this tube, where the large droplets (greater than ~10 µm in diameter) fall out by gravity and exit through the drain tube at the end of the spray chamber. The fine droplets (~5–10 µm in diameter) then pass between the outer wall and the central tube, where they eventually emerge from the spray chamber and are transported into the sample injector of the plasma torch.

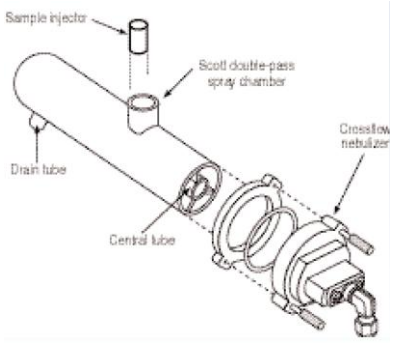

Fig. 5: Double-pass spray chamber [32]

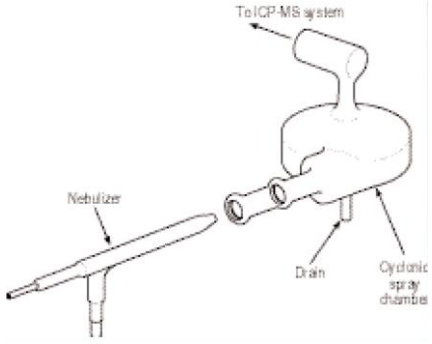

Fig. 6: Cyclonic spray chamber [32]

The cyclonic spray chamber operates by centrifugal force. Droplets are discriminated according to their size by means of a vortex produced by the tangential flow of the sample aerosol and argon gas inside the chamber. Smaller droplets are carried with the gas stream into the ICP-MS, while the larger droplets impinge on the walls and fall out through the drain. It is generally accepted that a cyclonic spray chamber has a higher sampling efficiency, which, for clean samples, translates into higher sensitivity and lower detection limits. [32]

2.2.2 The Plasma Source

The source where the plasma is generated consists of three components: a plasma torch, a radio frequency generator (RF) coil and RF power supply. Fig. 7 shows a detailed view of a plasma torch and RF coil

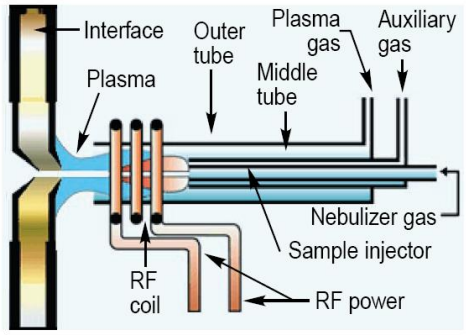

Fig. 7: Detailed view of a plasma torch and RF coil [33]

The plasma torch consists of three concentric tubes, which are usually made from quartz. In Fig. 7, these are shown as the outer tube, middle tube, and sample injector. The gas (usually argon) used to form the plasma (plasma gas) is passed between the outer and middle tubes at a flow rate of 12–17 L/min. A second gas flow, the auxiliary gas, passes between the middle tube and the sample injector at 1 L/min and is used to change the position of the base of the plasma relative to the tube and the injector. A third gas flow, the nebulizer gas, also flowing at 1 L/min carries the sample, in the form of a fine-droplet aerosol, from the sample introduction system and physically punches a channel through the center of the plasma.

The sample injector is often made from materials other than quartz, such as alumina, platinum, and sapphire, if highly corrosive materials need to be analyzed.

The plasma torch is mounted horizontally and positioned centrally in the RF coil, approximately 10–20 mm from the interface. [33]

2.2.2.1 Formation of an ICP discharge

The process of ICP discharge is conceptionally shown in Fig. 8:

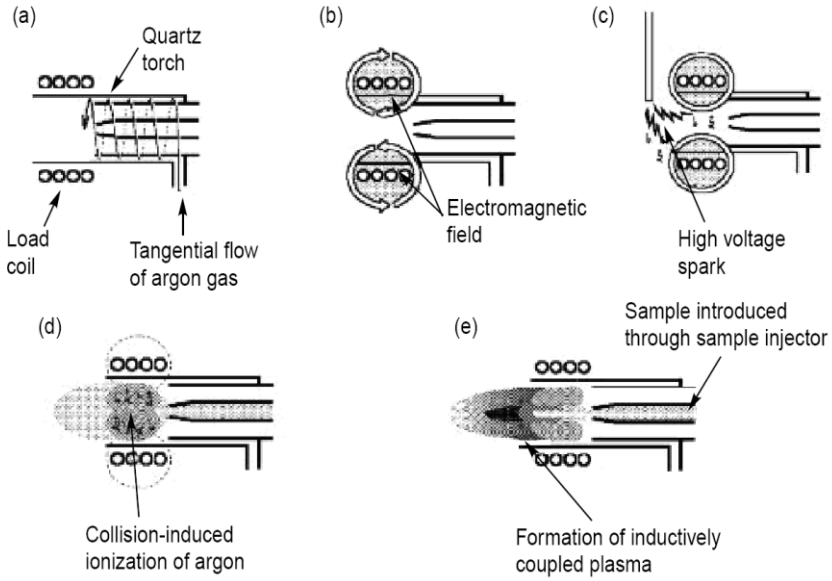

Fig. 8: Schematic of ICP discharge [33]

First, a tangential (spiral) flow of argon gas is directed between the outer and middle tube of a quartz torch (Fig. 8a). A load coil, usually copper, surrounds the top end of the torch and is connected to a radio frequency generator. When RF power (typically 750–1500 W, depending on the sample) is applied to the load coil, an alternating current oscillates within the coil at a rate corresponding to the frequency of the generator. In most ICP generators this frequency is either 27 or 40 MHz. This RF oscillation of the current in the coil causes an intense electromagnetic field to be created in the area at the top of the torch (Fig. 8b). With argon gas flowing through the torch, a high-voltage spark is applied to the gas, which causes some electrons to be stripped from their argon atoms (Fig. 8c). These electrons, which are caught up and accelerated in the magnetic field, then collide with other argon atoms, stripping off still more electrons. This collision-induced ionization of the argon continues in a chain reaction, breaking down the gas into argon atoms, argon ions and electrons, forming what is known as an inductively coupled plasma discharge (Fig. 8d).

The ICP discharge is then sustained within the torch and load coil as RF energy is continually transferred to it through the inductive coupling process. The sample aerosol is then introduced into the plasma through a third tube called the sample injector (Fig. 8e). [33]

2.2.2.2 Ionization of the sample

Fig. 9 shows a cross-sectional representation of the discharge along with the approximate temperatures for different region of plasma.

The sample aerosol enters the injector via the spray chamber. When it exits the sample injector, it is moving at such a velocity that it physically punches a hole through the center of the plasma discharge. It then goes through a number of physical changes, starting at the preheating zone and continuing through the radiation zone before it eventually becomes a positively charged ion in the analytical zone.

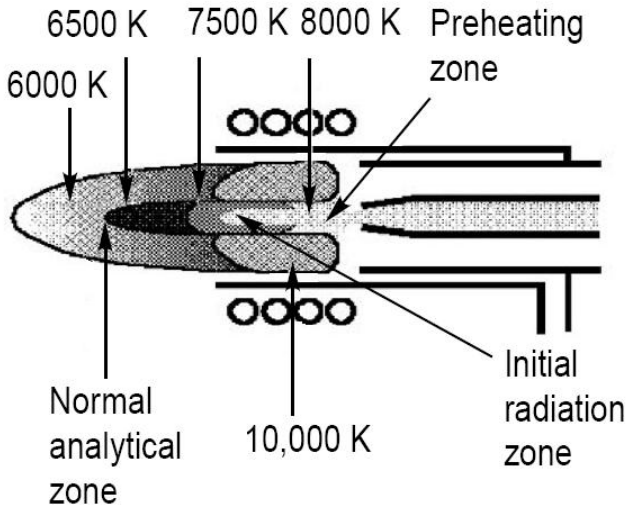

Fig. 9: different temperatures zones in the plasma [33]

The process of conversion of droplets into ions is represented in Fig. 10.

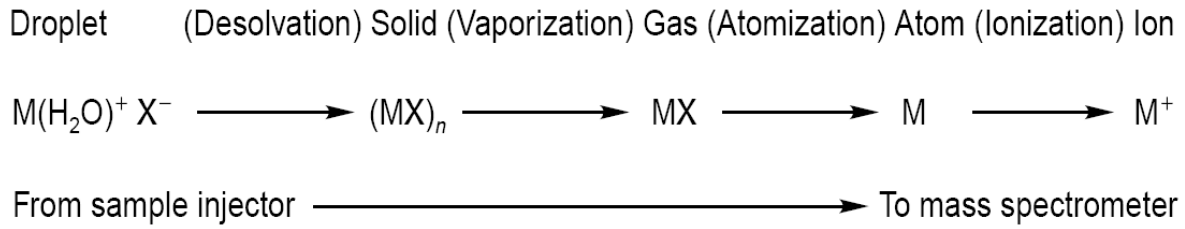

Fig. 10: Ionization process of a sample [33]

The first step that takes place is desolvation of the droplet. With the water molecules stripped away, it then becomes a very small solid particle. As the sample moves further into the plasma, the solid particle changes first into a gaseous form and then into a ground-state atom. The final process of conversion of an atom to an ion is

achieved mainly by collisions of energetic argon electrons (and to a lesser extent by argon ions) with the ground-state atom. The ion then emerges from the plasma and is directed into the interface of the mass spectrometer. [33]

2.2.3 The interface region

The interface region is probably the most critical area of the whole inductively coupled plasma mass spectrometry (ICP-MS) system, because the most challenging part of an ICP-MS is the movement of the ions from the plasma to the mass spectrometer.

Fig. 11 shows a detailed view of the interface region.

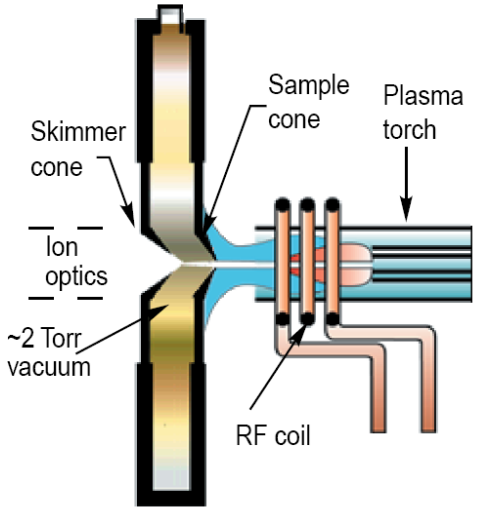

Fig. 11: detailed view of the interface region [34]

The role of the interface is to transport the ions efficiently, consistently, and with electrical integrity from the plasma, which is at atmospheric pressure (760 Torr), to the mass spectrometer analyzer region, which is at approximately 10^{-6} Torr. One first achieves this by directing the ions into the interface region. The interface consists of two metallic cones with very small orifices, which are maintained at a vacuum of approx. 2 Torr with a mechanical roughing pump. After the ions are generated in the plasma, they pass through the first cone, known as the sampler cone, which has an orifice diameter of 0.8–1.2 mm. From there they travel a short distance to the skimmer cone, which is generally sharper than the sampler cone and has a much smaller orifice (0.4–0.8 mm i.d.). Both cones are usually made of nickel, but they can be made of materials such as platinum that are far more tolerant to corrosive liquids. To reduce the effects of the high-temperature plasma on the cones, the interface housing is water-cooled and made from a material that dissipates heat easily, such as copper or aluminum. The ions then emerge from the skimmer cone, where they are directed through the ion optics, and finally are guided into the mass separation device.

The main problem to overcome in the interface region is capacitive coupling. The capacitive coupling is an undesired electrostatic effect between the load coil and the plasma discharge, producing a potential difference of 100–200 V. Although this potential is a physical characteristic of all inductively coupled plasma discharges, it is particularly serious in an ICP mass spectrometer because the capacitive coupling creates an electrical discharge between the plasma and the sampler cone. This discharge, commonly called the pinch effect or secondary discharge, shows itself as arcing in the region where the plasma is in contact with the sampler cone.

If not taken care of, this arcing can cause all kinds of problems, including an increase in doubly charged interfering species, a wide kinetic energy spread of sampled ions, formation of ions generated from the sampler cone, and a decreased orifice lifetime.

To overcome this problem it is necessary to install grounding In today's instrumentation the grounding is achieved in a number of different ways, depending on the design of the interface. Some of the most popular designs include balancing the oscillator inside the circuitry of the RF generator, positioning a grounded shield or plate between the coil and the plasma torch or using two interlaced coils where the RF fields go in opposing directions. They all work differently but achieve a similar result of reducing or eliminating the secondary discharge. [34]

2.2.4 Ion optics

The inherent problem lies in the fact that ICP-MS is relatively inefficient; out of every million ions generated in the plasma, only one actually reaches the detector. One of the main contributing factors to the low efficiency is the higher concentration of matrix elements compared with the analyte, which has the effect of defocusing the ions and altering the transmission characteristics of the ion beam. The role of the ion focusing system is therefore to transport the maximum number of analyte ions from the interface region to the mass separation device, while rejecting as many of the matrix components and nonanalyte-based species as possible.

The ion optics are positioned between the skimmer cone and the mass separation device.

The function of the ion optic system is to take ions from the hostile environment of the plasma at atmospheric pressure via the interface cones and steer them into the mass analyzer, which is under high vacuum.

A secondary but also very important role of the ion optic system is to stop particulates, neutral species, and photons from getting through to the mass analyzer and the detector. These species cause signal instability and contribute to background levels, which ultimately affect the performance of the system. For example, if photons or neutral species reach the detector, they will elevate the background noise and

therefore degrade detection capability. In addition, if particulates from the matrix penetrate farther into the mass spectrometer region, they have the potential to deposit on lens components and, in extreme cases, get into the mass analyzer. In the short term this will cause signal instability and, in the long term, increase the frequency of cleaning and routine maintenance.

Basically two approaches will reduce the chances of these undesirable species making it into the mass spectrometer.

The first method is to place a grounded metal stop (disk) behind the skimmer cone. This stop allows the ion beam to move around it but physically blocks the particulates, photons, and neutral species from traveling downstream. The other approach is to set the ion lens or mass analyzer slightly off axis. The positively charged ions are then steered by the lens system into the mass analyzer, while the photons and neutral and nonionic species are ejected out of the ion beam.

To fully understand the role of the ion optics in ICP-MS, it is important to have an appreciation of the dynamics of ion flow from the plasma through the interface region into the mass spectrometer. When the ions generated in the plasma emerge from the skimmer cone, there is a rapid expansion of the ion beam as the pressure is reduced from 760 Torr (atmospheric pressure) to approximately 10^{-23} to 10^{-24} Torr in the lens chamber with a turbomolecular pump. The composition of the ion beam immediately behind the cone is the same as the composition in front of the cone because the expansion at this stage is controlled by normal gas dynamics and not by electrodynamics.

One of the main reasons for this is that, in the ion sampling process, the Debye length (the distance over which ions exert influence on each other) is small compared with the orifice diameter of the sampler or skimmer cone. Consequently there is little electrical interaction between the ion beam and the cone and relatively little interaction between the individual ions in the beam. In this way, compositional integrity of the ion beam is maintained throughout the interface region. With this rapid drop in pressure in the lens chamber, electrons diffuse out of the ion beam. Because of the small size of the electrons relative to the positively charged ions, the electrons diffuse farther from the beam than the ions, resulting in an ion beam with a net positive charge.

The generation of a positively charged ion beam is the first stage in the charge separation process. Unfortunately, the net positive charge of the ion beam means that there is now a natural tendency for the ions to repel each other. If nothing is done to compensate for this, ions with a higher mass-to-charge ratio will dominate the center of the ion beam and force the lighter ions to the outside. The degree of loss will depend on the kinetic energy of the ions: those with high kinetic energy (high mass elements) will be transmitted in preference to ions with medium (midmass elements) or low kinetic energy (low-mass elements). The second stage of charge

separation is therefore to electrostatically steer the ions of interest back into the center of the ion beam by placing voltages on one or more ion lens components. [35]

Fig. 12 shows a modern ion optics which consists of a single ion lens and a grounded photon stop.

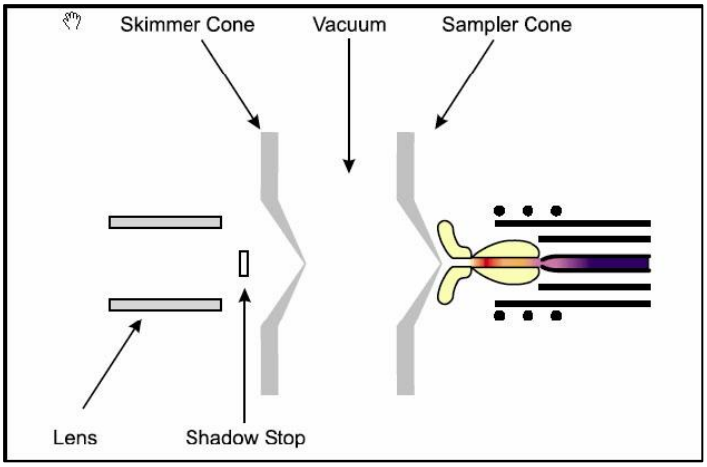

Fig. 12: Ion optics consisting of a single ion lens and a grounded photon stop [36]

2.2.5 The mass analyzer – quadrupol mass filter

The mass analyzer is positioned between the ion optics and the detector and is maintained at a vacuum of approximately 10^{-6} Torr with a second turbomolecular pump. Assuming the ions are emerging from the ion optics at the optimum kinetic energy, they are ready to be separated according to their mass-to-charge ratio by the mass analyzer.

There are basically four kinds of commercially available mass analyzers:

Quadrupole mass filters, double focusing magnetic sector, time-of-flight, and collision–reaction cell technology. They all have their own strengths and weaknesses. Since the ICP-MS device used for measurements in this work contained a quadrupole mass filter corresponding technology is described in this section.

Quadrupole-based systems were developed in the early 1980s and represent approximately 90% of all ICP mass spectrometers used today. This design was the first to be commercialized; as a result, today's quadrupole ICP-MS technology is considered a very mature, routine, high throughput, trace-element technique.

A quadrupole consists of four cylindrical or hyperbolic metallic rods of the same length and diameter. They are typically made of stainless steel or molybdenum, and sometimes have a ceramic coating for corrosion resistance. Quadrupoles used in ICP-MS are typically 15–20 cm in length and about 1 cm in diameter and operate at a frequency of 2–3 MHz. [37]

2.2.5.1 Basic principles of operation

By placing a direct current (dc) field on one pair of rods and a radio frequency (rf) field on the opposite pair, ions of a selected mass are allowed to pass through the rods to the detector, while the others are ejected from the quadrupole. Fig. 13 shows this in greater detail.

In this simplified example, the analyte ion (black) and four other ions (colored) have arrived at the entrance to the four rods of the quadrupole. When a particular rf-dc voltage is applied to the rods, the positive or negative bias on the rods will electrostatically steer the analyte ion of interest down the middle of the four rods to the end, where it will emerge and be converted to an electrical pulse by the detector.

The other ions of different mass-to-charge ratios will pass through the spaces between the rods and be ejected from the quadrupole.

This scanning process is then repeated for another analyte at a completely different mass-to-charge ratio until all the analytes in a multielement analysis have been measured.

Quadrupole scan rates are typically on the order of 2500 atomic mass units (amu) per second and can cover the entire mass range of 0–300 amu in about 0.1 s. However, real-world analysis speeds are much slower than this, and in practice 25 elements can be determined in duplicate with good precision in 1–2 min. [37]

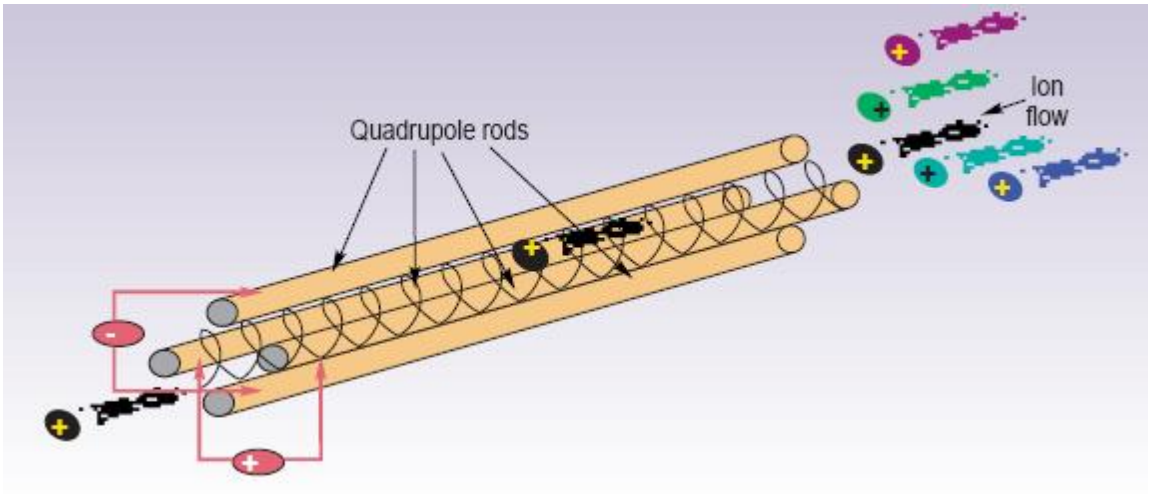

Fig. 13: Schematic of the principle of a quadrupole [37]

2.2.5.2 Resolution

The ability to separate different masses with a quadrupole is determined by a combination of factors including shape, diameter, and length of the rods, frequency of quadrupole power supply, operating vacuum, applied rf-dc voltages, and the motion and kinetic energy of the ions entering and exiting the quadrupole. All these factors will have a direct impact on the stability of the ions as they travel down the middle of the rods and thus the quadrupole's ability to separate ions of differing mass-to-charge ratios.

In theory, the resolution of a quadrupole mass filter can be varied between 0.3 and 3.0 amu. However, improved resolution is always accompanied by a sacrifice in sensitivity.

In practice, the quadrupole is normally operated at a resolution of 0.7–1.0 amu for most applications. [37]

2.2.6 Dual-stage detector

There are two possible cases when analyzing samples. For samples with low analyte concentration it is necessary to use detectors with high sensitivity. These detectors operate in digital counting mode. For samples with high analyte concentration the analog counting mode is used to reduce the sensitivity of detector.

Accordingly detectors with a wide analytical range are required. Since in real-samples the analyte concentration is unknown two scans of one sample are required. A first scan, in which the detector is operated in the analog mode, provides signals for elements present at high concentrations. A second scan, in which the detector voltage is switched to digital pulse counting mode, provides high sensitivity detection for elements present at low levels.

The disadvantage of such an analysis is that two independent mass scans are required to gather data across an extended signal range. This not only results in degraded measurement efficiency and slower analyses, but it also means that the system cannot be used for fast transient signal analysis of unknown samples because mode switching is generally too slow.

The limitations of using two scans can be overcome by using a dual-stage discrete dynode detector.

This technology uses measurement circuitry that allows both high and low concentrations to be determined in one scan. This is achieved by measuring the ion signal as an analog signal at the midpoint dynode.

When more than a threshold number of ions are detected, the signal is processed through the analog circuitry. When fewer than the threshold number of ions are

detected, the signal cascades through the rest of the dynodes and is measured as a pulse signal in the conventional way. This process is completely automatic and means that both the analog and the pulse signals are collected simultaneously in one scan.

The pulse-counting mode is typically linear from zero to about 10^6 counts/s, while the analog circuitry is suitable from 10^4 to 10^9 counts/s. To normalize both ranges, a cross calibration is performed to cover concentration levels, which could generate a pulse and an analog signal. This is possible because the analog and pulse outputs can be defined in identical terms of incoming pulse counts per second, based on knowing the voltage at the first analog stage, the output current, and a conversion factor defined by the detection circuitry electronics.

By performing a cross calibration across the mass range, a dual-mode detector of this type is capable of achieving approximately eight to nine orders of dynamic range in one simultaneous scan. [38]

2.2.7 Interferences

The interferences which can occur in ICP-MS are generally classified in three major groups: spectral, matrix and physical.

2.2.7.1 Spectral interferences

Spectral interferences are classified in spectral overlaps, isobaric interferences, interferences which are produced by doubly charged species.

Spectral overlaps are probably the most serious types of interferences. The most common type is known as a polyatomic or molecular spectral interference, which is produced by the combination of two or more atomic ions. They are usually associated with either the plasma and nebulizer gas used, matrix components in the solvent and sample, other analyte elements, or entrained oxygen or nitrogen from the surrounding air.

For example, ^{40}Ar from argon plasma interferes dramatically with the most abundant isotope of calcium ^{40}Ca, whereas the combination of argon and oxygen in an aqueous sample generates the $^{40}Ar^{16}O$ interference, which has a significant impact on the major isotope of Fe at mass 56.

Isobaric overlaps are mainly produced by different isotopes of other elements in the sample that create spectral interferences at the same mass as the analyte. For example, vanadium has two isotopes at 50 and 51 amu. However, mass 50 is the only practical isotope to use in the presence of a chloride matrix, because of the large contribution from the $^{16}O^{35}Cl$ interference at mass 51. Unfortunately mass 50 amu, which is only 0.25% abundant, also coincides with isotopes of titanium and

chromium, which are 5.4% and 4.3% abundant, respectively. This makes the determination of vanadium in the presence of titanium and chromium very difficult unless mathematical corrections are made. [39]

2.2.7.2 Matrix interferences

Matrix interferences cause suppression of the signal by the matrix itself.

There are basically two types of matrix-induced interferences. The first and simplest to overcome is often called a sample transport effect and is a physical suppression of the analyte signal, brought on by the matrix components. It is caused by the sample's impact on droplet formation in the nebulizer or droplet-size selection in the spray chamber.

In some matrices, signal suppression is caused not so much by sample transport effects, but by its impact on the ionization temperature of the plasma discharge. This is exemplified when different concentrations of acids are aspirated into a cool plasma. The ionization conditions in the plasma are so fragile that higher concentrations of acid result in severe suppression of the analyte signal (Fig. 14).

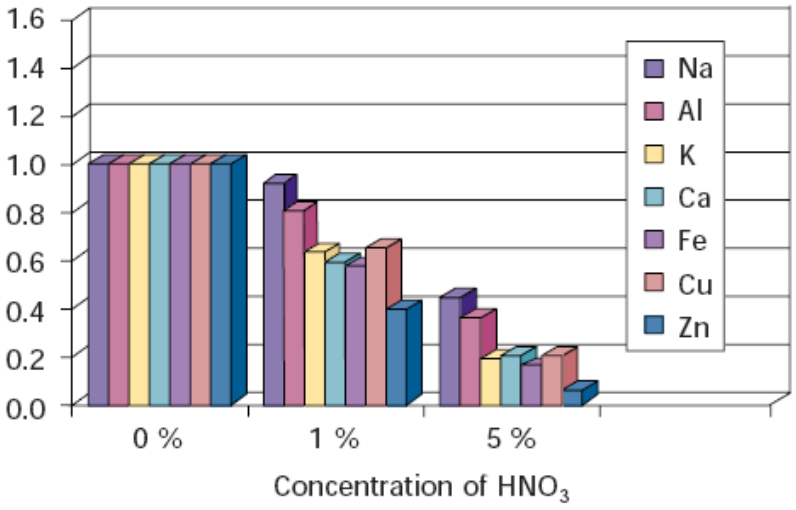

Fig. 14: Matrix suppression caused by increasing concentration of nitric acid [39]

Another matrix interference is the so called space-charge interference. This has the effect of defocusing the ion beam, which leads to poor sensitivity and detection limits, especially when trace levels of low mass elements are being determined in the presence of large concentrations of high mass matrices. The high-mass matrix element will dominate the ion beam, pushing the lighter elements out of the way.

The suppression of low mass elements such as Li and Be is significantly higher than with high mass elements such as Tl and Pb in the presence of 1000 ppm uranium (Fig. 15).

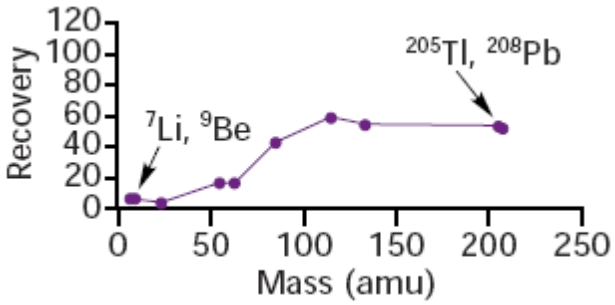

Fig. 15: Space charge matrix suppression caused by 1000ppm uranium [39]

2.2.7.3 Compensation of Interferences

There are some methods to compensate interferences including mathematical correction, using cool plasma, applying collision cells or by adding internal standards to the sample.

2.2.7.3.1 Mathematical correction equation

Mathematical correction is used to compensate for isobaric interferences.

This method works on the principle of measuring the intensity of the interfering isotope at another mass, which ideally is free of any interferences. A correction is then applied by knowing the ratio of the intensity of the interfering species at the analyte mass to its intensity at the alternate mass.

For example, a mathematical correction is used when measuring Cd in combination with Sn.

The most sensitive isotope for cadmium is at mass 114. However, there is also a minor isotope of tin at mass 114. This means that a quantitation using ^{114}Cd can only be carried out if a correction is made for ^{114}Sn. Fortunately Sn has a total of 10 isotopes, which means that at least one of them will probably be free of a spectral interference. Therefore, by measuring the intensity of Sn at one of its most abundant isotopes (typically ^{118}Sn with an abundance of 24.23%) and rationing it to ^{114}Sn (abundance of 0.65%), a correction is made in the method software by the following equation:

$$^{114}Cd = counts\ at\ mass\ 114 - \frac{^{114}Sn}{^{118}Sn} * {}^{118}Sn = mass\ 114 - 0.0268 * {}^{118}Sn$$ [39]

2.2.7.3.2 Cool Plasma Technology

If the intensity of the interference is large, and analyte intensity is extremely low, mathematical equations are not ideally suited as a correction method.

An alternative approach is to use cold/cool plasma conditions.

Under normal plasma conditions (typically 1000–1400 W rf power and 0.8–1.0 L/min of nebulizer gas flow), argon ions combine with matrix and solvent components to generate problematic spectral interferences such as ^{38}ArH, ^{40}Ar, and $^{40}Ar^{16}O$, which impact the detection limits of a small number of elements including K, Ca, and Fe. By using cool plasma conditions (500–800 W rf power and 1.5–1.8 L/min nebulizer gas flow), the ionization conditions in the plasma are changed so that many of these interferences are dramatically reduced.

The result is that detection limits for this group of elements are significantly enhanced.

Cool plasma conditions are limited to a small group of elements in simple aqueous solutions that are prone to argon-based spectral interferences. It offers very little benefit for the majority of the other elements, because its ionization temperature is significantly lower than a normal plasma. In addition, it is often impractical for the analysis of complex samples, because of severe signal suppression caused by the matrix.

Collision cells are applied to overcome these limitations. Collision cells use ion-molecule collisions and reactions to cleanse the ion beam of harmful polyatomic and molecular interferences before they enter the mass analyzer.

The best and probably most efficient way to remove spectral overlaps is to resolve them away using a high resolution mass spectrometer. During the past 10 years this approach, particularly with double-focusing magnetic sector mass analyzers, has proved to be invaluable for separating many of the problematic polyatomic and molecular interferences seen in ICP-MS, without the need to use cool plasma conditions or collision/reaction cells.

However, even though their resolving capability is far more powerful than quadrupole-based instruments, there is a sacrifice in sensitivity if extremely high resolution is used, as shown in Fig. 16.

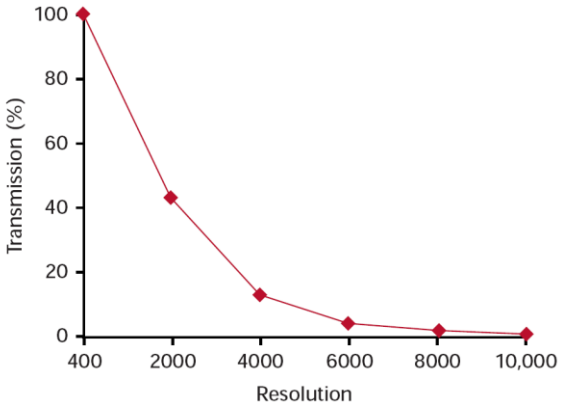

Fig. 16: Transmission characteristics of a magnetic sector ICP-MS decreases as the resolving power increases [39]

2.2.7.4 Internal standardization

The classic way to compensate for a physical interference is to use internal standardization. With this method of correction, a small group of elements (usually at the parts-per-billion level) are spiked into the samples, calibration standards, and blank to correct for any variations in the response of the elements caused by the matrix. As the intensity of the internal standards change, the element responses are updated every time a sample is analyzed. The following criteria are typically used for selecting the internal standards:

- They are not present in the sample
- The sample matrix or analyte elements do not spectrally interfere with them
- They do not spectrally interfere with the analyte masses
- They should not be elements that are considered environmental contaminants
- They are usually grouped with analyte elements of a similar mass range.
- They should be of a similar ionization potential to the groups of analyte elements so they behave in a similar manner in the plasma
- Some of the common ones reported to be good candidates include ^{9}Be, ^{45}Sc, ^{59}Co, ^{74}Ge, ^{89}Y, ^{103}Rh, ^{115}In, ^{169}Tm, ^{175}Lu, ^{187}Re, and ^{232}Th.

Internal standardization is also used to compensate for long-term signal drift produced by matrix components slowly blocking the sampler and skimmer cone orifices. [39]

2.3 Liquid scintillation counting (LSC)

2.3.1 Introduction

The earliest organic scintillators were used in the form of crystals and as a logical extension of the work with the crystals, the early liquid scintillators were solutions of the crystalline materials. 1937 Kallmann noted that certain organic materials fluoresced under ultraviolet light and made a large crystal out of naphthalene, which he showed could be used for the detection of α-, β- and γ-rays [40]. Ten years later he showed that aromatic solvents with certain dissolved solutes were efficient scintillation sources for nuclear radiations. He used toluene and xylene solutions of fluorine, carbazole, phenanthrene and anthracene as scintillation detectors [41]. Ageno et al. used xylene solutions of naphthalene [42] and Reynolds et. al demonstrated the coincidence method of a counter with benzene and xylene solutions of p-terphenyl [43]. Hayes et al. evaluated hundreds of organic compounds for their use in liquid scintillation counting, most of which are still the best scintillator solutes.

Important names according to the theory and mechanism of energy transfer are Förster and Galanin. The Försters resonance energy transfer theory explained the quantitative energy transfer from excited solvent molecules to the solute molecules [44] and Galanins theory explained the quantitative transfer of excitation energy from primary solutes to secondary solutes [45].

Birks et al. have contributed to the understanding of the relationship between photophysical and scintillation processes [46] and Kallmann et al. contributed to the understanding of the mechanism of quenching [45].

2.3.2 Basic processes

The detection of energy, in the form of nuclear emanations, by organic solutions is dependent on a charged particle producing a number of excited molecules in the organic solution. These excited molecules will either emit photons or efficiently transfer the energy to an acceptor (solute) which in turn will emit photons. The photons can be measured by collection on the face of a multiplier phototube which will convert them into an electrical pulse [45].

2.3.2.1 Interaction of ionizing radiation with matter

Nuclear radiation will interact with molecules in many ways. The ionizing radiation, e. g. electrons, alphas etc., will make a “track” as the particle passes through a material. Along the track there will be a large number of molecules which will be given energy from the particles, but the majority of the molecules in the materials will not be affected at all; that is, the effects are very local (Fig. 17).

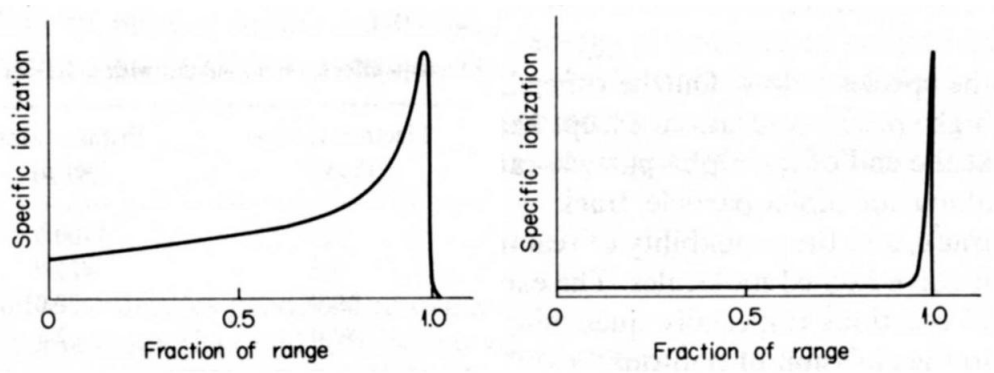

Fig. 17: energy loss of alpha- (left) and beta-particles (right) along the track [45]

The energy loss by the ionizing particle will produce ions, excited molecules, free radicals and secondary particles. Along the track the concentration of the excited and ionized molecules will determine the types of processes (chemical and physical) that occur as the result of the interaction which follow the passage of the particle.

The types of chemical reactions that occur are neutralization, free radical reactions, decomposition, excimer formation and many others. Physical processes are X-ray emission, fluorescence, phosphorescence, energy migration, energy transfer, radiationless deactivation and many others. In many systems, including liquid scintillation solutions, almost all of these processes will occur. The final result, the emission of photons, will be effected by the competition between all of these reactions. [45]

2.3.2.2 Scintillation in organic material

The energy of the ionizing particle is partly transformed into luminescence emissions. The luminescence has a characteristic spectrum which seems to be a property associated with conjugated and aromatic organic molecules. It is an inherent molecular property and arises from the electronic structure of the molecule.

Saturated hydrocarbons such as cyclohexane contain no π-electrons and therefore show no optical absorption at energies less than ~6eV. However, many molecules which contain nonlocalized π-electrons require much less energy to cause electronic excitation. Generally three π-electronic absorption bands are readily observed which corresponds to transition from the singlet ground state (S_0) into the π-electronic excited states (S_1, S_2, S_3). A simplified diagram of the energy levels involved in a typical excitation of an organic molecule with π-electronic levels is shown in Fig. 18.

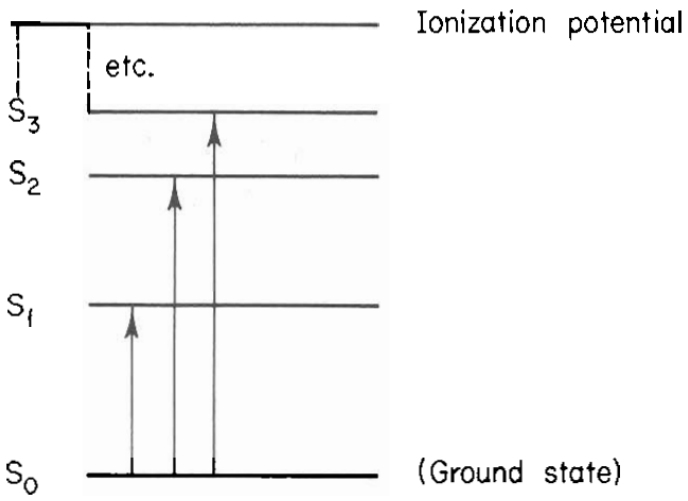

Fig. 18: typical excitation of an organic molecule with π-electrons [45]

The S_3 state is predominantly produced when an aromatic solvent is excited by an ionizing particle. However, the S_1 excited state is the state that is responsible for the fluorescence emission from all excited organic molecules. The upper excited states are converted to the lower excited states by the process of internal conversion. Internal conversion is a radiationless process where no photons are emitted. For each excited state there is a competition between photon emission and internal conversion. Most upper excited states (>S_2) undergo deexcitation by internal conversion. Only the S_1 state of many organic molecules has a higher probability for photon emission than for radiationless transition between S_1 state and ground-state vibrational levels. [45]

2.3.2.3 Energy transfer

Most aromatic solvents are not good scintillators by themselves. Therefore solutes that are efficient scintillators are added to the solvents. However, the energy has to find its way from the excited solvent molecules to the solute molecules. The efficiency of the transfer process is a function of the solute concentration (Fig. 19).

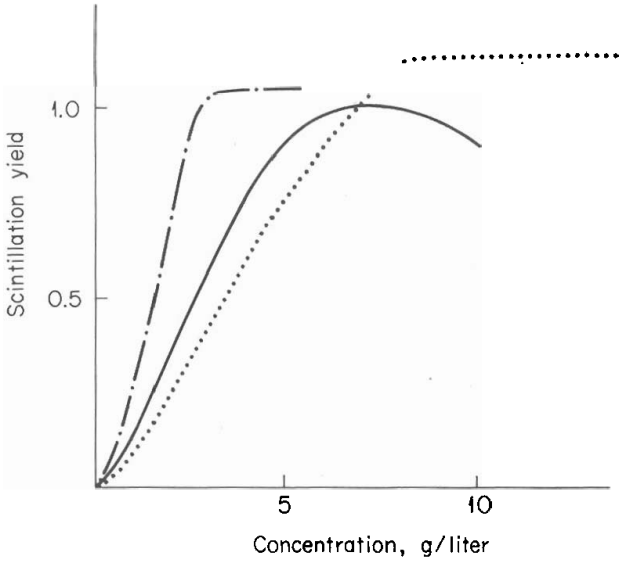

Fig. 19: relative scintillation yield as a function of the concentration of three typical solutes: PPO (—), butyl-PBD (···) and p-terphenyl (—·—·) [45]

2.3.2.3.1 Solvent-solvent transfer

The primary energy transfer process occurs between solvent molecules. Solvent-solvent energy transfer takes place in subnanosecond time and can occur over a distance of many molecular diameters. Furthermore solvent-solvent energy transfer is in part diffusion controlled and monoenergetic. There are two theories which describe the possible energy transfer mechanism.

One theory was proposed by Birks [47] and describes the formation of solvent excimers, which upon breaking apart find the excitation energy on the previously unexcited molecule. This solvent excimer formation and breaking up occurs many times, allowing the energy to migrate a long distance in the time, which is very short compared to the fluorescence emission time:

$$S_1^* + S_2 \leftrightarrows (S_1S_2)^* \leftrightarrows S_1 + S_2^*$$
$$S_2^* + S_3 \leftrightarrows (S_2S_3)^* \leftrightarrows S_2 + S_3^* \quad [48]$$

Each of these reactions is an equilibrium. Thus it is possible to have excimer formation and breaking apart without energy transfer.

A second theory was proposed by Voltz et al. [49]. This theory describes the energy transfer between solvent molecules as an energy migration from one solvent molecule to its adjacent neighbors:

$$S_1^* + S_2 \leftrightarrows S_1 + S_2^*$$
$$S_2^* + S_3 \leftrightarrows S_2 + S_3^* \quad [48]$$

Again these energy transfer reactions are equilibriums so that not every contact will lead to energy transfer.

Both of these mechanisms explain the observed evidence of energy transfer between solvent molecules. [45]

2.3.2.3.2 Solvent-solute transfer

As the energy transfers from solvent to solvent molecule it will move from environment to another. If solute molecules are present at the relatively low concentrations of 3-10 g/liter, it is likely that the excited solvent molecule will have direct contact with a solute molecule. However, at these low solute concentrations the energy is quantitatively transferred from excited molecules to solute molecules.

The energy transfer from solvent to solute is nonradiative, because no photons are emitted by the solvent molecule or absorbed by the solute molecules. Energy transfer occurs in 10^{-11} sec, whereas photon emission by the solvent occurs with a decay time of $30x10^{-9}$ sec. The energy transfer is also not diffusion controlled, which occurs in the order of 10^{-6} sec at these concentrations.

The energy transfer occurs by a resonance transfer process. A theory of the interaction of the dipoles of the two molecules has been developed by Förster [44].

The strength of the dipole-dipole interaction has been shown to be related to the degree of the overlap of the fluorescence spectrum of the donor molecule (solvent) and the absorption spectrum of the acceptor molecule (solute). [45]

2.3.2.3.3 Solute-solute energy transfer

Because of the low concentration of the solute it is very improbable that the energy transfer will be diffusion controlled. In fact, because the solute concentrations are low, the radiative probability, e. g. fluorescence, is many times greater than the other types of energy transfer processes. [45]

2.3.2.3.4 Energy transfer in liquid scintillation solutions

In liquid scintillation counting the excitation energy is in the form of kinetic energy of an ionizing particle produced by a nuclear emission. All of the primary excitations result in the formation of excited solvent molecules. The energy than migrates from one solvent molecule to another until the energy is trapped by a solute molecule. If there is a secondary solute, the energy is subsequently transferred from the primary

solute to the secondary solute where it is trapped. Finally the energy is released in the form of a photon which is characteristic of the fluorescent species. [45]

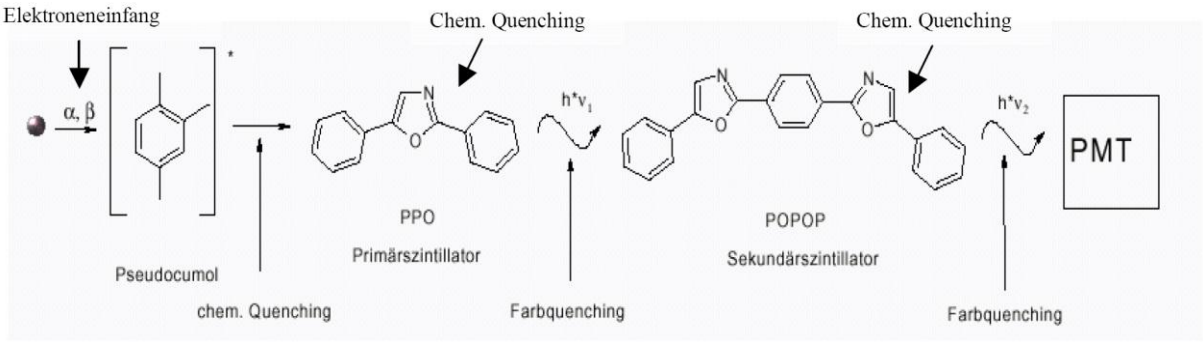

Fig. 20: Principle of the energy transfer in liquid scintillation counting [48]

2.3.2.3.5 Fluorescence

The general term luminescence is used to describe the emission of light from an excited state. Fluorescence describes emission from the singlet excited state S_1 and phosphorescence is the emission from the tripled excited state. Phosphorescence is a forbidden transition and is not observed in liquid media, because a triplet state has a long life and therefore triplet energy is usually lost through quenching or triplet-triplet-type processes.

Fluorescence usually occurs between the first excited state S_1 and the ground state S_0. The emission is not monoenergetic. The energies of the photons cover a rather wide band. These bands correspond to the energy difference between the zero vibrational level of S_1 state and many vibrational levels of the ground state.

The fluorescence between $S_{10} \rightarrow S_{00}$ corresponds to the maximum energy of a photon emitted by this excited molecule. However in most cases this band is either weak or missing and the probability of this transition is very small. The transition between S_{10} and the low vibrational levels of the ground state is the most probable. Because absorption can occur between the $S_{00} \rightarrow S_{10}$ levels and not between other ground –state vibrational levels, it is that the $S_{10} \rightarrow S_{00}$ fluorescence is not observed due to reabsorption of the emitted photon.[45]

Fig. 21 summarizes the processes described above.

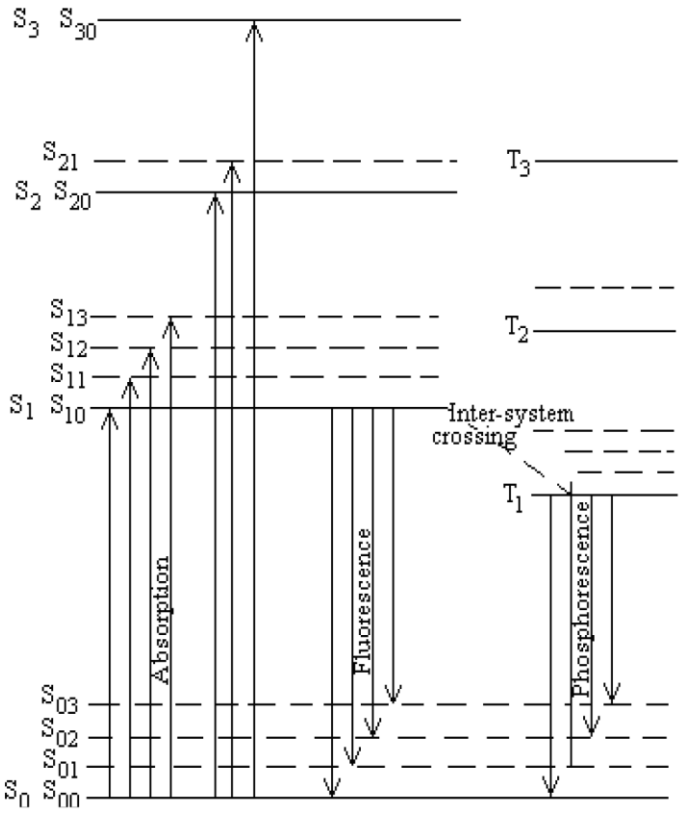

Fig. 21: Processes that can occur upon excitation of an organic molecule [48]

2.3.2.4 Scintillator solutions

The scintillator solution is composed of a solvent or solvents and a solute or solutes. The solvent acts as medium for absorbing the energy of the nuclear radiation and for dissolving the sample. The solute acts as an efficient source of photons after accepting energy from the excited solvent molecules.

Fig. 22 shows some commonly used LSC solution and Fig. 23 and Fig. 24 show some primary and secondary solutes.

Solvent	Primary solute (g/liter)	Secondary solute (mg/liter)	Other additives	Type of sample
Toluene	PPO (4–6)	M_2-POPOP (50–200)	—	Organic soluble
Toluene	Butyl-PBD (8–12)	—	—	Organic soluble
p-Xylene	Butyl-PBD (8–12)	—	Ethanol	Aqueous
Dioxane (Bray's solution)	PPO (4)	M_2-POPOP (200)	Methanol (100 ml) Ethylene glycol (200 ml) Naphthalene (60 g)	Aqueous
Dioxane	PPO (7)	M_2-POPOP (300)	Naphthalene (100 g)	Aqueous
p-Xylene	PPO (4–6)	—	Emulsifier (i.e., Triton N-101)	Water and aqueous

Fig. 22 Some commonly used LSC solutions [45]

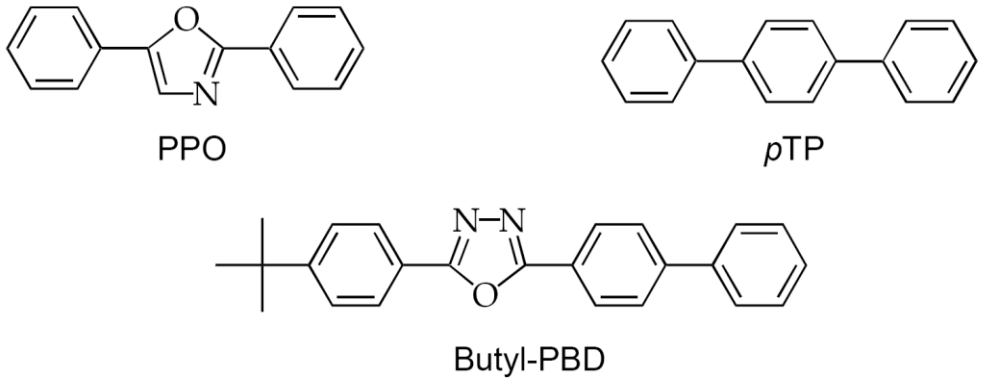

Fig. 23 some commonly used primary solutes [48]

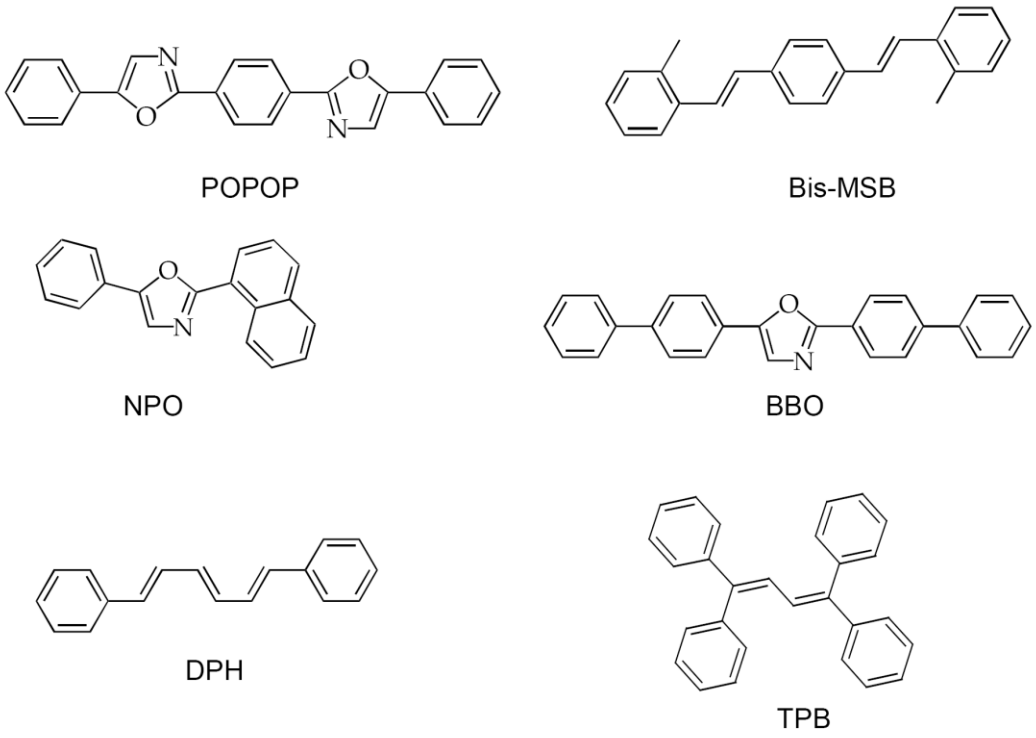

Fig. 24 some commonly used secondary solutes [48]

2.3.2.5 Quenching effects

As a result of the complicated energy transfer processes in liquid scintillator counting solutions various disturbances can appear, so-called quenching effects. Quenching effects are processes, which lead to a radiationless energy transfer.

2.3.2.5.1 Concentration quenching

Concentration quenching is the process of solute self-quenching through solute-solute interactions. It occurs with selecting the optimum solute concentration.

Ideally the solute concentration is chosen to give a maximum of energy transfer. However it is necessary to have an excess of solute over the minimum required for maximum energy transfer. This excess will allow for any dilutions which occur when introducing the sample. At the concentration C_B shown in Fig. 25 it can be readily seen that dilutions (up to a certain degree) will not alter the relative scintillation yield and thus the counting efficiency will remain constant. If the initial concentration were C_A, small dilutions would decrease the relative scintillation yield.

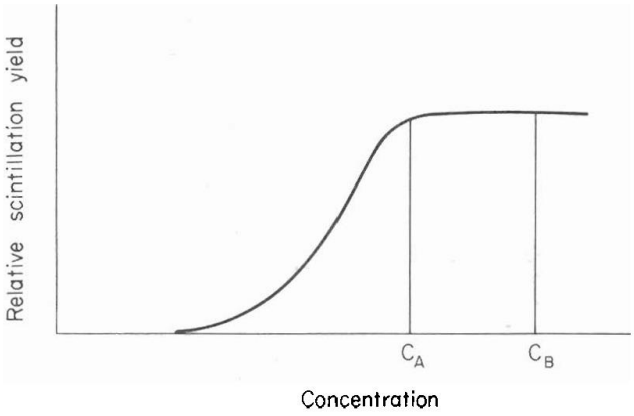

Fig. 25: Choice of proper solute concentration (C_B) [45]

Therefore concentration quenching leads to a decrease in the scintillation yield by decreasing the number of excited molecules. In the selfquenching process the energy is shared by two molecules. When they separate each molecule will possess some energy, but less than what is necessary to produce a photon:

$$(F_1^* \cdot F_0) \rightarrow 2F_0 + \text{energy}$$

Most molecules which undergo concentration quenching have the ability for the chromophoric part of the molecule to obtain a planar configuration, e. g. anthracene, which is unhindered by the approach of a second like molecule.

To eliminate concentration quenching it is necessary to alter the structural constitution by introducing side groups. For example 9,10-diphenyl-anthracene undergoes no self quenching in opposite to anthracene.

Introducing the so called “bumper groups” eliminates self-quenching too. These groups are not a part of the chromophore group, but are large bulky groups that interfere with two molecules coming together in a proper orientation for energy exchange. For example the tetramethyl derivative of p-quaterphenyl has no self quenching contrary to p-quaterphenyl. [45]

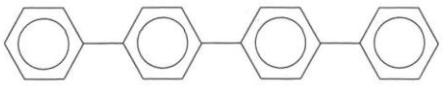

(a)

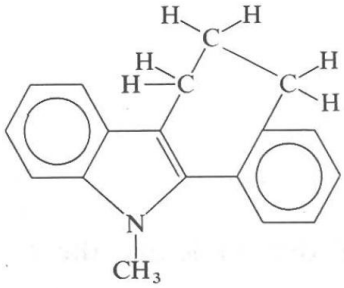

(b)

Fig. 26: p-quaterphenyl (a) vs. tetramethyl derivative of p-quaterphenyl [45]

2.3.2.5.2 Color quench

Additives that absorb light in the ultraviolet and near-ultraviolet wavelength reagions, e.g. $MnSO_4$, $CuSO_4$, $FeCl_3$ etc., will lead to reductions in the number of photons that escape the sample vial.

Several methods are used to correct the measured counting rate for color quench.

Decoloration

In this method chemicals for destroying the color by changing the oxidation state of metal ions to noncolored species are used.

Internal standard

The internal standard technique is probably the oldest method. It involves the addition of a known amount of the nuclide in high specific activity to the same sample that is being measured. The counting efficiency is then calculated from:

$$\varepsilon = \frac{cpm\ (standard+sample) - cpm\ (sample)}{dpm\ (standard)} \qquad \textbf{eq. 9}$$

The advantages of the method are: the method is rapid, it is not necessary to run a series of quenched standards (see sample channel ratio method) and different types of quenchers will not affect the validity of the method.

The disadvantages are: the sample cannot be recounted to check its cpm value and there are certain hazards to open the vial and add something extra to the scintillator solution, e.g. risk of contaminating the sample with other quenchers (by a contaminated pipet) or condensation of moisture in refrigerated samples since water is a very strong quencher.

Sample channels ratio method (SCR method)

In this method the amount of quench is measured by monitoring the ratio of counts in two channels.

The distribution of pulses for a beta-emitting nuclide in a liquid scintillator is shown in Fig. 27.

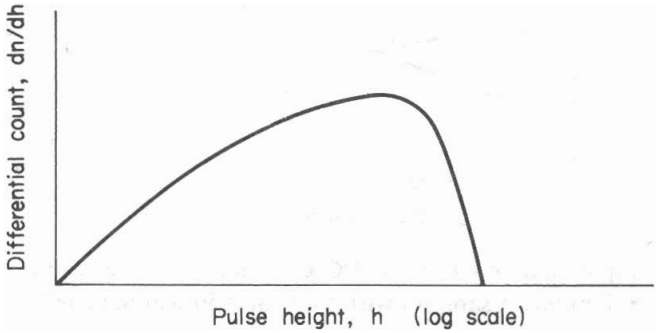

Fig. 27 typical spectrum of a beta-emitting nuclide [45]

The two counting channels can be selected in several ways. Three typical counting modes are given in Fig. 28.

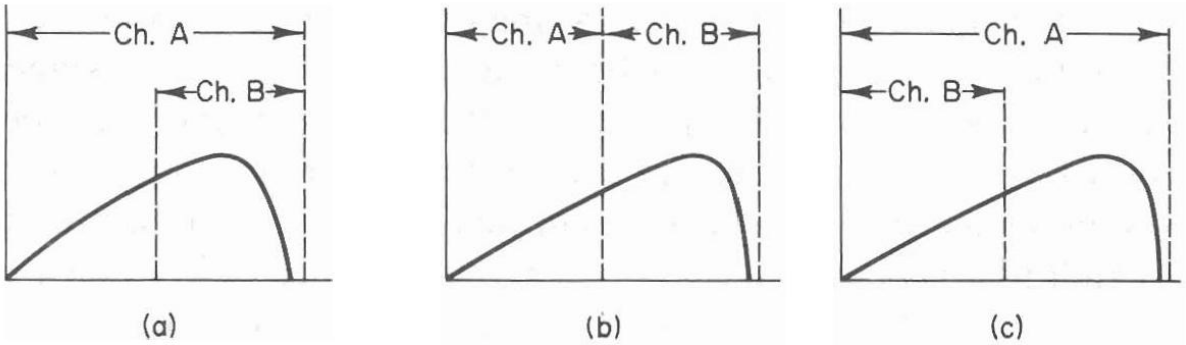

Fig. 28 Selections of counting channels for SCR method [45]

This method requires a standard quench curve. A series of samples, as nearly identical as possible with the sample to be measured, are counted which have known amounts of the radioactive nuclide and increasing amounts of quenching agent. The counting efficiency and the sample channels ratio are measured for each quenched

standard. The counting efficiency is plotted as a function of the sample channels ratio (Fig. 29).

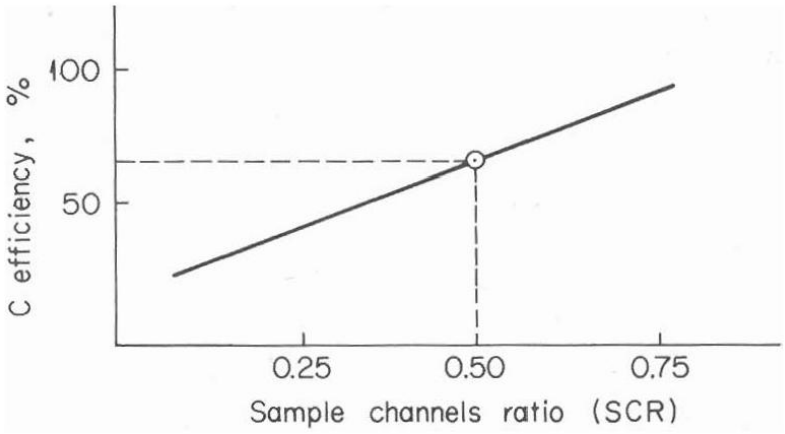

Fig. 29:standard quench plot [45]

Subsequently, an unknown sample is counted and its sample channels ratio measured. The counting efficiency for the unknown sample is obtained from the standard quench plot. For example in Fig. 29, any sample which measures an SCR value of 0.5 will be counted with an efficiency of 60%.

The method does not require the addition of anything to the scintillator solution, and the sample can be recounted as often as needed (advantages). But the method is very time-consuming and does not give as reliable results if the quench is great (drawbacks of the method). [45]

2.3.2.6 Background

There are many sources of background events in liquid scintillation counting. The main division of these sources is into those produced in the liquid scintillator solution and those which result from events outside the scintillation solution (Fig. 30). [45]

Source	Contributors
Liquid scintillator materials	Natural radioactivity in the materials which constitute the liquid scintillator Chemiluminescence and phosphorescence of certain solvents enhanced by the presence of the solutes
Sample	Natural radioactivity in the sample which may be the same or different from the nuclide to be assayed Contamination with the same or other radioactive material Chemiluminescence and phosphorescence produced by the sample or impurities in the sample
Vial	Natural radioactivity in the vial walls or cap Cosmic-ray-induced background—Cerenkov and secondary electrons and γ rays Chemiluminescence and phosphorescence produced by sun light or impurities on the vial walls Static charge buildup during movement in the sample changer
MPT	Natural radioactivity in materials which make up the MPT Cosmic rays which produce Cerenkov radiation, secondary electrons, and γ rays Thermionic and secondary electron emission from photocathode and dynodes—in coincidence systems this is mostly eliminated, because of its randomness Cross talk from electric discharges and/or Cerenkov radiation Afterpulses
Other radioactive sources	Radioactive sources (usually γ rays) in the area of the liquid scintillation counter. The movement of these sources can be very detrimental, because it will lead to changes in the background level

Fig. 30: Sources of background [45]

2.3.2.6.1 Chemiluminescence

Chemiluminescence (CL) is the emission of photons as the result of a chemical reaction where an excited molecule is produced:

$$Rubrene^{+} + Rubrene^{-} \rightarrow Rubrene^{*} + Rubrene$$

$$Rubrene^{*} \rightarrow Rubrene + hv$$

CL is often associated with the type of sample or the type of treatment given to the sample in its preparation for counting with LSC.

One source of CL is the dissolved oxygen present in all aerated solutions. In alkaline milieus or when peroxides are present the oxygen is excited to singlet oxygen. Then CL is produced by the emission of photons as the excited singlet oxygen returns to

the ground state oxygen. So flushing the sample with an inert gas will eliminate this type of CL.

Other sources of CL are impurities present in the scintillator solution, reagents used to solubilize the sample or the sample itself. All this sources can initiate chemical reactions with components of scintillator solution. This induced chemical reactions and therefore the chemiluminiscence will continue as long as chemical reactants are present.

The major problem with CL is that it will vary with time. Thus the background of a sample that has a very small amount of CL will appear to decrease over a period of time. The rate of the decrease will be determined by the rate of the chemical reaction, which produces the excited species which lead to CL. In those cases where the CL rate is very fast, it is possible to wait a period of time before measuring the background and/or the sample count rate.

In those cases where the CL rate is low, it can be helpful to increase the temperature. Since the rate of a chemical reaction is a function of temperature, an increase in temperature would mean an increase in the rate of the chemical reaction and therefore CL would be eliminated after a short period of time.

If the count rate of the sample is orders of magnitude greater than background and chemiluminescence, it is only necessary to be sure that CL intensity remains fairly constant during the counting time. In this case it is necessary to maintain a constant temperature. [45]

2.3.2.6.2 Photoluminescence

Photoluminescence describes the production of photon-induced species by light, e.g. sunlight or room light. Often the photoluminescent species are very long-lived, especially those produced in glass vials. To overcome this problem is to use polyethylene vials (Fig. 31). In general, the background rate of PE-vials is about 10-20% less than glass vials.

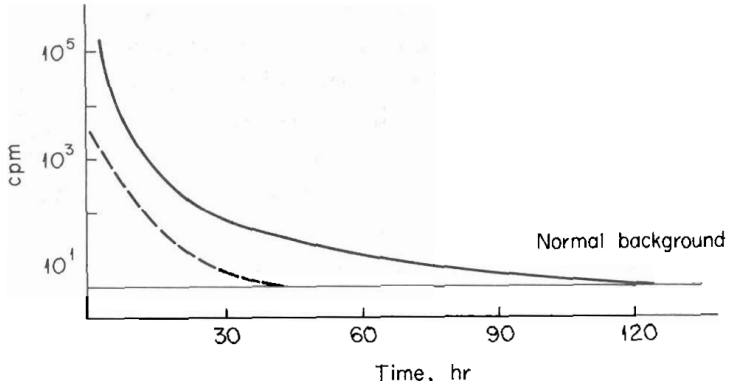

Fig. 31: Vials irradiated with sunlight, placed in counter and kept in darkness between counting times: — glass vial; - - - PE-vial [45]

2.3.2.6.3 Cerenkov and natural radioactivity

Natural radioactivity of different kinds is present in all the materials used for LSC. For example scintillator solutions contain H-3 and C-14 from atmospheric equilibriums. Stuff made of glass contains K-40, Th-232 and daughters and U_{nat}.

Those nuclides that emit high-energy β-particles, e.g. K-40, cause Cerenkov radiation (Fig. 32). Cerenkov radiation is produced by the slowing down of high-energy electrons in the glass envelope of MPT or glass vials. Since the Cerenkov radiation is photons, the MPTs will count it with a good efficiency. [45]

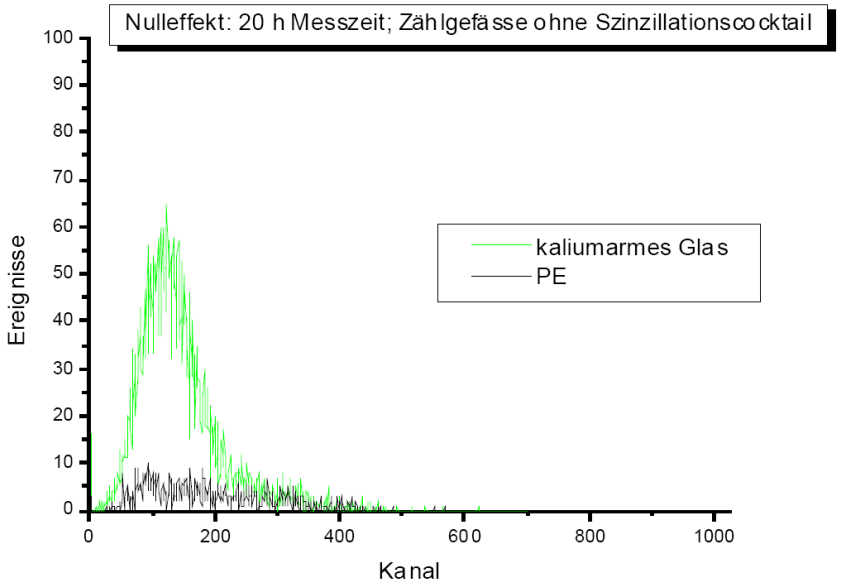

Fig. 32: background of glass- and PE-vial without scintillator solution [48]

2.3.3 Liquid scintillation counter

For sample counting a liquid scintillation counter TriCarb 1600TR (Packard Instrument Company) was used (Fig. 33).

The core of a liquid scintillation counter is the coincidence system, that is, two multiplier phototubes (MPT) viewing the sample (Fig. 34). The main advantage of the coincidence system is the reduction of background rates due to randomly generated pulses produced within each MPT, commonly called electronic noise.

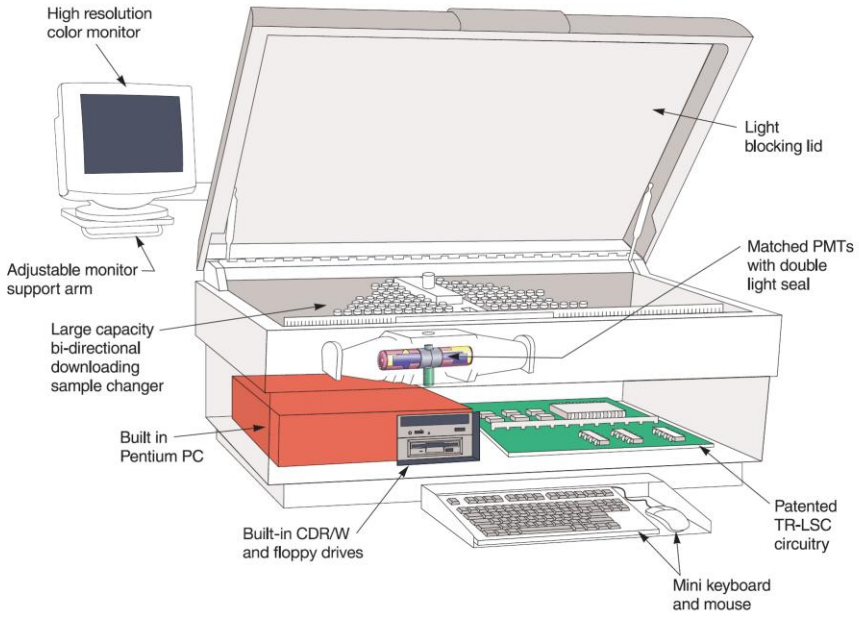

Fig. 33: TriCarb 3170 TR/SL counter, main features similar to TriCarb 1600TR [50]

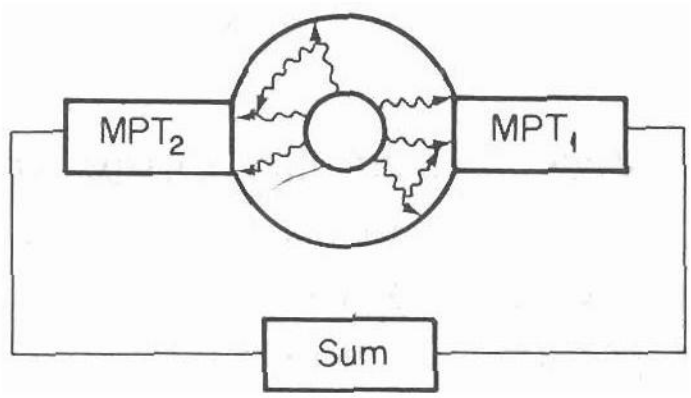

Fig. 34: Coincidence system [45]

2.3.3.1 Photomultiplier tubes

Photons of the scintillation emerge from the vial containing the scintillation solution, and are detected by a light-sensitive device known as a photomultiplier tube (PMT). The photons interact with the photocathode and eject photoelectrons. The photoelectrons are accelerated toward the first of a series of metallic elements - dynodes. Each dynode of the series is at a higher position voltage than the previous one. The accelerated electrons strike the first dynode and release secondary electrons. The secondary electrons in turn are accelerated toward the next dynode

stage and release more electrons. In the course of 12 dynode stages, the number of electrons is increased by a factor of about 10^7: An electrical pulse appears at the output of the PMT as a result of the photons which interacted with the photocathode. The amplitude - height - of this pulse (as a voltage) is proportional to the number of photons which interact with the photocathode; therefore, the pulse height at the output of the PMT is proportional to the energy of the beta particle in the sample.

2.3.3.2 Coincidence Circuity

Electronic noise from the PMT can result from electrons emitted from the photocathode due to heat ions within the tube, Cerenkov radiation, cold cathode emission and other sources. Noise pulses at the output of the PMT are identical to pulses due to scintillations from the sample. To distinguish noise pulses from sample pulses, two photomultipliers are mounted to "view" the sample in the dark enclosure of the counting chamber. The output pulses from each PMT are fed into a coincidence circuit.

Noise pulses are random events, and the fact that noise pulses are due to events which are peculiar to an individual PMT suggests that the probability of two PMTs producing noise pulses simultaneously is relatively small. This is in contrast to the production of pulses from photoelectrons due to beta particles in the sample because most beta particles have sufficient energy to produce more than one photon in interactions with the scintillation solution. It is probable that both PMTs will simultaneously receive photons due to a single beta decay event. To distinguish pulses due to beta emissions from those due to electronic noise, two PMTs are arranged to detect the scintillations from the sample. A coincidence circuit is established to check if a pulse from one PMT is accompanied by a corresponding pulse from the other. The time interval allowed, within which both tubes must produce a pulse, is about 2×10^{-8} sec. The requirement that both PMTs produce a pulse within the coincidence resolving time, for this event to be accepted, excludes the vast majority of noise pulses from the sample.

2.3.3.3 Pulse summation

The use of two PMTs not only distinguishes between electronic noise and single photon events, but it provides a means of producing electrical signals proportional to the energy of the beta-event. A beta event depositing its energy in the scintillation solution produces multiple photons, the number entering each PMT depends upon the energy and the position of the event within the vial. Thus, an event close to one PMT will produce a higher pulse amplitude in the nearest PMT than the pulse amplitude of the more remote PMT.

A circuit is incorporated into the counter which adds the amplitude of the individual PMT pulses, which are coincident in time, to produce a summed pulse proportional to the total photon yield of the event.

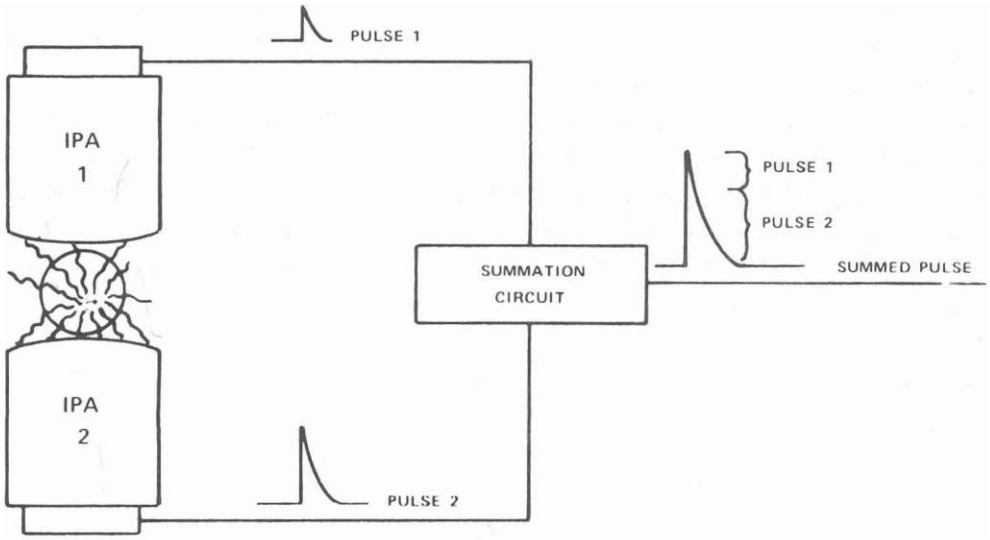

Fig. 35: summation circuit [51]

2.4 Validation

The ISO definition of validation is the confirmation by examination and provision of objective evidence that the particular requirements for a specific intended use are fulfilled. Validation is the process of making sure that an analytical method or procedure is fit for the intended purpose. [52]

The term validation is used in two ways, instrument validation and method validation.

Instrument validation is used to describe the process of establishing that an instrument at any given moment is able to perform according to its design specification. This process might be achieved for example by means of calibration or performance checks.

Method validation is the process of establishing the performance characteristics and limitations of a method and the identification of the influences which may change these characteristics and to what extent. Method validation is usually considered to be very closely tied to method development, indeed it is often not possible to determine exactly where method development finishes and validation begins. [53]

However, there are two main reasons to perform method validation.

The first reason is for the importance of an analytical measurement.

Every day millions of analytical measurements are made in thousands of laboratories around the world. There are innumerable reasons for making these measurements, for example: as a way of valuing goods for trade purposes, supporting healthcare, checking the quality of drinking water, analyzing the elemental composition of an alloy to confirm its suitability for use in aircraft construction, forensic analysis of body fluids in criminal investigations. Virtually every aspect of society is supported in some way by analytical measurement.

The cost of carrying out these measurements is high and additional costs arise from decisions made on the basis of the results. For example, tests showing food to be unfit for consumption may result in compensation claims; tests confirming the presence of banned drugs could result in fines, imprisonment or even, in some countries, execution. Clearly it is important to determine the correct result and be able to show that it is correct.

The second reason is for the professional duty of the analytical chemist.

A customer always expects to be able to trust results. Therefore an analytical result to be fit for its intended purpose it must be sufficiently reliable that any decision based on it can be taken with confidence. Thus the method performance must be validated and the uncertainty on the result, at a given level of confidence, estimated.

Implicit in this is that the tests carried out are appropriate for the analytical part of the problem that the customer wishes solved, and that the final report presents the analytical data in such a way that the customer can readily understand it and draw

appropriate conclusions. Uncertainty should be evaluated and quoted in a way that is widely recognized, internally consistent and easy to interpret.

Method validation enables chemists to demonstrate that a method is ‘fit for purpose’. [53]

A method should be validated when it is necessary to verify that its performance parameters are adequate for use for a particular analytical problem. For example when a new method is developed for particular problem, an established method is to be revised to incorporate improvements or extended to a new problem, when quality control indicates an established method is changing with time, an established method used in a different laboratory, or with different analysts or different instrumentation.

The extent of validation or revalidation required will depend on the nature of the changes made in reapplying a method to different laboratories, instrumentation, operators, and the circumstances in which the method is going to be used. Some degree of validation is always appropriate even when using apparently well-characterized standard or published methods. [53]

Typical performance characteristics of analytical methods are: applicability, selectivity, calibration, trueness, precision, recovery, operating range, limit of quantification, limit of detection, sensitivity, and ruggedness. To these can be added measurement uncertainty and fitness-for-purpose [54].

2.4.1 Applicability

After validation, the documentation should provide, in addition to any performance specification, the following information:

- the identity of the analyte, including speciation where appropriate (e.g., “total arsenic”);
- the concentration range covered by the validation (e.g., “0–50 ppm”);
- a specification of the range of matrices of the test material covered by the validation (e.g.,“seafood”);
- a protocol, describing the equipment, reagents, procedure (including permissible variation in specified instructions, e.g., “heat at 100 +/- 5 °C for 30 +/- 5 min”), calibration and quality procedures, and any special safety precautions required;
- the intended application and its critical uncertainty requirements (e.g., “The analysis of food for screening purposes. The standard uncertainty $u(c)$ of the result c should be less than $0.1 \times c$.”). [54]

2.4.2 Selectivity

Selectivity is the degree to which a method can quantify the analyte accurately in the presence of interferences.

Ideally, selectivity should be evaluated for any important interferent likely to be present. It is particularly important to check interferents that are likely, on chemical principles, to respond to the test.

Selectivity is expressed by decontamination factors DF, which are calculated by

$$D_f \geq \frac{N_{A0}}{N_A} \qquad \textbf{eq. 10}$$

where N_{A0} is the netto counting rate in the reference sample before treatment , e.g. loading onto the resin, and N_A is counting rate in the sample, i.e. after treatment.

The criterion of acceptance for selectivity is $D_f \geq 100$.

2.4.3 Linearity and operating range

Linearity is defined as the ability of the method to obtain test results proportional to the concentration of analyte [53].

A method is to be tested for linearity by using six or more calibration standards which are evenly spaced over the concentration range of interest. The range should encompass 0–150 % or 50–150 % of the concentration likely to be encountered and depending on which of these is the more suitable. The calibration standards should be run at least in duplicate, and preferably triplicate or more, in a random order. [54]

Linearity was evaluated by the correlation coefficient R^2. The criterion of acceptance was set to $R^2 \geq 0.995$.

2.4.4 Trueness

Trueness is the closeness of agreement between a test result and the accepted reference value of the property being measured. Trueness is stated quantitatively in terms of “bias”, with smaller bias indicating greater trueness. Bias is typically determined by comparing the response of the method to a reference material with the known value assigned to the material (eq. 11 [55]).

$$\boldsymbol{B}\,[\%] = \frac{\boldsymbol{c_{det} - c_{ref}}}{\boldsymbol{c_{ref}}} \cdot \mathbf{100} \qquad \textbf{eq. 11}$$

where c_{det} is the determined concentration of an analyte and c_{ref} the concentration of the referenced material

Test for trueness is ideally performed by using certified reference materials (CRMs). CRMs are traceable to international standards with known uncertainty and should always be preferred in method validation.

In the absence of reference materials, bias can be investigated by spiking and recovery. A typical test material is analyzed by the method under validation both in its original state and after the addition (spiking) of a known mass of the analyte to the test portion. The difference between the two results as a proportion of the mass added is called the surrogate recovery or sometimes the marginal recovery. [54]

According to ISO/IEC 17043 [55] results for trueness were evaluated following eq. 12

$$E_n = \frac{\left|A_D - A_R\right|}{\sqrt{U(A_D)^2 - U(A_R)^2}} \qquad \textbf{eq. 12}$$

wherein U = u_c×k with k=2, A_R = reference activity, A_D = determined activity

with an criterion of acceptance of $E_n \leq 1$ [55].

2.4.5 Precision

Precision is the closeness of agreement between independent test results obtained under stipulated conditions. Precision depends only on the distribution of random errors and does not relate to the true value or specified value. The measure of precision is usually expressed in terms of imprecision and computed as a standard deviation of the test results. [53]

For single-laboratory validation, two sets of conditions are relevant:

1. precision under repeatability conditions, describing variations observed during a single run as expectation 0 and standard deviation s_b

$$s_b = \sqrt{\frac{\sum(\overline{x_j} - \bar{x})^2}{n-1}} \qquad \textbf{eq. 13}$$

where $\bar{x}_j$ is the mean of a daily run, $\bar{x}$ is the mean

of all runs and n is the number of runs

2. and precision under run-to-run conditions, describing variations in run bias as expectation 0 and standard deviation s_w.

$$s_w = \sqrt{\frac{\sum s_j^2}{n}} \qquad \textbf{eq. 14}$$

where s_j is the standard deviation of a daily run

Usually, both of these sources of error are operating on individual analytical results, which therefore have a combined precision s_t

$$s_t = \sqrt{s_w^2 + s_b^2} \qquad \textbf{eq. 15}$$

The two precision estimates can be obtained most simply by analyzing the selected test material (a spiked sample or preferably a CRM) in duplicate in a number of successive runs [54].

For environmental analyses combined precision $s_t \leq 15\%$ is choosen as criterion of acceptance [56]

2.4.6 Recovery

Recovery is the fraction of analyte added to a test sample (fortified or spiked sample) prior to analysis, the unfortified and fortified samples, percentage recovery (%R) is calculated as follows:

$$\%R = \frac{c_f - c_u}{c_a} \cdot 100 \qquad \textbf{eq. 16}$$

Where c_f is the concentration of analyte measured in the fortified sample; c_u is the concentration of analyte measured in the unfortified sample; c_a is the concentration of analyte added (measured value, not determined by method) in fortified sample. [53]Recovery are often discussed in conjunction with trueness [54].

Recovery was evaluated by calculating t – values (eq. 37).

2.4.7 Limit of detection (LOD)

The limit of detection of an individual analytical procedure is the lowest amount of an analyte in a sample which can be detected but not necessarily quantified as an exact value.

The limit of detection, expressed as a concentration c_{LOD} or a quantity q_{LOD}, is derived from the smallest signal x_{LOD} which can be detected with reasonable certainty for a given analytical procedure. The value of x_{LOD} is given by the equation:

$$x_{LOD} = \bar{x}_b + k \cdot s_b \qquad \textbf{eq. 17}$$

where $\bar{x}_b$ is the mean of the blank measurements, s_b is the standard deviation of the blank measurements, and k is a numerical factor chosen according to the level of confidence required.

For many purposes, the limit of detection is taken to be 3 x s_b or 3 x signal to noise ratio [57].

Since nuclear decay is following poisson statistics, in case of beta-spectrometry LOD is calculated by [58]

$$LOD = \left(k_{1-\alpha} + k_{1-\beta}\right) \cdot \sqrt{N_0 \cdot \left(\frac{1}{t_0} + \frac{1}{t_m}\right)} + \frac{1}{4}\left(k_{1-\alpha} + k_{1-\beta}\right)^2 \cdot \left(\frac{1}{t_0} + \frac{1}{t_m}\right)$$ **eq. 18**

where $k_{1-\alpha}$ and $k_{1-\beta}$ = quintiles of the normal distribution, N_0 = background count rate, t_0 = background counting time and t_m = sample counting time

2.4.8 Limit of quantification (LOQ)

The limit of quantification of an individual analytical procedure is the lowest amount of an analyte in a sample which can be determined as an exact value.

The limit of quantification, expressed as a concentration c_{LOQ} or a quantity q_{LOQ}, is derived from the smallest signal x_{LOQ} which can be determined with reasonable certainty for a given analytical procedure.

The value of x_{LOQ} is given by the eq. 17, where the factor *k* is chosen to be 9.[57]

For ß-spectrometry calculation of LOQ is not reported in literature.

2.4.9 Sensitivity

Sensitivity is the change in the response of a measuring instrument divided by the corresponding change in the stimulus [57]. Stimulus may for example be the amount of the measurand present. Sensitivity may depend on the value of the stimulus. Although this definition is clearly applied to a measuring instrument [53].

However, the sensitivity of an analytical method is equal to the slope of the calibration graph [57].

2.4.10 Robustness

The robustness of an analytical procedure is a measure of its capacity to remain unaffected by small, but deliberate variations in method parameters and provides an indication of its reliability during normal usage [53].

Examples of the factors that a robustness test could address are: changes in the instrument, operator, or brand of reagent, concentration of a reagent, pH of a solution, temperature of a reaction, time allowed for completion of a process, etc [54]

2.4.11 Matrix variation

Matrix variation is, in many sectors, one of the most important but least acknowledged sources of error in analytical measurements.

Matrix variation uncertainties need to be quantified separately, because they are not taken into account elsewhere in the process of validation. The information is acquired by collecting a representative set of the matrices likely to be encountered within the defined class, all with analyte concentrations in the appropriate range. The materials are analyzed according to the protocol, and the bias in the results estimated. Unless the test materials are CRMs, the bias estimate will usually have to be undertaken by means of spiking and recovery estimation. The uncertainty is estimated by the standard deviation of the biases. [54]

2.4.12 Fitness for purpose

Fitness for purpose is the extent to which the performance of a method matches the criteria, agreed between the analyst and the end-user of the analysis report, that describe the end-user's needs [54].

2.4.13 Measurement uncertainty

Measurement uncertainty combines all parameters, associated with the result of a measurement, which characterizes the dispersion of the values that could reasonably be attributed to the measurand.

Uncertainty sets the limits within which a result is regarded accurate, i.e. precise and true.

Uncertainty of measurement comprises, in general, many components. Some of these components may be evaluated from the statistical distribution of the results of series of measurements and can be characterized by experimental standard deviations. The other components, which can also be characterized by standard deviations, are evaluated from assumed probability distributions based on experience or other information. [59]

According to Eurachem Guide [60] the process for the estimation of measurement uncertainties is the following:

1. Specify the measurand, e.g. analyte concentration or activity
2. Identify uncertainty sources, e.g. sampling, instrument effects, uncertainty for CRM, data processing etc.
3. Quantify uncertainty sources by measuring or estimating the size of the uncertainty component associated with each potential source of uncertainty identified.
4. Calculate combined uncertainty

2.4.13.1 Calculation of uncertainties

Before combination, all uncertainty contributions must be expressed as standard uncertainties, that is, as standard deviations. There are rules for converting an uncertainty component to a standard deviation:

Rule 1 Where the uncertainty component was evaluated experimentally from the dispersion of repeated measurements, it can readily be expressed as a standard deviation

$$s = \sqrt{\frac{\sum_{i=1}^{n}(x_i - \bar{x})^2}{n-1}} \qquad \textbf{eq. 19}$$

The relative standard deviation RSD is given by

$$RSD = \frac{s}{\bar{x}} \qquad \textbf{eq. 20}$$

For results subjected to averaging, the standard deviation of the mean is used

$$s_{\bar{x}} = \frac{s}{\sqrt{n}} \qquad \textbf{eq. 21}$$

Rule 2 where a confidence interval is given with a level of confidence (in the form ±*a* at *p*%) then divide the value *a* by the appropriate percentage point of the Normal distribution for the level of confidence given to calculate the standard deviation.

Rule 3 If limits of ±*a* are given without a confidence level and there is reason to expect that extreme values are likely, it is normally appropriate to assume a rectangular distribution, with a standard deviation of $a/\sqrt{3}$

Rule 4 If limits of ±*a* are given without a confidence level, but there is reason to expect that extreme values are unlikely, it is normally appropriate to assume a triangular distribution, with a standard deviation of $a/\sqrt{6}$. [60]

2.4.13.2 Calculation of combined uncertainty

The general relationship between the combined standard uncertainty $u_c(y)$ of a value y and the uncertainty of the independent parameters $x_1, x_2, \ldots x_n$ on which it depends is

$$u_c\big(y(x_1, x_2, \ldots)\big) = \sqrt{\sum_{i=1,n} c_i^2\, u(x_i)^2} \qquad \textbf{eq. 22}$$

where $y(x_1,x_2,..)$ is a function of several parameters $x_1,x_2...$, c_i is a sensitivity coefficient evaluated as $ci=\partial y/\partial x_i$, the partial differential of y with respect to x_i.

In some cases and given uncertainties are not correlated, the expression for combining uncertainties reduces to much simpler form:

For models involving only a sum or difference of quantities, *e.g. y*=(*p*+*q*+*r*+...), the combined standard uncertainty $u_c(y)$ is given by

$$u_c\big(y(p,q,\dots)\big) = \sqrt{u(p)^2 + u(q)^2 + \dots.} \qquad \textbf{eq. 23}$$

For models involving only a product or quotient, *e.g. y=(p* × *q* × *r* ×*...)* or *y*= *p* / (*q* × *r* ×*...)*, the combined standard uncertainty $u_c(y)$ is given by

$$u_c\big(y(p,q,\dots)\big) = \sqrt{\left(\frac{u(p)}{p}\right)^2 + \left(\frac{u(q)}{q}\right)^2 + \dots.} \qquad \textbf{eq. 24}$$

where (*u*(*p*)/*p*) *etc*. are the uncertainties in the parameters, expressed as relative standard deviations. [60]

2.4.13.3 Expanded uncertainty

The final stage is to multiply the combined standard uncertainty by the chosen coverage factor in order to obtain an expanded uncertainty.

The expanded uncertainty is required to provide an interval which may be expected to encompass a large fraction of the distribution of values which could reasonably be attributed to the measurand.

For most purposes it is recommended that *k* is set to 2. [60]

$$\boldsymbol{U = k \cdot u_c} \qquad \textbf{eq. 25}$$

3 Experimental

3.1 Reagents and apparatus

All reagents used were of analytical grade, 18 MΩ deionized water was used throughout all experiments. pH values were measured using a pH meter (pHep® HANNA) and adjusted when necessary using NaOH and H_2SO_4. The FClA and F49A resin samples prepared by TrisKem International were used as received without further purification.

Ag^+ loaded FClA resin was prepared by contacting 10 g of the FClA resin with 100 mL of a 1 M H_2SO_4 solution containing 650 mg of $AgNO_3$ in a 250 mL PE flask on a vortex shaker over a period of 2 h. The resin was then filtered, rinsed with 1 M H_2SO_4 (until absence of Ag^+ in the filtrate) and dried.

2 mL PE columns with appropriate funnels (both TrisKem International) were employed for elution studies and separation tests, 2 mL Eppendorf centrifuge tubes for batch experiments. Element concentrations were determined by ICP-MS measurement using an ELAN 6000 (PerkinElmer), all samples were measured after appropriate dilution and addition of a suited internal standard. LSC measurements were performed using either a TriCarb 1600TR (Packard) or a 1220 Quantulus (PerkinElmer) and ProSafe HC (Meridian) as liquid scintillation cocktail.

The used chemicals, element standards and certified materials will be mentioned in the respective chapter.

3.2 General procedures

3.2.1 General procedure for batch experiments

Weight distribution ratios, interferences and maximum uptakes were determined in batch experiments. 50 mg of the respective resin were weighted into 2 mL centrifugation tubes and 0.3 mL of the acid for which the D_w was to be determined were added. The tubes were closed and shaken for 30 minutes in order to precondition the resin. 1 mL of a solution of a well defined pH value, containing defined amounts of selected cations, in general 1 µg per cation, was then added (A_0 sample). The tubes were again closed, shaken for 30 minutes and finally centrifuged. A 1 mL aliquot was withdrawn from the tube using a micro-pipette (A sample). The aliquot was diluted appropriately using 3% HNO_3 and measured by ICP-MS. Measurements were performed relative to the A_0 sample.

Iodide and chloride weight distribution ratios were determined using Ag^+ loaded FClA resin prepared as described before and A_0 samples containing known activities of ^{36}Cl or ^{129}I. The withdrawn aliquots were mixed with 10 mL of liquid scintillation cocktail

and measured by liquid scintillation counting (counting time t = 10 minutes) relative to A_0 samples. All D_w values were determined in triplicate.

Whenever measuring the elements by ICP-MS Rh and Ir were used as internal standard for Pd and Pt respectively, Cs was used as internal standard for Cl and I and Bi was used as internal standard for all other elements.

D_w values were calculated according to eq. 26 and maximum uptake according to eq. 27, net count rates refer to ICP-MS count rates as well as to LSC count rates:

$$D_W = \frac{(N_{A0} - N_A)}{N_A} \times \frac{V}{m_R} \qquad \textbf{eq. 26}$$

where N_{A0} = net count rate in the A_0 sample; N_A = net count rate in the A sample; V = Volume of the aqueous phase (1.3 mL) and m_R = amount of the resin in g

$$K = \frac{\left(c_{Ag,A0} \cdot V_{A0}\right) - \left(c_{Ag,A} \cdot V_A\right)}{m_R} \qquad \textbf{eq. 27}$$

where $c_{Ag,A0}$ = silver concentration in the A_0 sample, $c_{Ag,A}$ = silver concentration in the A sample, V_{A0} = volume of the A_0 sample, V_A = volume of the A sample, m_R = mass of the resin in g

3.2.2 General procedure for column experiments

Elution studies and method validation were performed in column experiments.

The columns used for these studies were prepared by soaking 0.65 g of FClA resin (in case of ^{36}Cl / ^{129}I experiments Ag^+ loaded FCIA resin) in 10 mL of appropriate acid for 2 h under shaking; the resin was subsequently transferred into an empty 2 mL column. The packed columns were then loaded with elements to be preconcentrated and separated and subsequently rinsed with appropriate rinsing and elution agents. The agents, concentrations and volumes are specified in the respective chapter.

All samples (fractions) were analyzed by ICP-MS after appropriate dilution or by LSC after adding 10ml of ProSafe HC liquid scintillation cocktail.

To consider matrix effects additionally two blank columns were prepared. The respective fractions (e.g. rinsing step) from one of the column were spiked with elements to be analyzed (A_0 samples). Appropriate fractions from the second column were used as blank samples.

3.3 Validation

Method validation was performed in both cases, for the method for preconcentration and separation of ^{36}Cl and ^{129}I as well as for the method for preconcentration and separation of Pd and Pt.

Details on the performed experiments for method validation are given in the appropriate chapters.

4 Results and discussion

4.1 Characterization of extraction chromatographic resins

4.1.1 Maximum uptake

Maximum uptakes were determined for different species of Pd and Pt and for the resins FClA and F49A. Solutions containing 5 mg/ml Pd and Pt, respectively, were used. The procedure described in section 3.2.1 was applied.

Table 1 and Table 2 summarize the results. The FClA resin shows higher capacities for all Pd species and a slightly higher capacity for tetravalent platinum. The F49A resin only shows a noticeable higher capacity for the divalent platinum.

Maximum uptake Pd@pH1 mg/g	**FClA**			**F49A**		
	Mean	**SD**	**RSD / %**	**Mean**	**SD**	**RSD / %**
$PdNO_3$	97.94	0.77	0.79	87.14	0.60	0.69
$(NH_4)_2[PdCl_4]$	63.94	0.13	0.21	49.73	1.20	2.41
$PdSO_4$	98.97	1.27	1.29	87.72	1.43	1.63

Table 1: Maximum uptake [mg Pd/g resin] for different Pd species and resins

Maximum uptake Pt@pH1 mg/g	**FClA**			**F49A**		
	Mean	**SD**	**RSD / %**	**Mean**	**SD**	**RSD / %**
$Pt(NO_3)_2$	35.81	3.52	9.82	55.36	1.95	3.53
$PtCl_4$	24.39	1.64	6.72	22.67	3.58	15.81

Table 2: Maximum uptake [mg Pt/g resin] for different Pt species and resins

4.1.2 Weight distribution ratios

Weight distribution ratios were determined in batch experiments following the procedure described in section 3.2.1.

4.1.2.1 Weight distribution ratios in HNO_3

Weight distribution ratios in HNO_3 were determined for FClA and F49A resins for the following elements: Cu(II), Ni(II), Cr(III), Zn(II), Cd(II), Pb(II), Co(II), Mn(II), U(IV), Hg(I), Pd(II), Ag(I), Tl(III), Rh(III), and Ca(II).

Both resins show selectivity for Ag(I), Pd(II), Pt(II) and Hg(I) and the F49A resin additionally for U(IV). No selectivity is observed for the remaining elements.

Fig. 36 and Fig. 37 summarize the results on weight distribution ratios in nitric acid for FClA and F49A resin respectively. For Hg, Ag, Pd and Pt a comparison between the both resins is given in Fig. 38 - Fig. 41.

Very high D_w values are observed at high HNO_3 concentrations for Ag, Pd (pH=0) and Hg (2M HNO_3). For divalent platinum a high D_w value is observed at low HNO_3 concentration (pH=5).

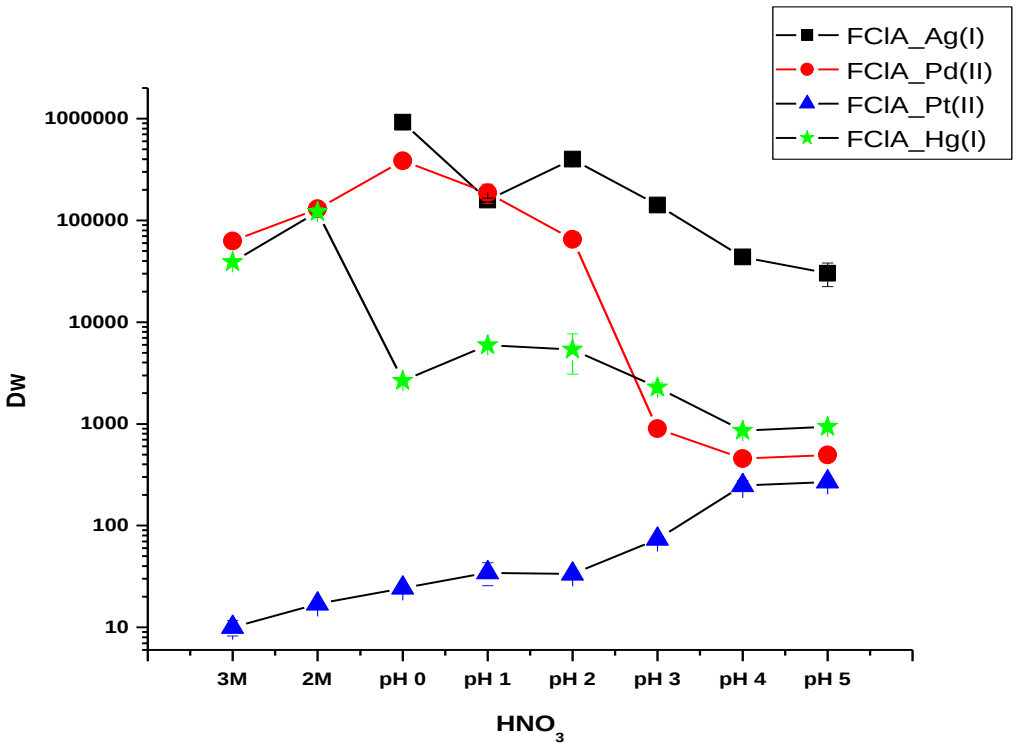

Fig. 36: FClA resin: Weight distribution ratios for Ag(I), Pd(II), Pt(II) and Hg(I) in HNO_3

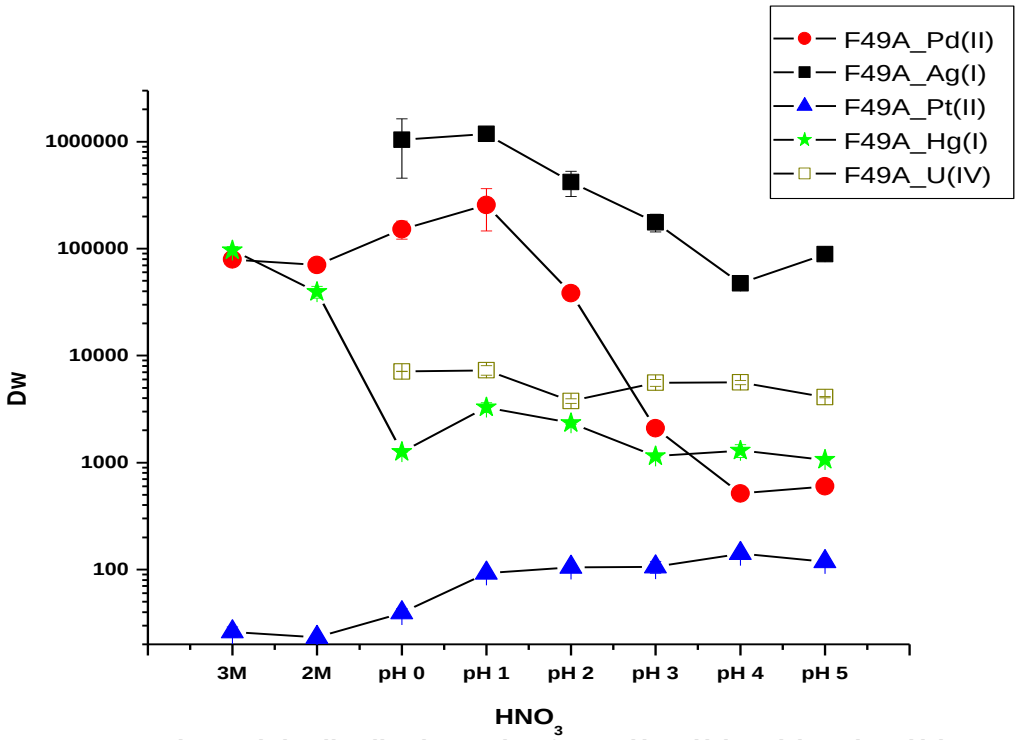

Fig. 37: F49A resin: Weight distribution ratios for Ag(I), Pd(II), Pt(II) and Hg(I) in HNO_3

For Ag and Pd none of the two resins show advantages with respect to element uptake (Fig. 39 and Fig. 40). Both resins seem to be equal with respect to the selectivity for these metals, whereas for Hg and Pt the FClA resin shows a slightly higher selectivity at considered concentrations in comparison to the F49A resin (Fig. 38 and Fig. 41).

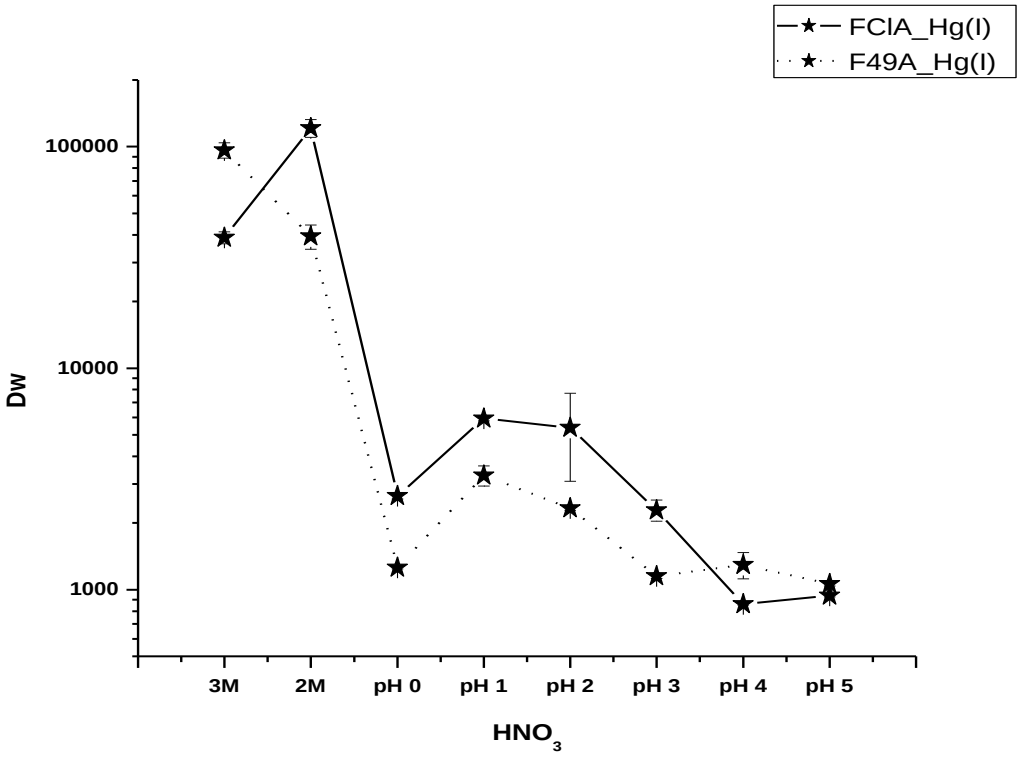

Fig. 38 Hg(I) in HNO_3: Comparison of the weight distribution ratios between the two resins

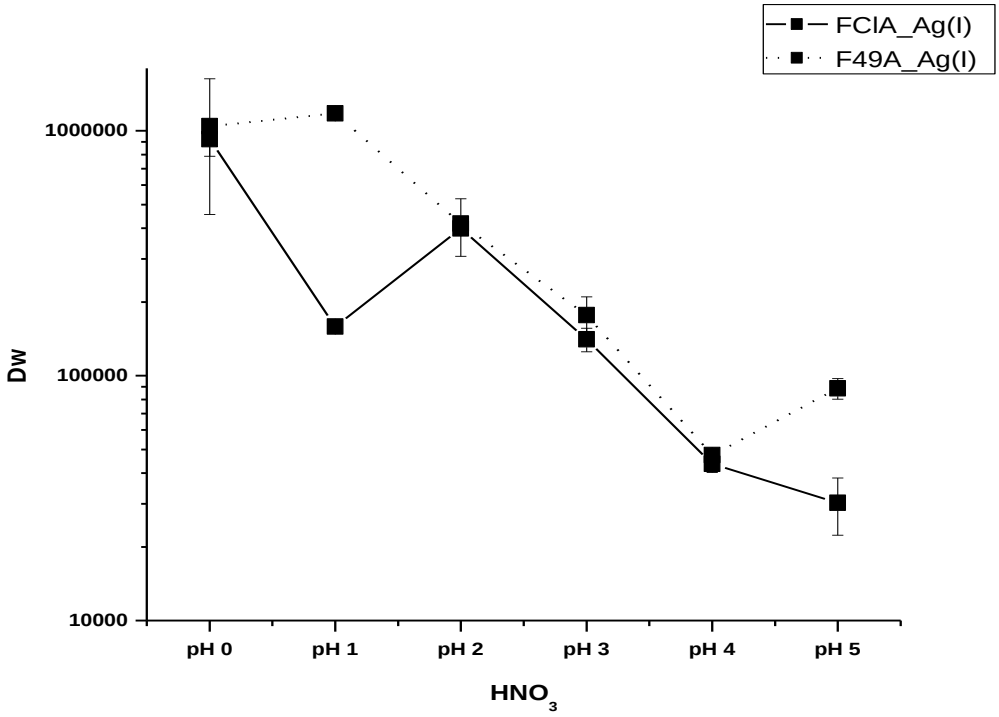

Fig. 39 Ag(I) in HNO_3: Comparison of the weight distribution ratios between the two resins

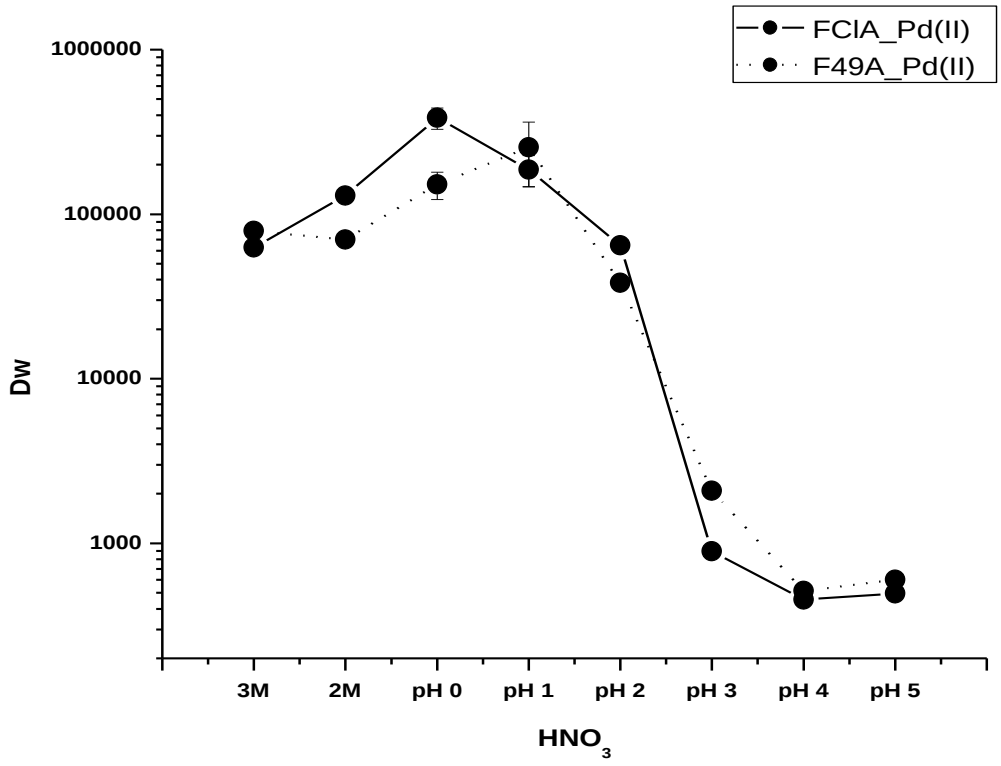

Fig. 40 Pd(II) in HNO_3: Comparison of the weight distribution ratios between the two resins

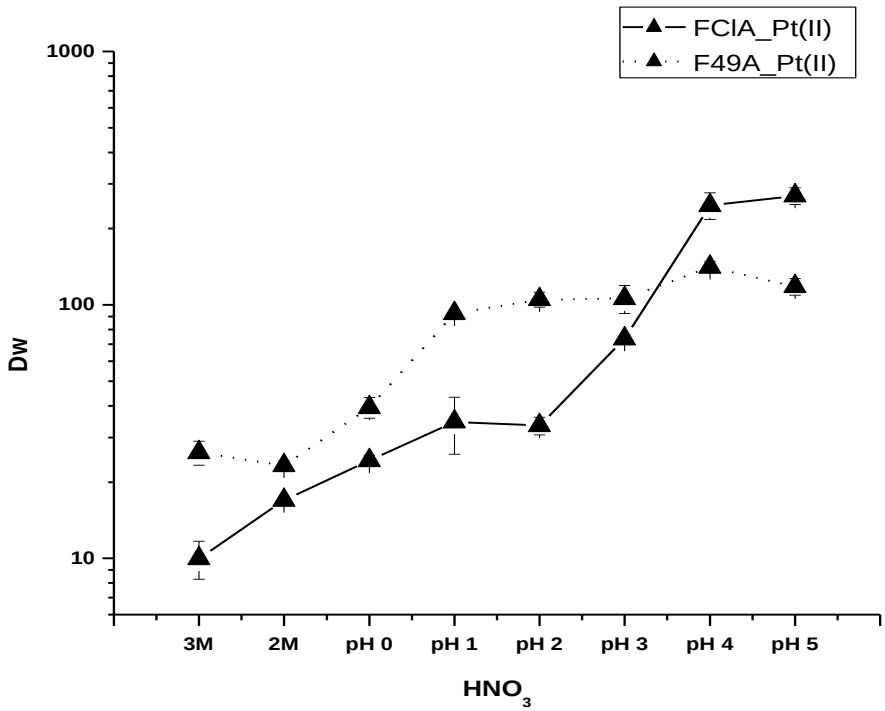

Fig. 41 Pt(II) in HNO_3: Comparison of the weight distribution ratios between the two resins

4.1.2.2 Weight distribution ratios in HCl

Weight distribution ratios in HCl were determined for FClA and F49A resins for the following elements: Cu(II), Co(II), Ni(II), Y(III), Cr(III), Sm(III), Zn(II), Fe(III), V(III), Eu(III), Cd(II), Yb(III), Tb(III), La(III), Ce(III), Ir(III), Ru(III), Hg(II), Ca(II), Pt(IV), Au(III)

Both resins show selectivity for Au(III), Pt(IV), Pd(II) and Hg(II) and the F49A resin additionally for V(III), Zn(II) and Y(III). There is no selectivity observed for the remaining elements.

Fig. 42 and Fig. 43 summarize graphically the results on weight distribution ratios for the FClA and F49A resin in hydrochloric acid. For Pt, Au, Hg and Pd a comparison between the both resins is given in Fig. 44 - Fig. 47.

For F49A resin very high D_w values are observed at high HCl concentrations for Pd, Pt, Zn (pH=0) and Au (pH=1). A selectivity for Hg, V and Y is observed at low HCl concentrations (pH=3-5).

A similar result was obtained for the FClA resin. Very high D_w values are observed at high HCl concentrations for Pd, Au (pH=1) and Pt (pH=2). For Hg a selectivity is only observed at a low HCl concentration (pH=5).

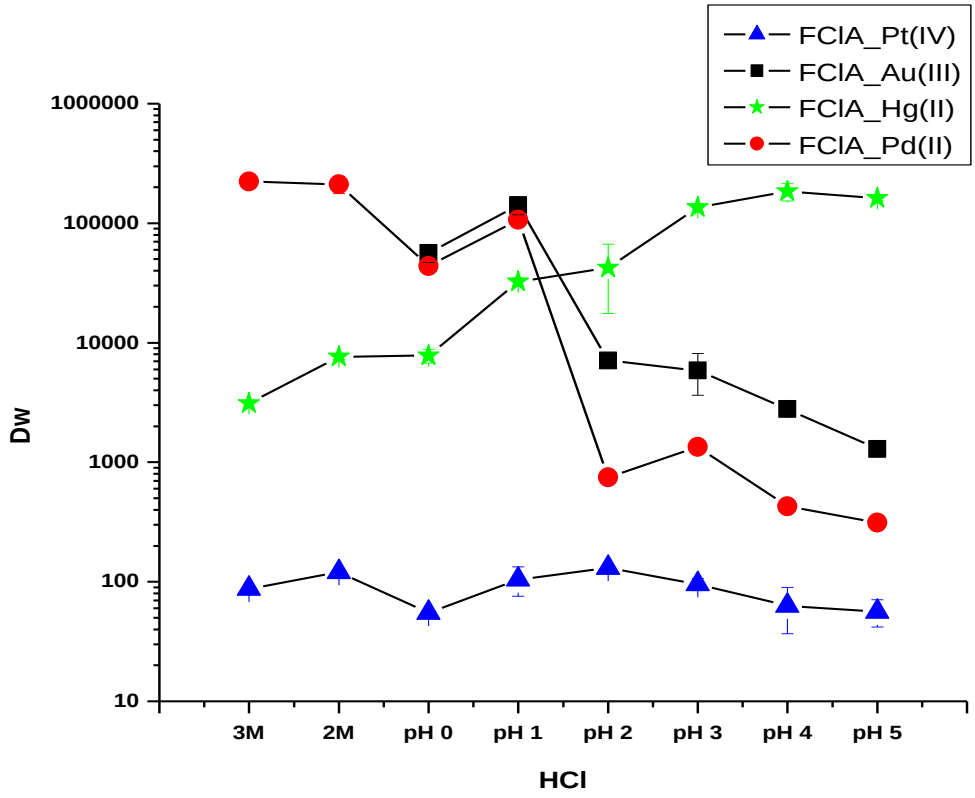

Fig. 42: FClA resin: Weight distribution ratios for Au(III), Pt(IV), Pd(II) and Hg(II) in HCl

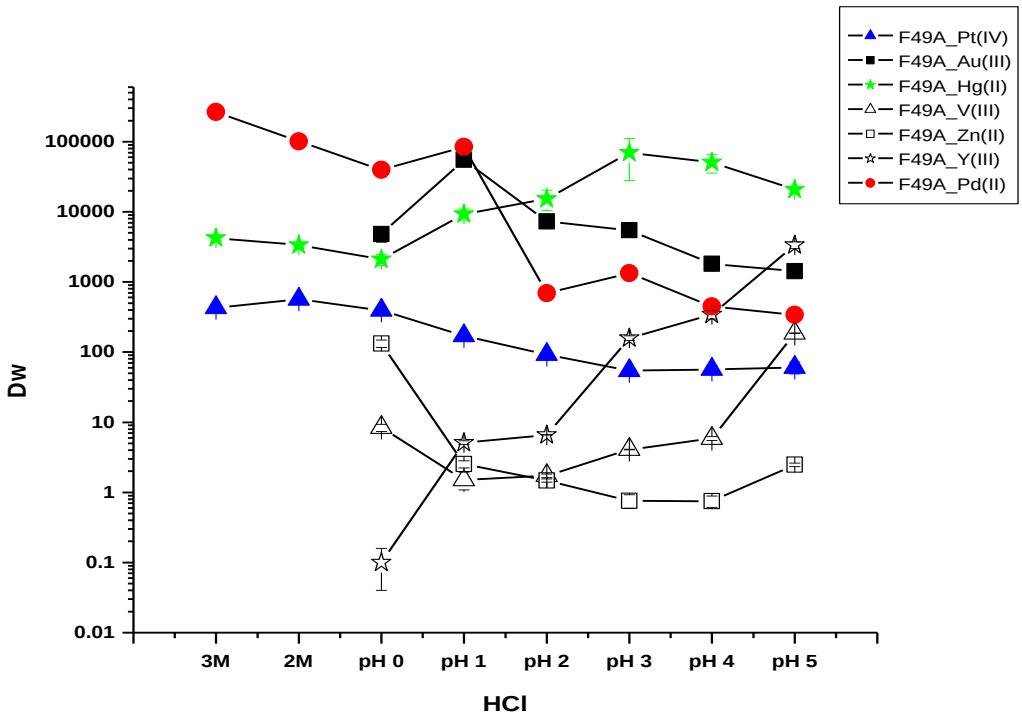

Fig. 43: F49A resin: Weight distribution ratios for Au(III), Pt(IV), Pd(II), V(III), Zn(II), Y(III) and Hg(II) in HCl

When comparing both resins for selected elements (Fig. 44 - Fig. 47) one comes to the conclusion that for Pd there is no difference between the resins, for Hg and Au FClA resin has slightly better properties than F49A resin, and that F49A resin has a higher selectivity for Pt at a pH value lower 0 and additionally shows selectivity for V, Zn and Y.

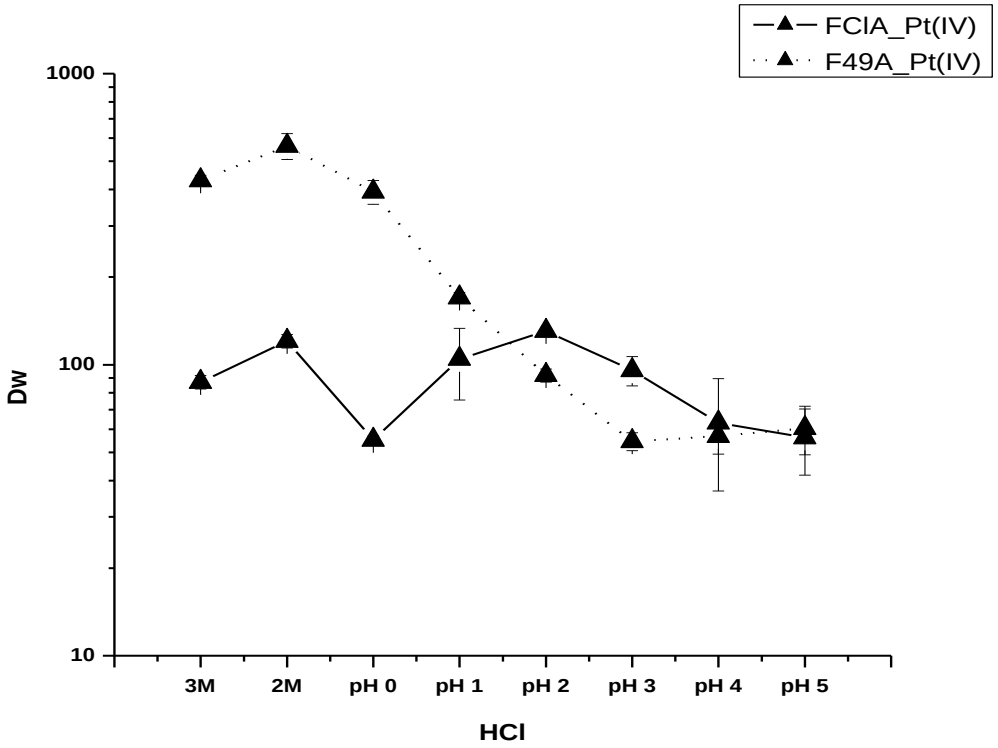

Fig. 44: Pt(IV) in HCl: Comparison of the weight distribution ratios between the two resins

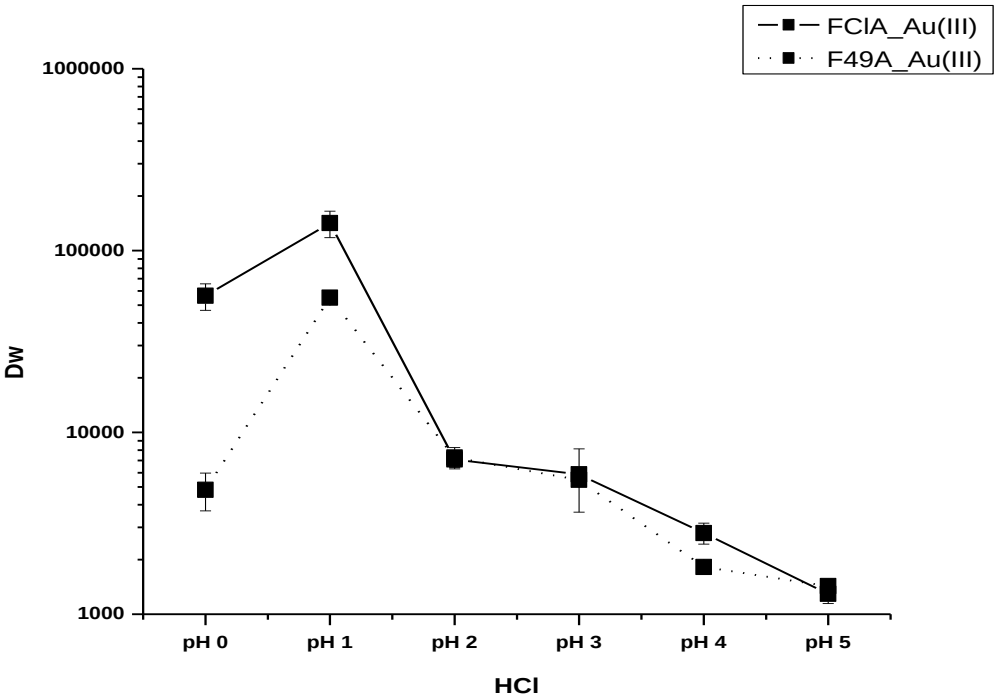

Fig. 45: Au(III) in HCl: Comparison of the weight distribution ratios between the two resins

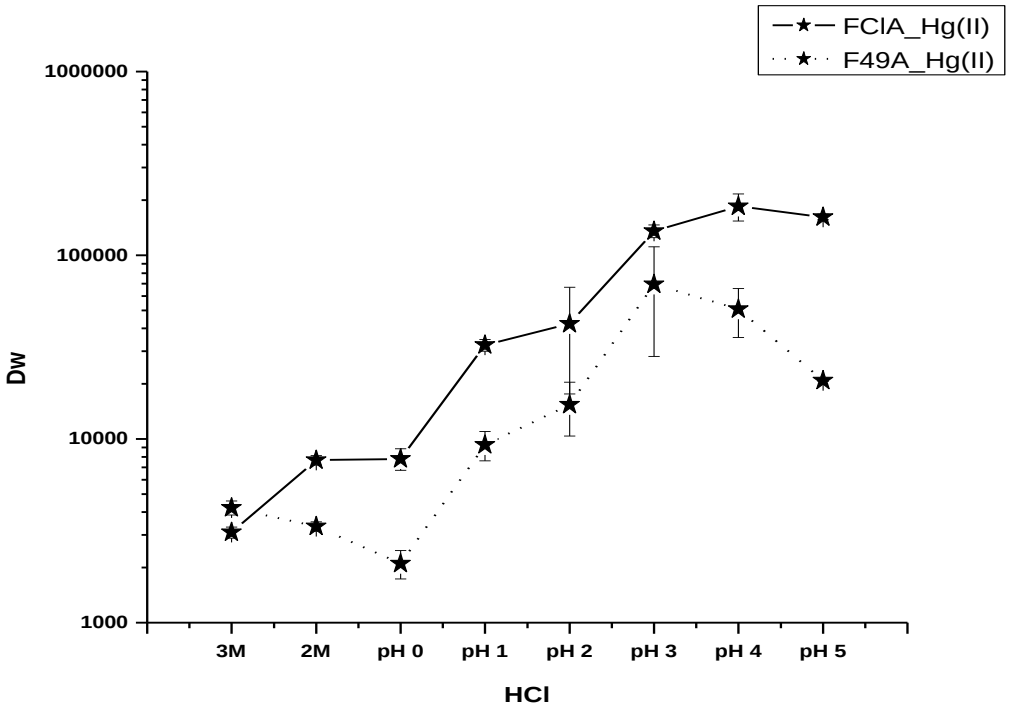

Fig. 46: Hg(II) in HCl: Comparison of the weight distribution ratios between the two resins

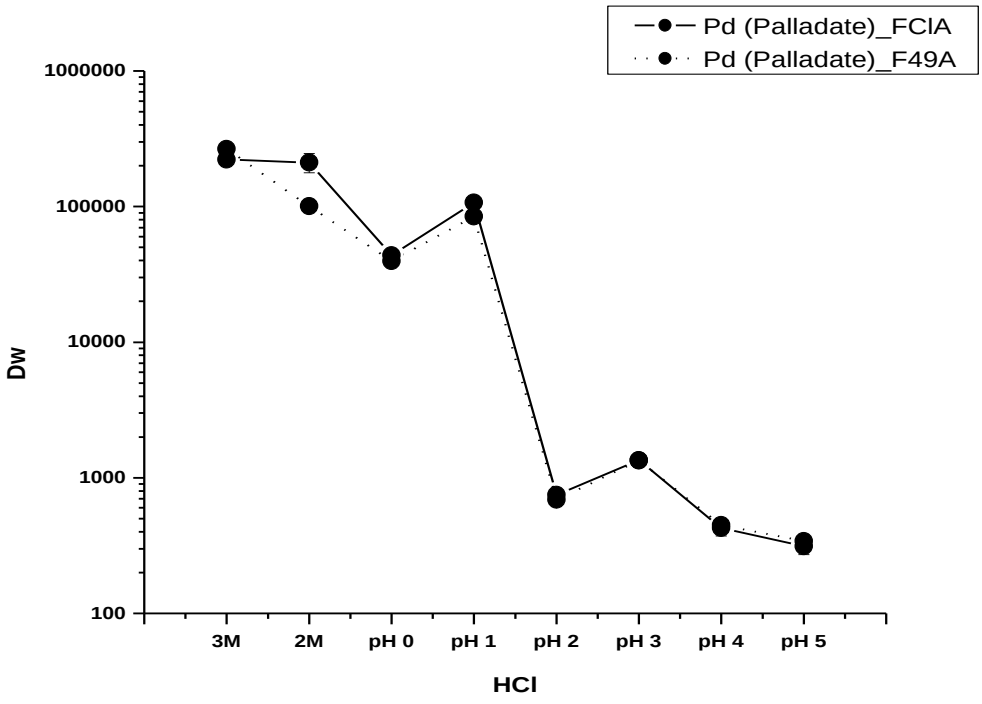

Fig. 47: Pd(II) in HCl: Comparison of the weight distribution ratios between the two resins

4.1.2.3 Weight distribution ratios in H_2SO_4

Weight distribution ratios in H_2SO_4 were determined for FClA and F49A resins for the following elements: Co(II), Cu(II), Ni(II), Zn(II), Fe(III), Cd(II), Mn(II), Ce(III) and Pd(II)

Both resins exhibit selectivity in sulfuric acid only for Pd, with F49A resin generally obtaining higher Dw values than FClA resin (Fig. 48). For all other elements analyzed no selectivity was observed (D_W < 10).

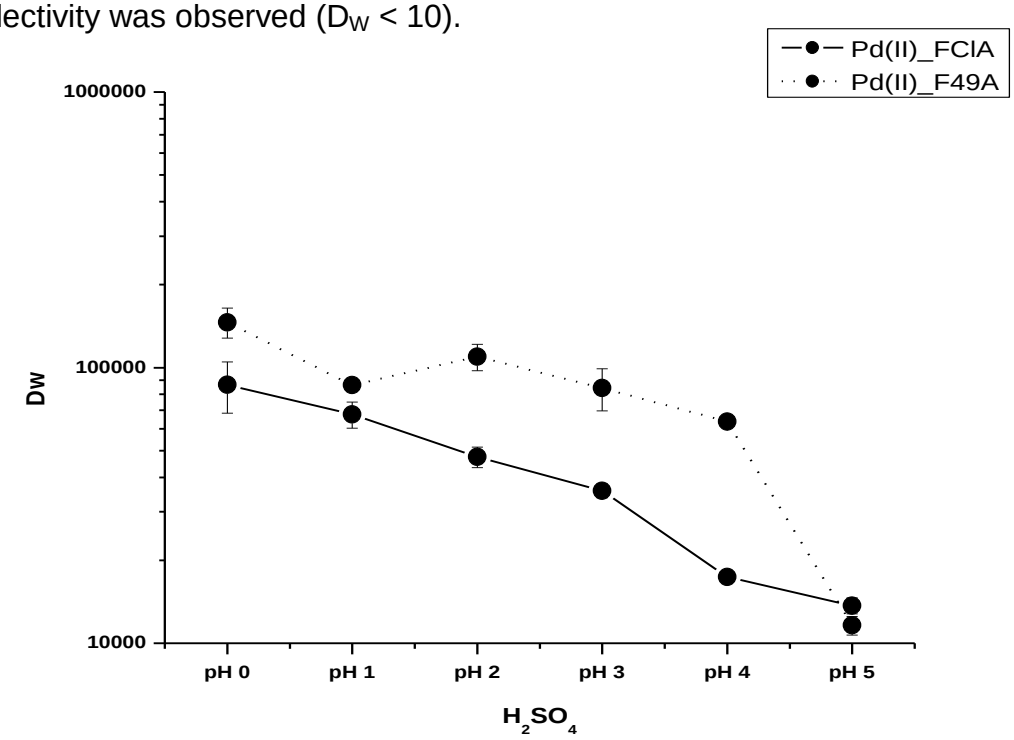

Fig. 48: Pd(II) in H_2SO_4: Comparison of the weight distribution ratios of the two resins

4.1.2.4 Comparison of weight distribution ratios depending on oxidation state

When comparing Pt(II) with Pt(IV) and Hg(I) with Hg(II) one can see that there is a higher selectivity for Hg(II) on both resins (Fig. 51 and Fig. 52) whereas the FClA resin is more suitable for Pt(II) and the F49A resin for Pt(IV) (Fig. 49 and Fig. 50).

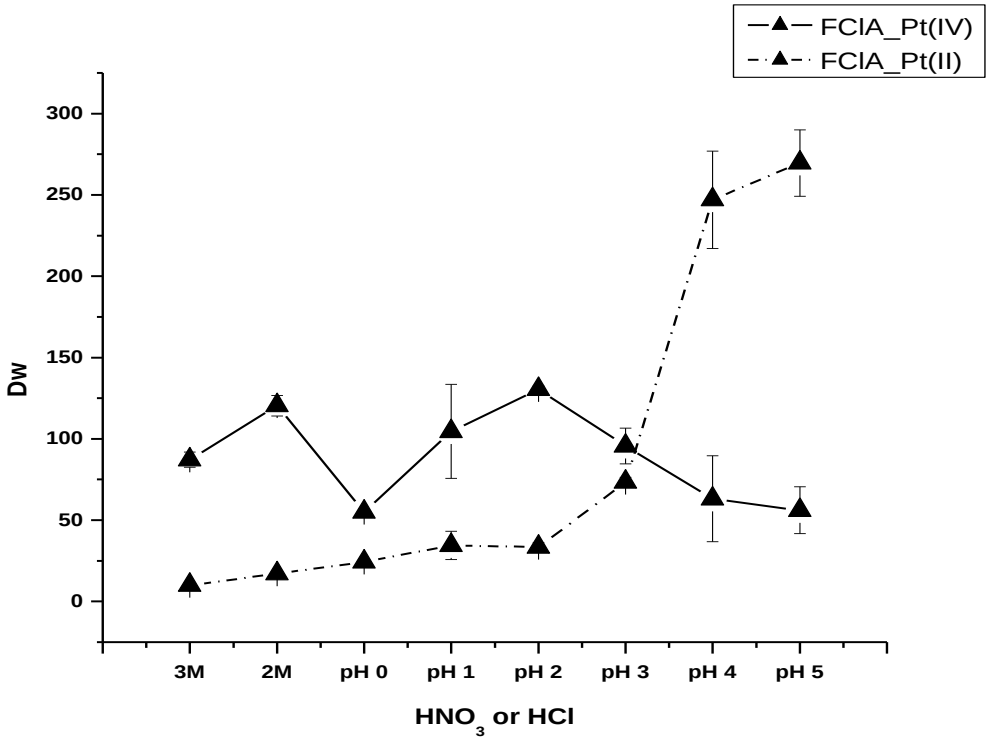

Fig. 49: Comparison of D_w-values for Pt(II) and Pt(IV) for FClA resin

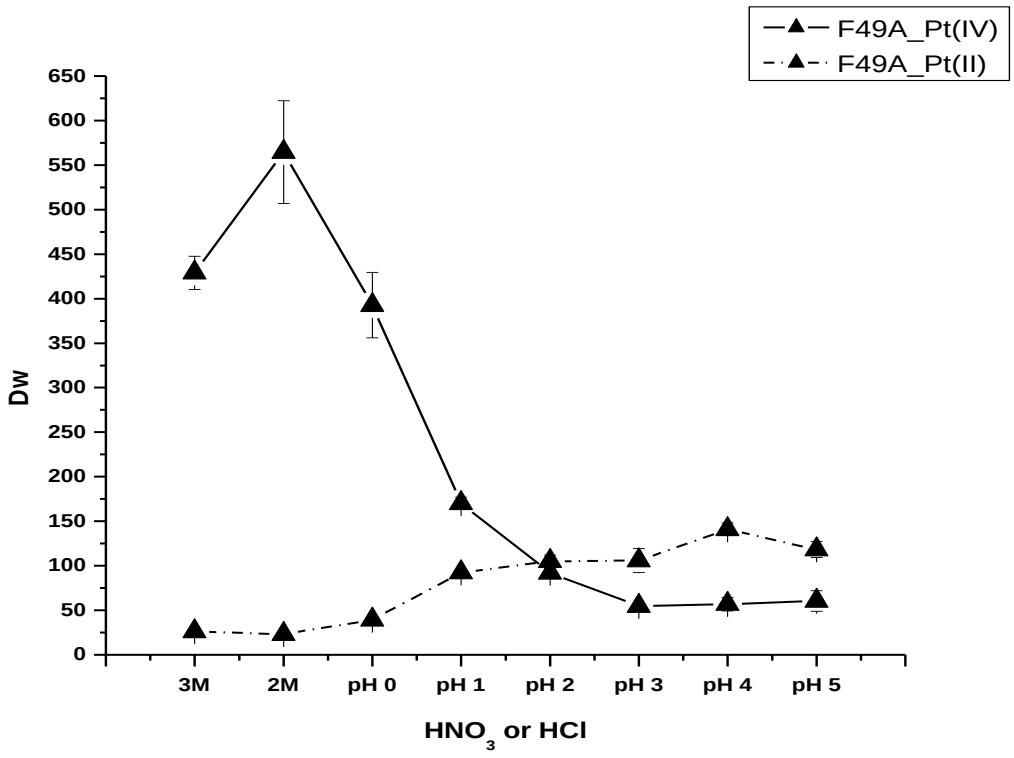

Fig. 50: Comparison of Dw-values for Pt(II) and Pt(IV) for F49A resin

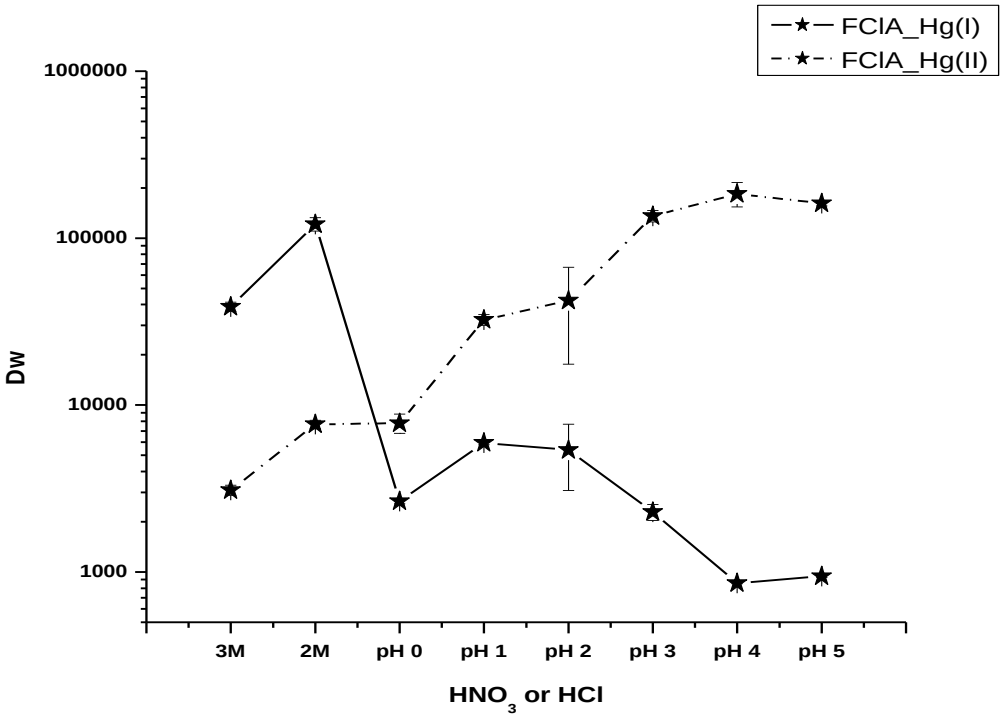

Fig. 51: Comparison of Dw-values for Hg(I) and Hg(II) for FClA resin

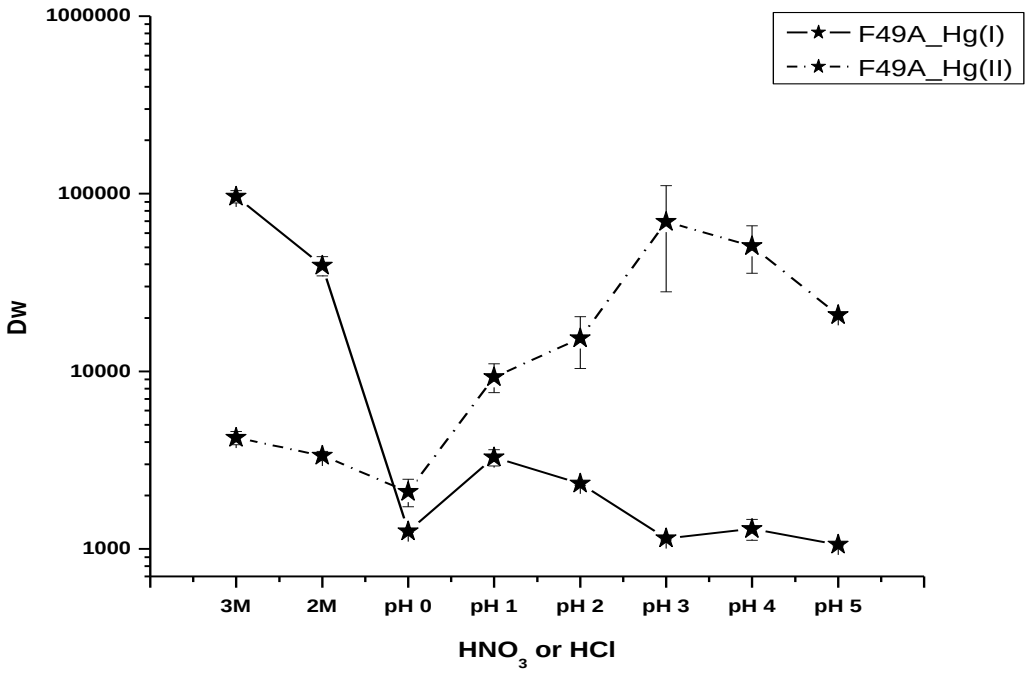

Fig. 52: Comparison of Dw-values for Hg(I) and Hg(II) for F49A resin

Summing up the results of the studies for weight distribution ratios with a view to Pd and Pt separation, best conditions seem to be using FClA resin and loading the elements from 3M HNO_3. Pt is then expected to be eluted during the loading and Pd is expected to be retained on the resin (Fig. 53).

However, before testing and optimizing the procedure in column experiments further studies were performed concerning some potential interferences and evaluating the conditions for eluting Pd from the resin.

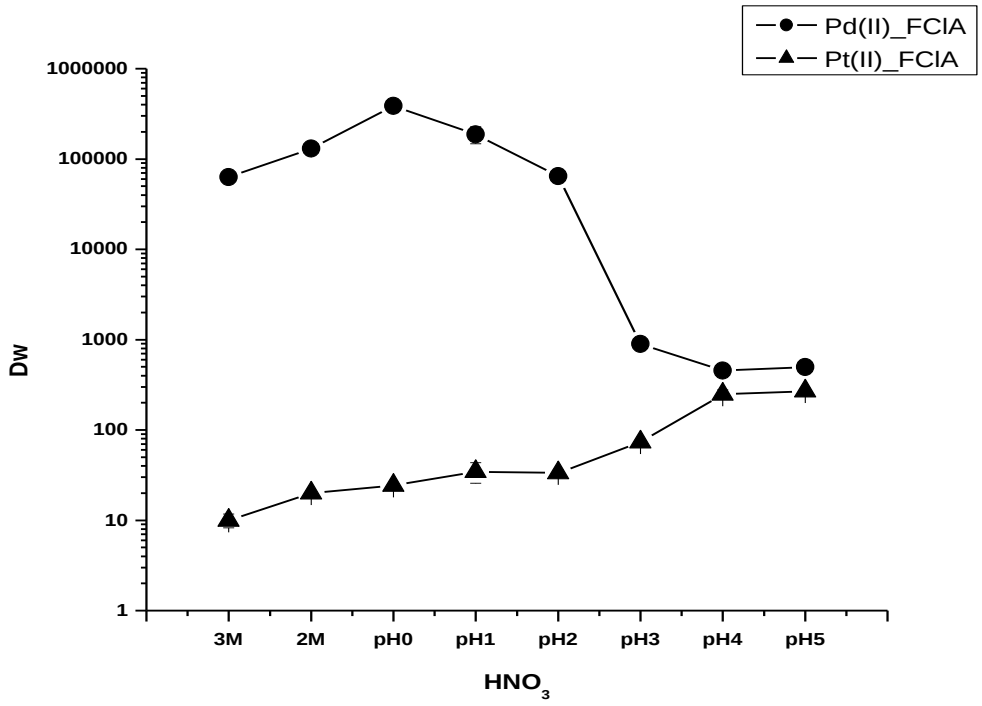

Fig. 53: Comparison of D_w values for Pd and Pt in HNO_3

4.1.2.5 Interferences

Cationic (Fig. 54 - Fig. 59) and ionic (Fig. 60 - Fig. 65) interferences were determined in batch experiments (procedure 3.2.1). D_w-values were calculated by eq. 26. The influence of the interferences was only determined for Pd since it is assumed that Pt will be eluted during loading, hence effects from interfering elements on Pt uptake are not of interest. However interferences for Pd are of a higher significance because interferences often lead to a lower uptake.

4.1.2.5.1 Cationic interferences

Cationic interferences were determined in 1M HNO_3 (Fig. 54 and Fig. 55), 1M HCl (Fig. 56 and Fig. 57) and 1M H_2SO_4 (Fig. 58 and Fig. 59). Sodium, calcium, manganese, ammonium and iron were chosen as interfering elements. A concentration range of 0.01 – 1M was examined. The results of the interference studies can be summarized as follows: For both resins, and in all acids, only iron shows significant interferences at very elevated concentrations, it is reducing the D_W value by several orders of magnitude. However, D_W values are still higher than 100 which is sufficient for quantitative uptake. Nevertheless, in case very high iron concentrations are expected in the sample, it is advisable to perform an appropriate sample treatment (e.g. reduction).

The effect of all other elements was found to be negligible.

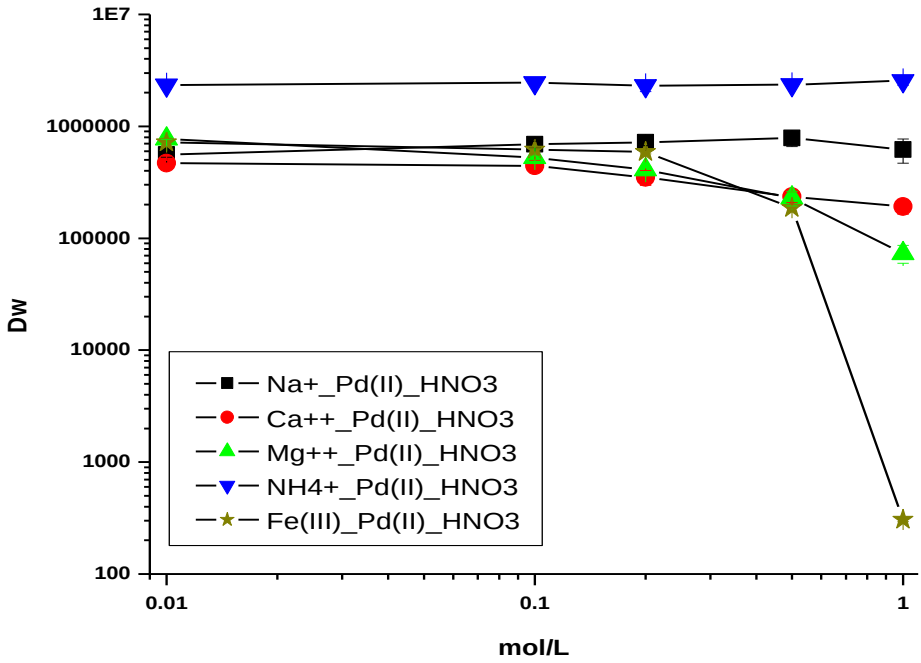

Fig. 54: Cationic interferences for Pd(II) and FCIA resin in nitric acid

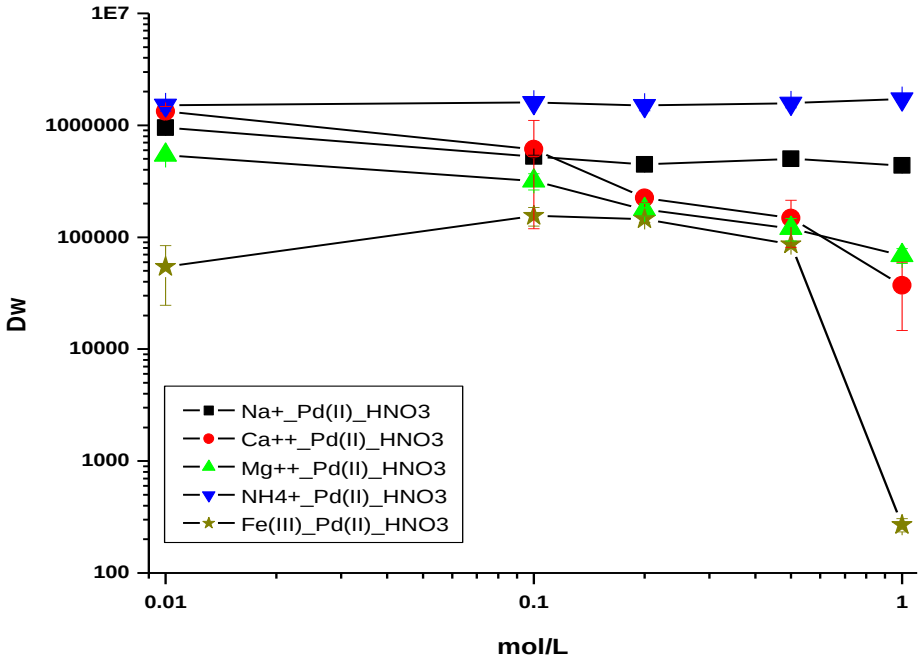

Fig. 55: Cationic interferences for Pd(II) and F49A resin in nitric acid

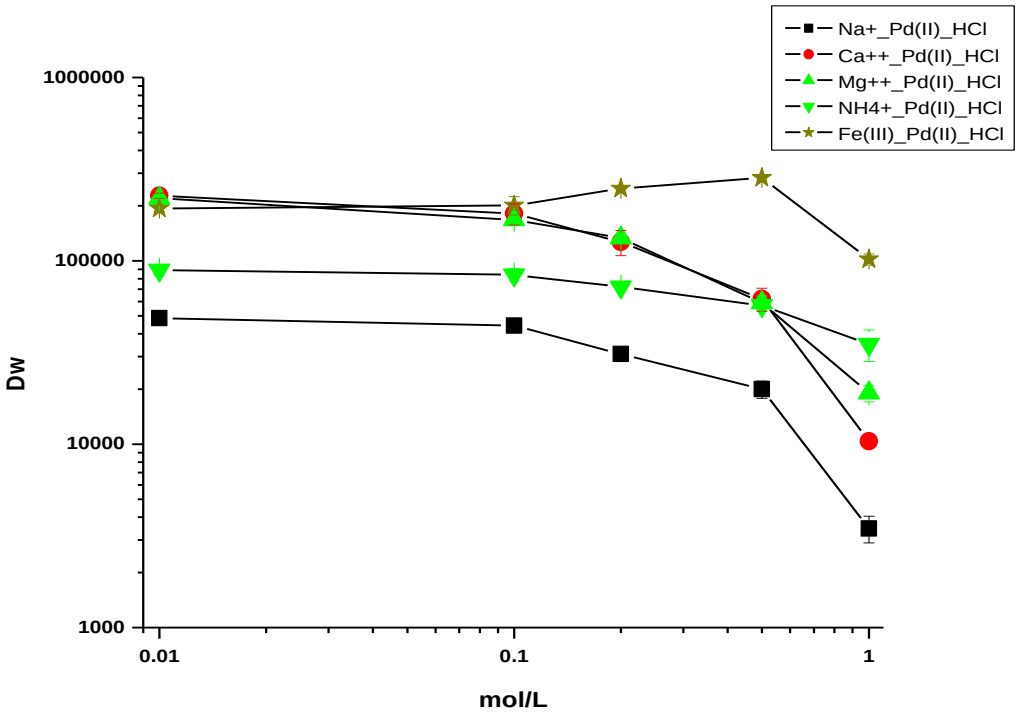

Fig. 56: Cationic Interferences for Pd(II) and FCIA resin in hydrochloric acid

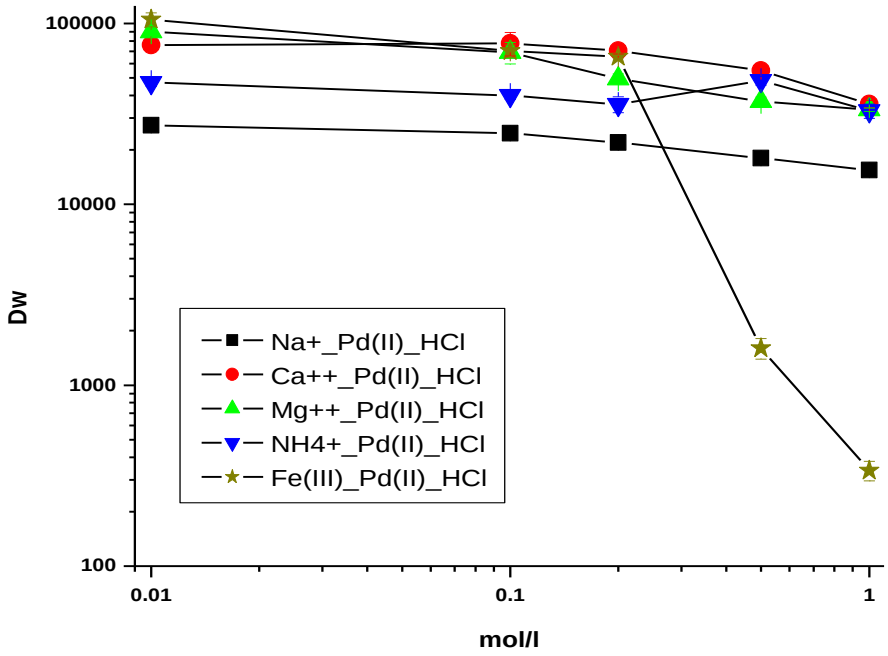

Fig. 57: Cationic interferences for Pd(II) and F49A resin in hydrochloric acid

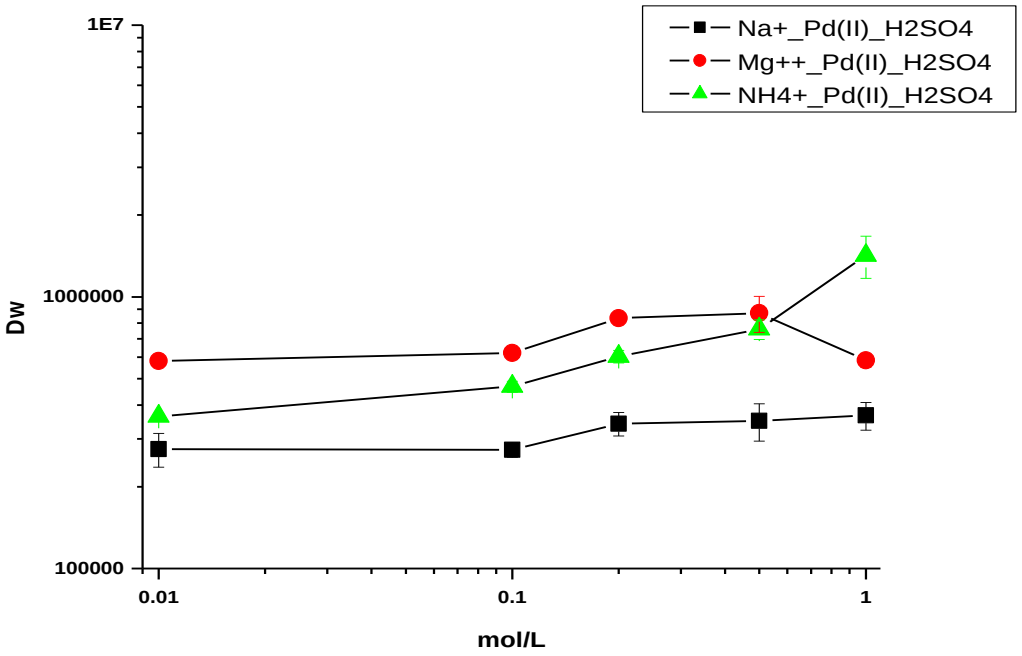

Fig. 58: Cationic interferences on Pd and FClA resin in sulphuric acid

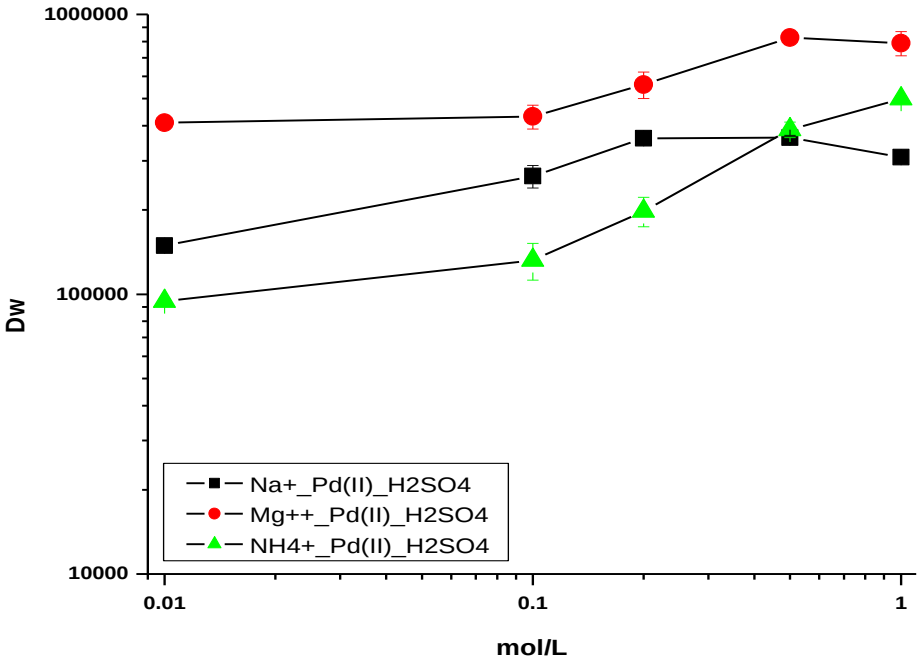

Fig. 59: Cationic interferences on Pd and F49A resin in sulphuric acid

4.1.2.5.2 Anionic interferences

The influence of anionic interferences was determined for Pd and Pt in their chloride, nitrate and sulfate forms. Ammonium oxalate and disodium phosphate in a concentration range of 0.01 – 1M were used as interfering agents. Fig. 60 and Fig. 62 show the results for oxalic interferences, Fig. 61 and Fig. 63 those for disodium phosphate.

The results of this study show strong interfering effects of oxalate and phosphate. For elevated oxalate and phosphate concentrations D_W values decrease below 10. That means on one hand that sample containing high oxalate and phosphate concentrations should be appropriately treated before loading on the resin (oxidative extraction of oxalate, addition of Al(III) in order to complex free phosphates). On the other hand both anions seem to be suitable to facilitate Pd elution.

However the results of this study are not that surprising since both anions are known to be strong complexing agents. As described in the theoretical part competing mechanism are involved in extraction chromatography. Phosphate as well as oxalate seems to have a stronger association for Pd than the extractant on the resin does.

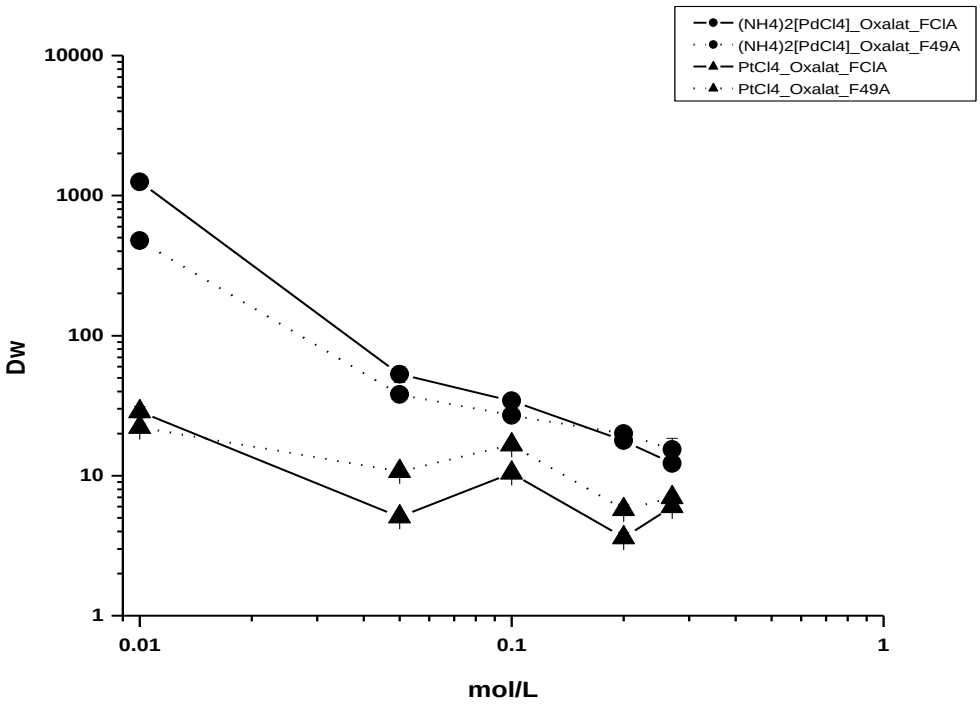

Fig. 60: Oxalic interferences for Pd and Pt in their chloride form for FClA and F49A resins

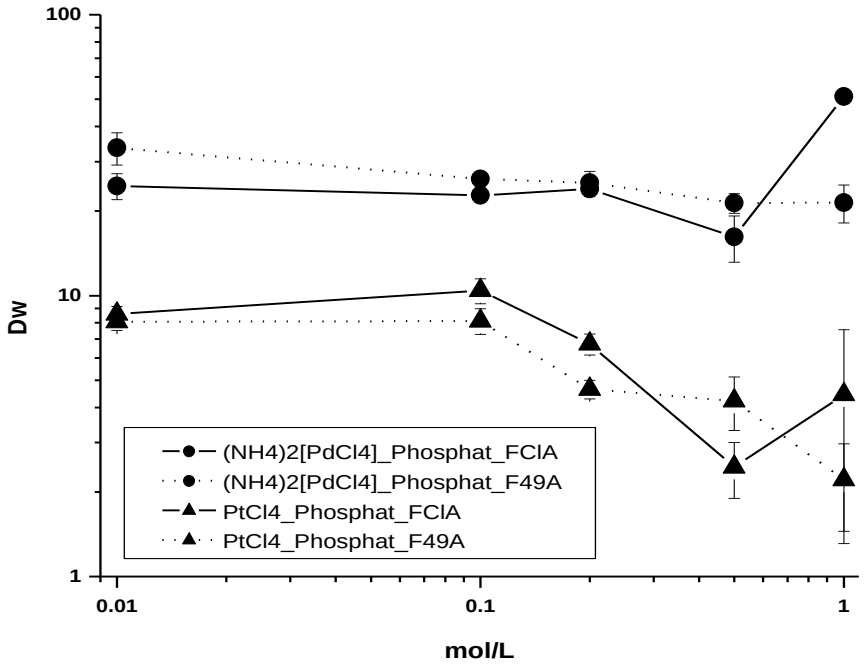

Fig. 61: Phosphatic interferences for Pd and Pt in their chloride form for FClA and F49A resins

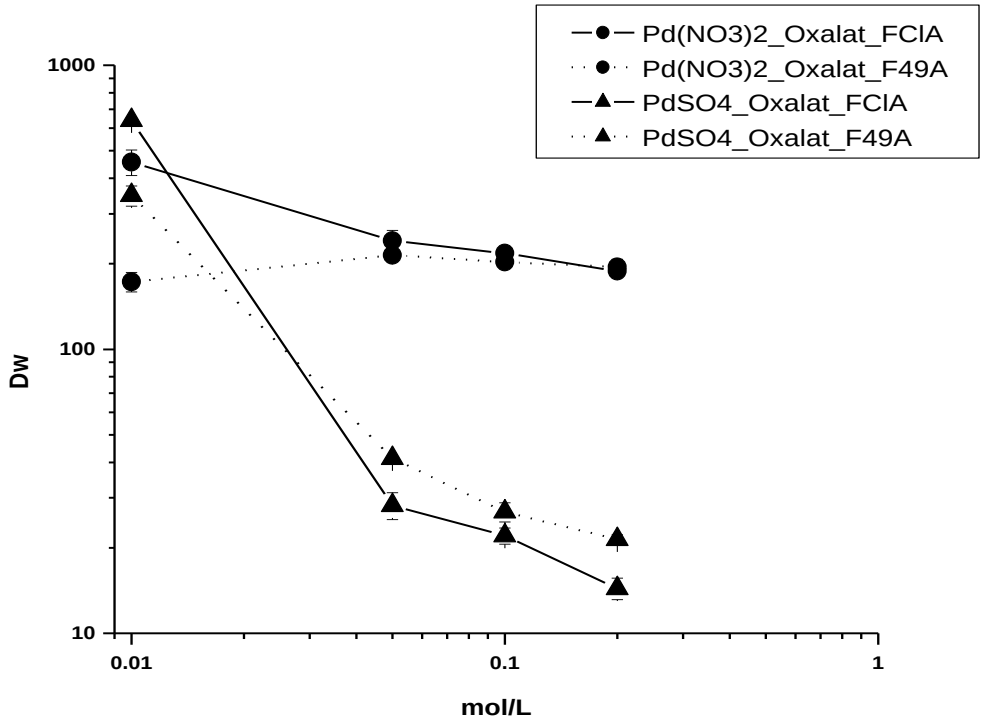

Fig. 62: Oxalic interferences for Pd in its nitrate and sulfate form for FClA and F49A resins

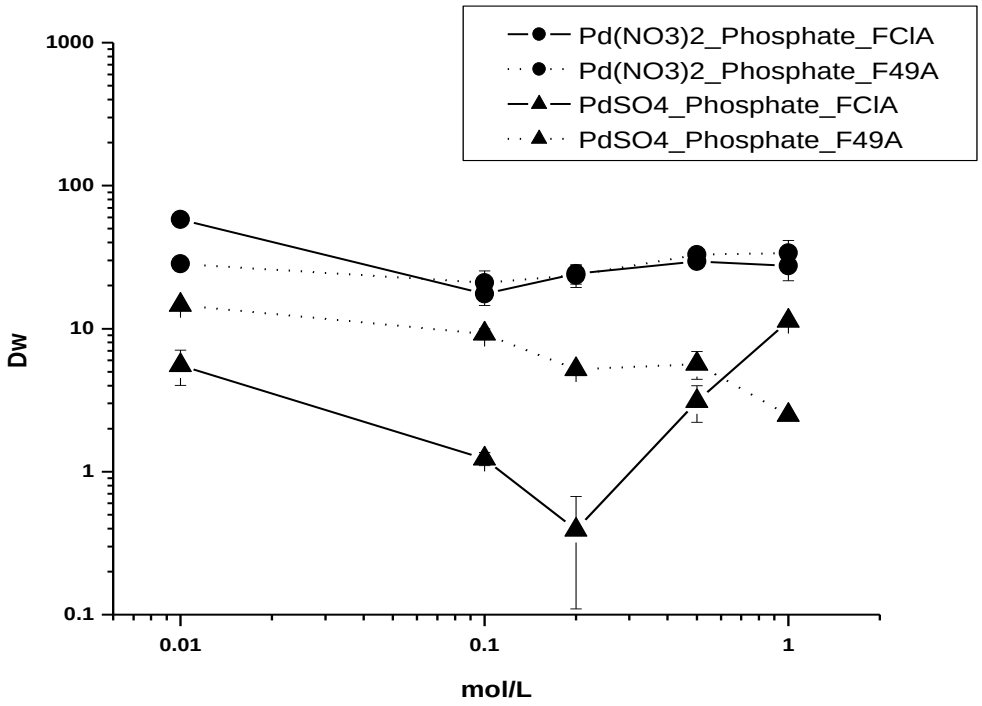

Fig. 63: Phosphatic interferences for Pd in its nitrate and sulfate form for FCIA and F49A resins

4.1.2.6 Evaluation of elution conditions for Pd

As can be seen from the anionic interference study, phosphates and oxalates interfere strongly with Pd retention, especially phosphate seems to be well suited for eluting Pd from the stationary phase.

Additionally it is reported [61] that ammonia also has high potential for Pd elution.

Hence, a study was performed to evaluate ammonia as eluting agent for Pd. Further EDTA (Na_2H_2EDTA) was also tested as eluting agent.

For both, ammonia and EDTA a concentration range of 0.1 -1M was tested. Elution conditions were tested by determination of weight distribution ratios D_w in batch experiments (section 3.2.1). Values were calculated by eq. 26.

Results are presented in Fig. 64 and Fig. 65. Both eluting agents are suitable for ammonium paladate elution ($D_W \leq 10$) but they are not suitable for palladium nitrate elution ($D_W \geq 100$) in this range. Later, in further optimization studies, it could be shown that ammonia can be used successfully for Pd elution at elevated concentrations (≥ 6M).

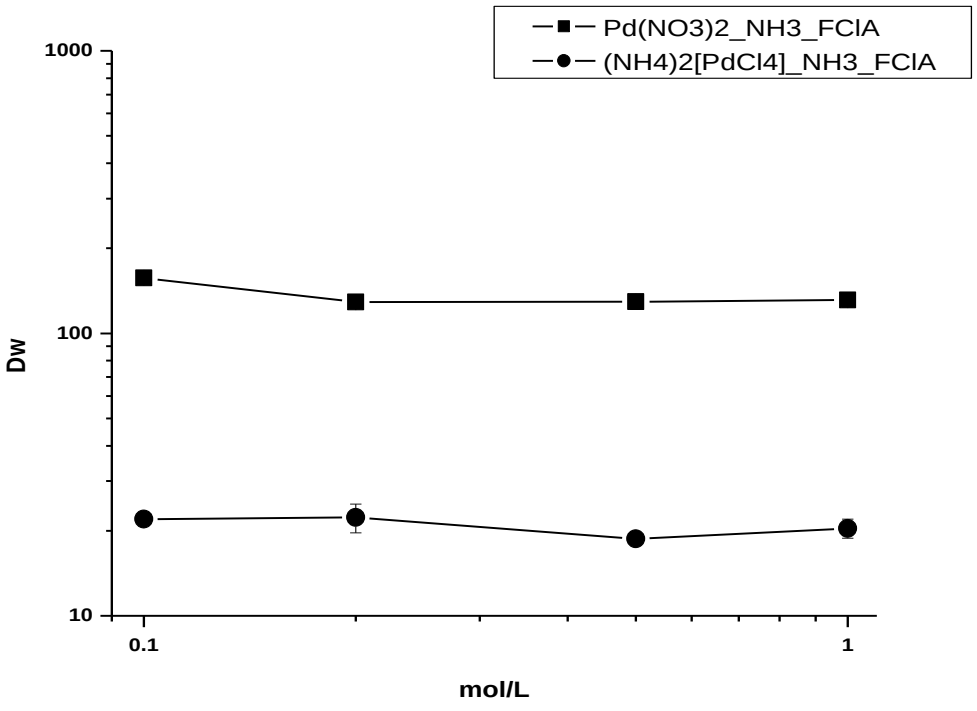

Fig. 64: Evaluation of ammonia as elution agent for Pd

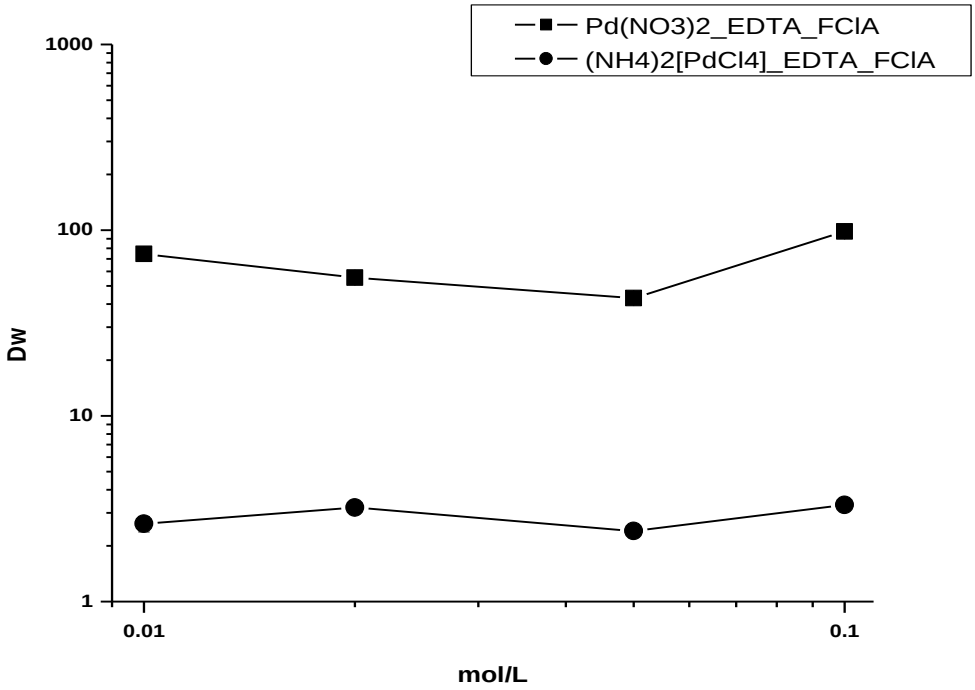

Fig. 65: Evaluation of Na_2H_2EDTA as elution agent for Pd

4.2 Method development for the separation of Pd and Pt

During the characterization studies (section 4.1) it was shown that both resins, FClA and F49A, have similar properties with respect to Pd and Pt uptake and influence of interferents. Furthermore it was shown that FClA resin has some advantages compared to F49A resin: The maximum uptake for Pd is higher (Table 1) and in 3M HNO_3 the difference of the D_W values of Pd and Pt is several orders of magnitude. Fig. 53 shows that a very good separation of Pd and Pt can be achieved when using FClA resin. Pt should be eluted during the loading whereas Pd should be retained on the resin and can be then eluted by 1M ammonium phosphate solution ($(NH_4)_2HPO_4$) (Fig. 63).

However, D_W values present only an indication on the behavior of the respective element on the column. Since contact times and contact surfaces are different in batch experiments and column experiments, it is difficult to transfer a result from batch experiments directly to column experiments. That means that a result obtained in batch experiments will not necessarily have exactly the same effect in column experiments, e.g. that 3M nitric acid will quantitatively elute Pd as observed in batch experiments. Therefore all conditions identified in batch experiments as seemingly optimal for the desired separation should always be tested in column experiments and further optimized, if necessary.

This section will thus deal with the development and optimization of the on-column separation.

Method development and optimization are performed in column experiments according to section 3.2.2. As mentioned above FClA resin was used for column experiments. In a preliminary study conditions for the separation and elution of Pd and Pt were directly tested on columns.

In order to do so three columns of FClA resin were prepared in 3M HNO_3 and loaded with 10 µg Pd^{2+} as $Pd(NO_3)_2$ and 8 µg Pt^{2+} as $Pt(NO_3)_2$, overall volume of the sample loading solution was 10 mL.

The column was then rinsed 3 times with 10 ml 3M HNO_3 and 5 times with 10 ml 1M $(NH_4)_2HPO_4$.

The results are summarized in Fig. 66.

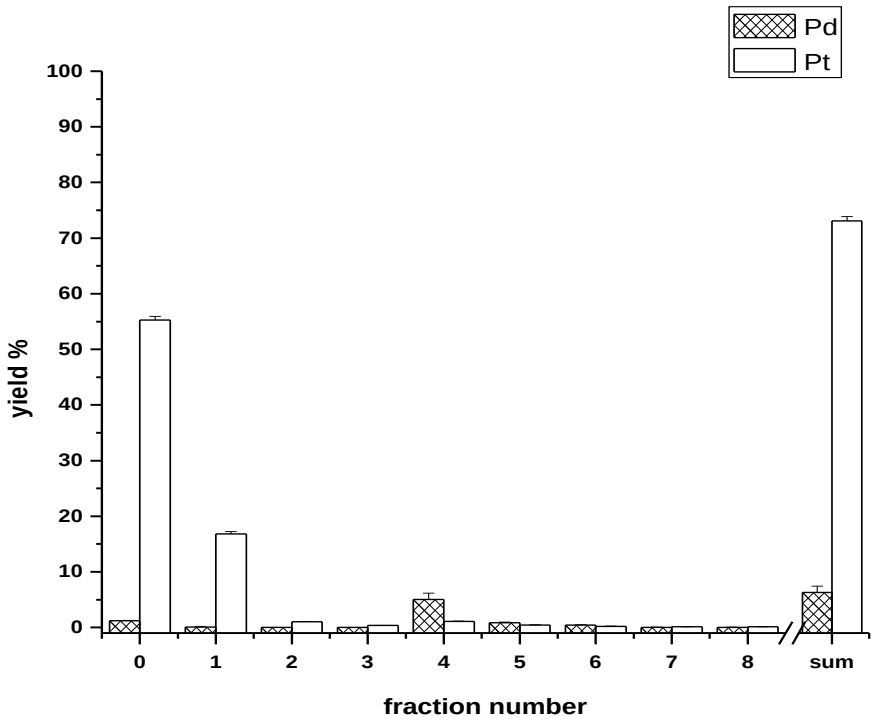

Fig. 66: Column experiments for the separation of palladium and platin. 0: loading solution, 1-3: 10 ml 3M HNO_3, 4-8: 10 ml of 1M $(NH_4)_2HPO_4$ respectively

Unfortunately, the results, especially for Pd, are not that as would have been expected from batch experiments. However, the yield for platinum is acceptable (73.1±0.8%) and although to be optimized. The yield for palladium is only 6.3±1.1%.

Duche et al. [62] have recently presented a liquid-liquid-extraction procedure for the separation of Pd(II) and Pt(IV). Quantitative Pd-extraction into the aqueous phase was achieved by using ammonia solution.

So further experiments were performed as described above, but rinsing the column with 5M HNO_3 (to further optimize the platinum yield) and then with 6M NH_3-solution in order to elute Pd. The results are presented in Fig. 67.

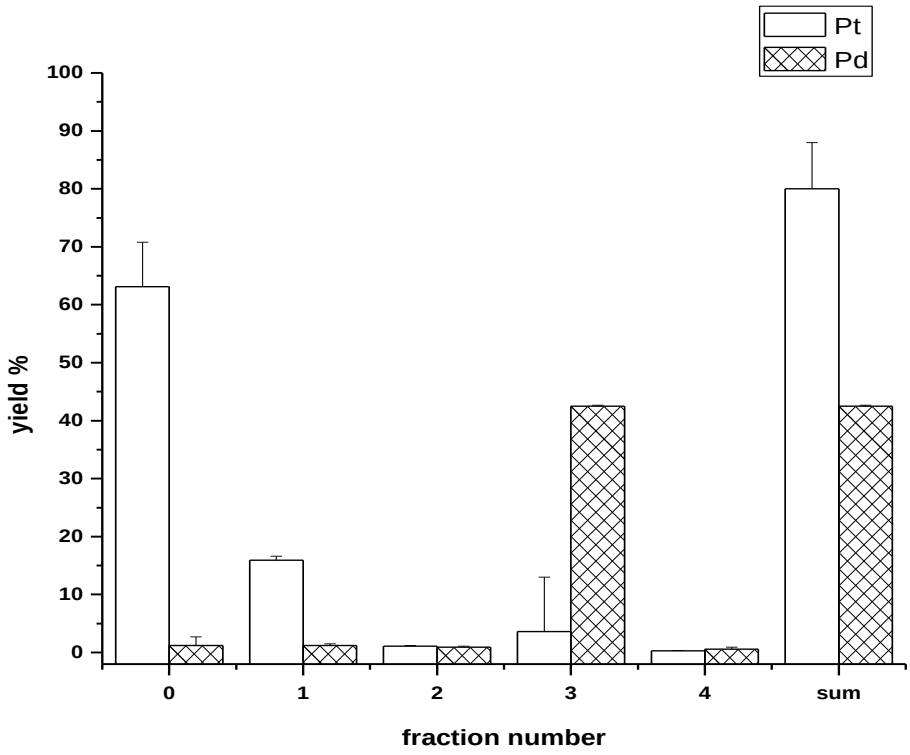

Fig. 67: Column experiments for the separation of palladium and platinum. Pd and Pt yields in respective collected fraction, 0: loading solution, 1-2: 10 ml 5M HNO_3, 3-4: 10 ml of 6M NH_3-solution respectively

As can be seen the yield for both elements is higher (Pt = 80±8%, Pd = 42.5±0.2%) under these conditions.

It is well known that the inertness of chloride complexes of platinum metals decreases after addition of stannous chloride to the solution. [63, 64]

Zolotov et al. [65] observed this “labilizing” effect of stannous chloride in the liquid-liquid extraction of platinum metals in the diphenylthiourea system.

This effect was also taken advantage of in other liquid-liquid extraction systems (Mojski, triphenylphosphine [66]; Duche, TOPO [62]). Best extraction yields were achieved with stannous chloride concentrations ≥ 0.1M [67].

In order to evaluate if the addition of $SnCl_2$ improved the separation performance of the FClA resin further experiments were performed. Pd and Pt were loaded from a 5M HNO_3/ 0.1 SnCl2 solution onto the FClA resin, following by two rinsing steps with 10ml 5M HNO_3 and one rinsing step with 10ml 5M NH_3. Results are shown in Fig. 68.

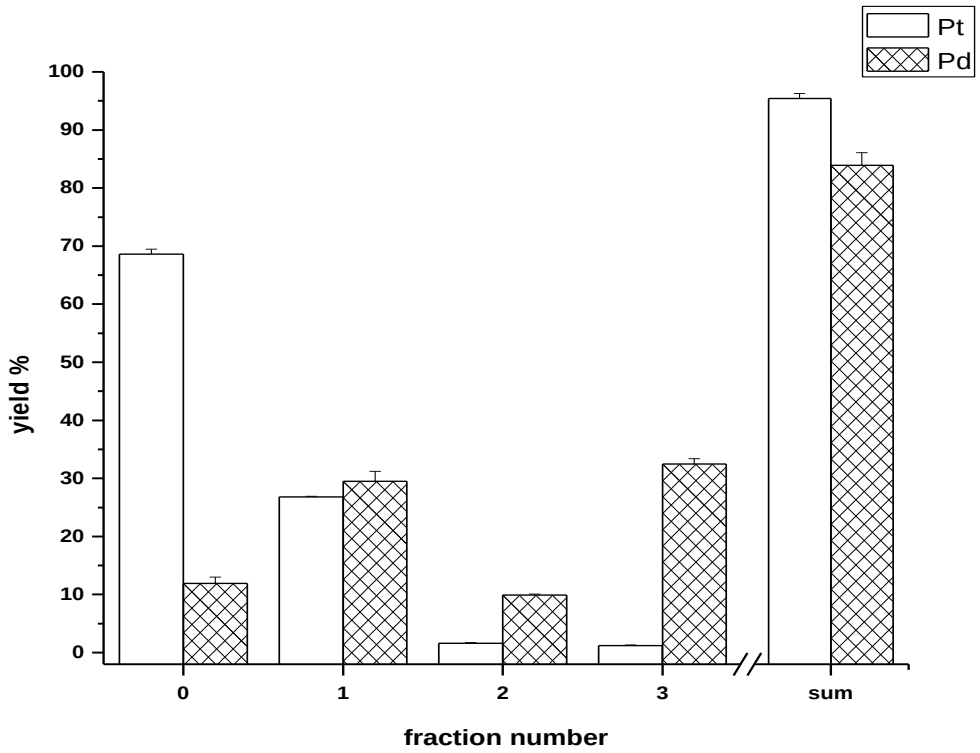

Fig. 68: Column experiments for the separation of palladium and platinum. Pd and Pt yields in respective collected fraction, 0: loading solution (5M HNO_3/ 0.1M $SnCl_2$), 1-2: 10 ml 5M HNO_3, 3: 10 ml of 5M NH_3-solution respectively

The addition of $SnCl_2$ leads to an almost quantitative elution of Pd (83.9±2.2%) and Pt (95.4±0.9%). Unfortunately a cross contamination occurs, that is Pd and Pt are present in each fraction, so no clear separation was achieved.

A similar set of experiment was performed, in which only the $SnCl_2$ concentration was lowered by the factor of ten compared to the previous experiment. Pd and Pt were thus loaded from a 5M HNO_3/ 0.01 $SnCl_2$ solution onto the FClA resin, following by four rinsing steps with 5ml 5M HNO_3 and two rinsing steps with 5ml 5M NH_3. Results are shown in Fig. 69.

Fig. 69 shows that by lowering the $SnCl_2$ concentration, palladium and platinum could be separated without cross contamination. Whereas Pt recovery is again very high (96.1±0.7%) unfortunately the Pd recovery decreases to only 22.8±1.7%. This experiment additionally shows that 5 ml 5M HNO_3 are sufficient to elute Pt with a high recovery when loading from 10 ml before (total volume: 15 ml).

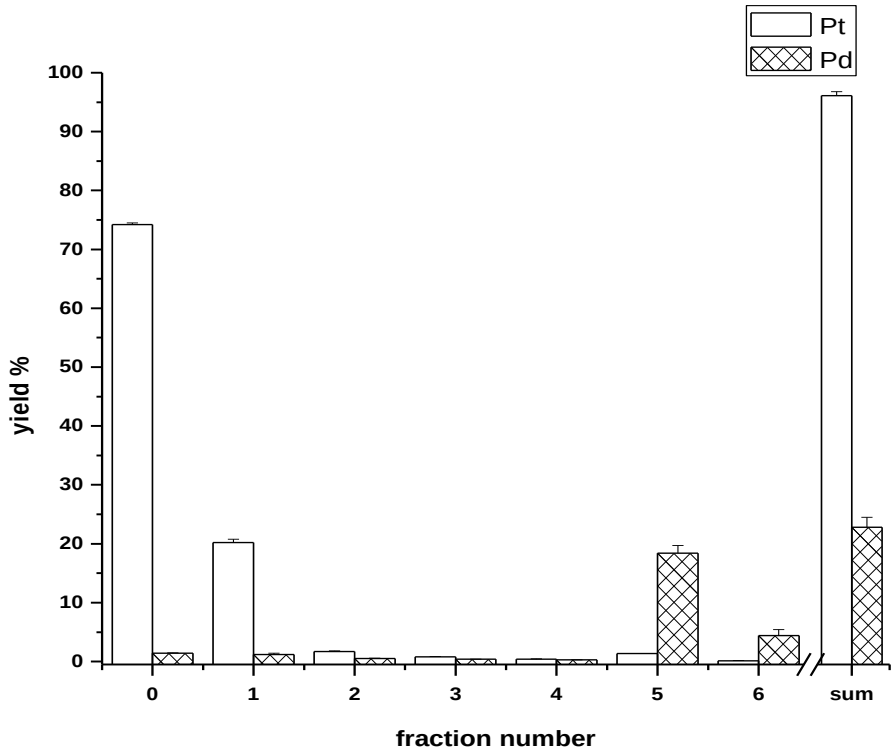

Fig. 69: Column experiments for the separation of palladium and platinum. 0: loading solution (10 ml 5M HNO_3/ 0.01M $SnCl_2$), 1-4: 5 ml 5M HNO_3, 5-6: 5 ml of 5M NH_3-solution respectively

In further experiments Pd recovery could be optimized. There are two possibilities of increasing Pd recovery.

By increasing the ammonia concentration of the Pd eluting agent (Fig. 70 shows the dependency of Pd yield on the ammonia concentration). The use of concentrated ammonia solution (13.4M) results in a Pd recovery of 87.6±2.6%.

Or by eluting Pt with 5 ml 5M HNO_3/0.01M $SnCl_2$ after loading (and not as in previous experiments with 5M HNO_3) followed by Pd elution with 9M NH_3.

The optimized method for preconcentration and separation of Pd and Pt is shown in Fig. 71. Pd and Pt were loaded from 10 ml 5M HNO_3/0.01M $SnCl_2$ solution and rinsed with 5 ml 5M HNO_3/0.01M $SnCl_2$ solution (fraction 1). Then the column was rinsed once with 10 ml and twice with 5 ml 9M NH_3 solution.

Obtained Pt recovery is 97.0±2.5% (fraction 1) and Pd recovery is 93.5±2.9% (in 20 ml 9M NH_3, sum of fraction 2-4).

As already known from literature $SnCl_2$ has a labilizing effect and is important for separation of Pd and Pt in liquid-liquid extraction. Also in extraction chromatography $SnCl_2$ was found to have a key function. This is especially true for Pd recovery. Compared to experiments performed without stannous chloride (Fig. 67) Pt recovery could be enhanced by approx. 20% and Pd recovery by approx. 55% when using stannous chloride.

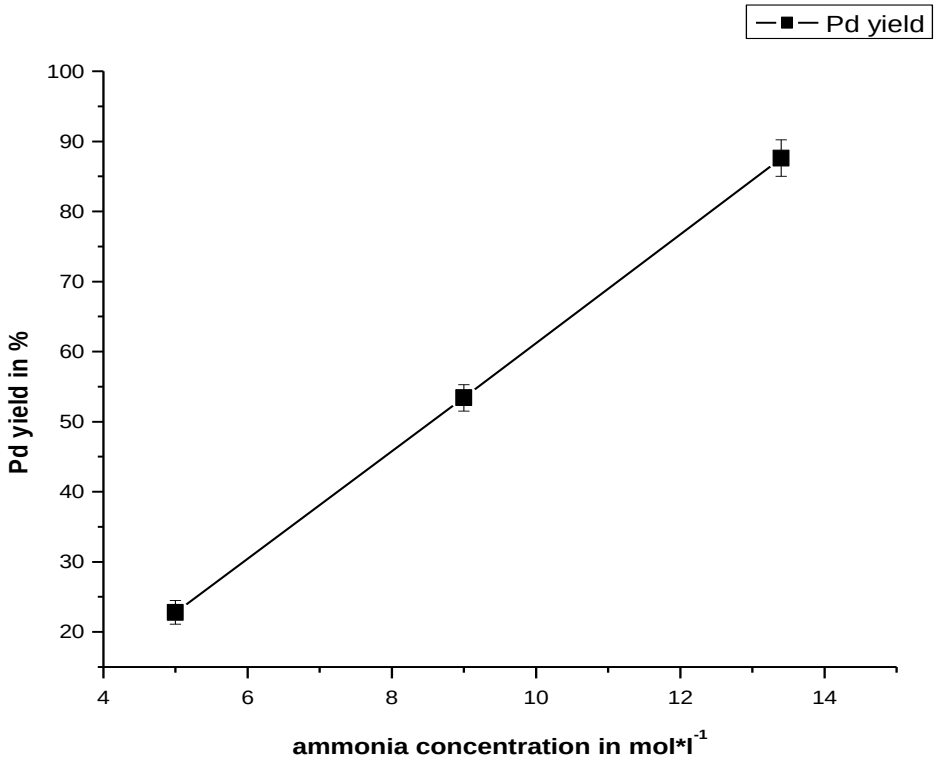

Fig. 70: Dependency of Pd yield on ammonia concentration

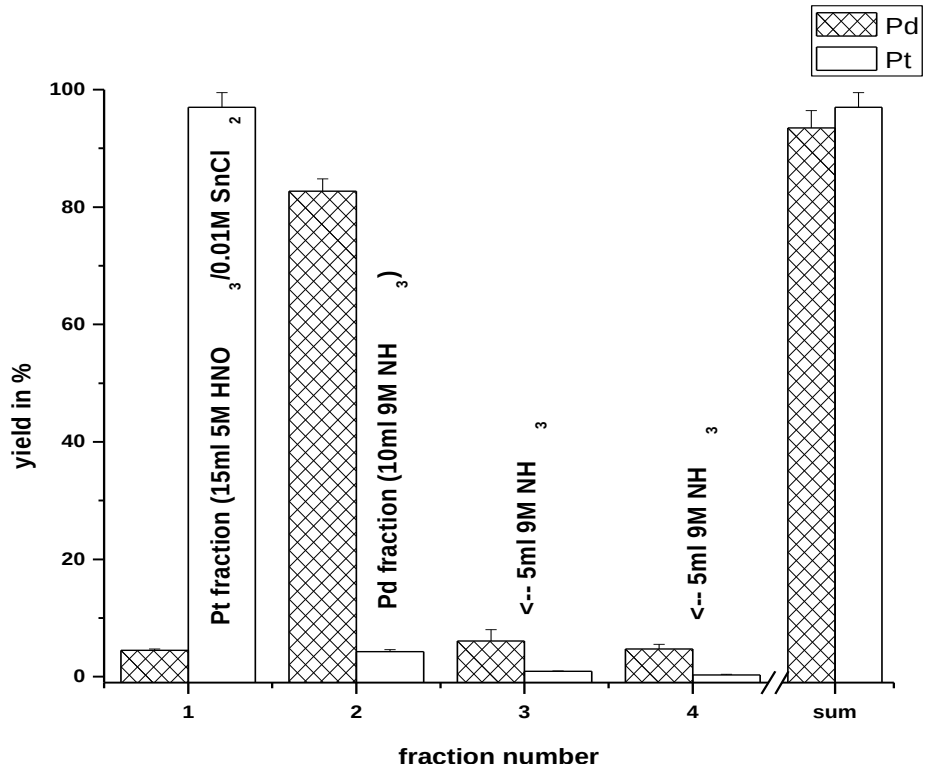

Fig. 71: Optimized method for preconcentration and separation of Pd and Pt . 1: loading solution (10 ml 5M HNO_3/ 0.01M $SnCl_2$) following by 5 ml 5M HNO_3 (Pt fraction), 2: 10 ml of 5M NH_3-solution (Pd fraction), 3-4: 5 ml of 5M NH_3-solution respectively

4.2.1 Validation of the method for the separation of Pd and Pt

After successfully developing and optimizing the method for preconcentration and separation of Pd and Pt the method was validated.

Unfortunately problems with new resin lots occurred during the validation. So only sensitivity and selectivity will be reported here.

4.2.1.1 Applicability

The method to be validated is shown in Fig. 72. And was performed according to section 3.2.2.

Chemicals used for the validation are

- 5M HNO_3/0.01M $SnCl_2$
- 9M NH_3
- Pd- and Pt standard solution
- Rh- and Ir standard solutions for internal standardization
- 3% HNO_3

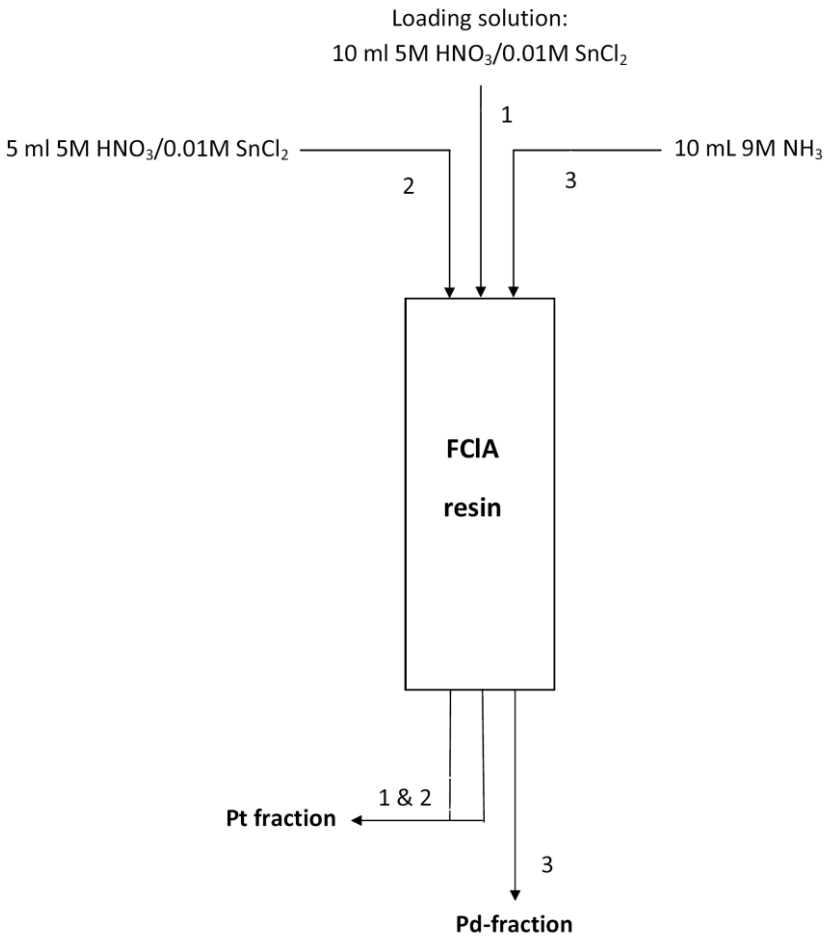

Fig. 72: Method for preconcentration and separation of Pd and Pt

4.2.1.2 Sensitivity

The sensitivity of an analytical method corresponds to the slope of the calibration graph and is a characteristic of the measuring device (section 2.4.9.).

However, the ICP-MS device (Perkin Elmer ELAN 6000) stood idle for a prolonged period and before starting it up some spare parts were changed. In order to make sure that the ICP-MS works properly the device was first of all calibrated and optimized and subsequently checked for linearity, precision, LOQ and LOD.

Mass calibration and optimization procedure

For calibration and optimization the auto-tune and auto-optimize functions of the software were used. For these procedures solutions containing either 10 µg/L or 200 µg/L of each Mg, Cu, Cd, Pb, Ce,and U were used. The results are summarized in Table 3:

Analyte	Exact Mass (amu)	Measured Mass (amu)	Measured Peak Width (amu)	Net Intensity (cps)	RSD %	Required Intensity (cps)
Mg	23.985	24.028	0.761	47318.5	0.9	> 20000
Cu	62.930	62.878	0.737	27145.4	1.5	
Cd	113.904	113.878	0.748	31656.7	1.5	
Ce	139.905	139.929	0.745	331048.2	1.0	
Pb	207.977	207.979	0.779	205114.9	0.9	>50000
U	238.050	237.977	0.771	47318.5	1.0	
CeO/Ce				0.012	0.2	≤0.03
Ba++/Ba+				0.034	1	≤0.03
Bkgd				20.4	10.7	<30

Table 3: Results for calibration and tuning of ICP-MS device

The results show that all measured values meet the required specifications. These values were controlled daily by a Daily Performance Test (DPT).

Lens voltage and auto lens, RF power, analogue and pulse stage voltage of the detector were also calibrated and optimized, a dual detector calibration also was performed. These procedures were performed periodically to check and assure the correct operation of the ICP-MS device.

Precision

Precision was controlled by analysing a standard calibration solution (Perkin Elmer) containing 10 µg/L of each Mg, Cu, Cd, Pb, Ce,and U. Measurements were taken three times a day for a period of time of 14 days.

From the obtained data inter-day standard (s_w) deviation was calculated following eq. 13, intra-day standard deviation (s_b) following eq. 14 and the combined standard deviation (s_t) following eq. 15; further the mean intensity $\overline{x_{ges}}$ was calculated. Since all values for common standard deviation are below 15% (section 2.4.5) the precision for the ICP-MS device is assumed to be given.

Results are summarized in Table 4.

Analyte	Mass	$\overline{x_{ges}}$	s_w	rel. s_w %	s_b	rel. s_b %	s_t	rel. s_t %
Mg	24.0	44669.31	3147.13	7.05	4196.60	9.39	5245.56	11.74
Cd	113.9	23019.01	1168.00	5.07	2570.38	11.17	2823.31	12.27
Cu	62.9	28416.68	1654.93	5.82	3687.90	12.98	4042.20	14.22
U	238.1	299593.48	16037.03	5.35	28258.81	9.43	32492.25	10.85
Pb	208.0	178058.30	7199.34	4.04	14366.03	8.07	16069.02	9.02

Table 4: Results of precision measurements of ICP-MS device

Linearity

The linearity of the ICP-MS was controlled by measuring standard solutions containing Mn, Cu, Ni, Pd, Pt, Ag, Cd, Pb and U. Each element was in a range of 12.5 – 800 µg/L

Each solution was measured three times; mean response values of each element were calculated and plotted (Fig. 73 - Fig. 81).

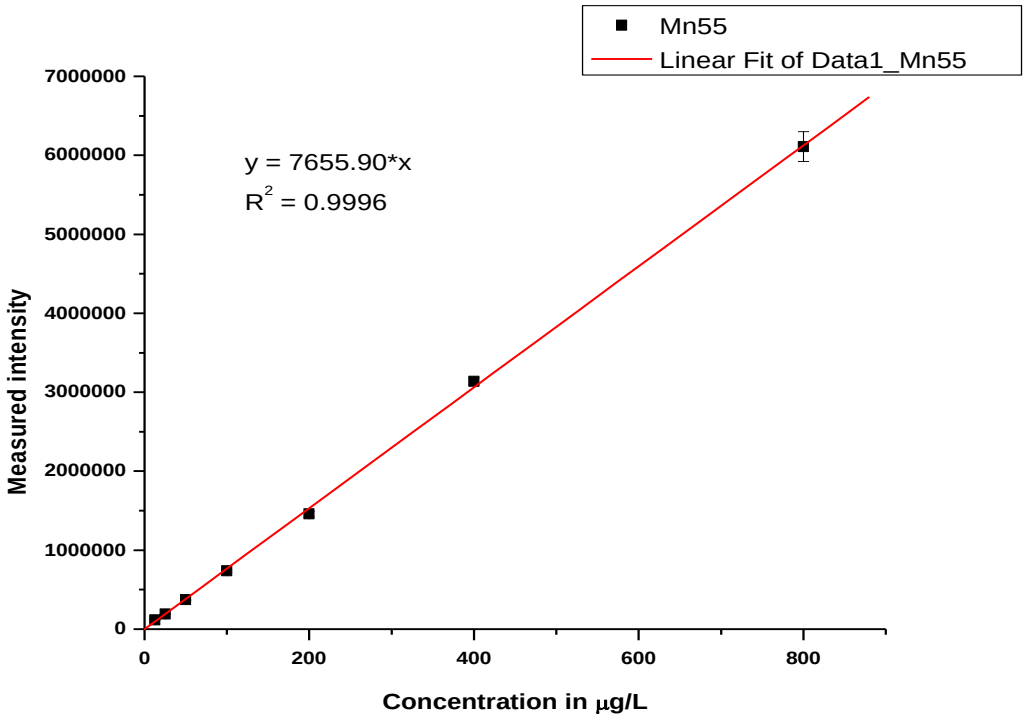

Fig. 73: Plot of mean intensity vs. concentration for Mn

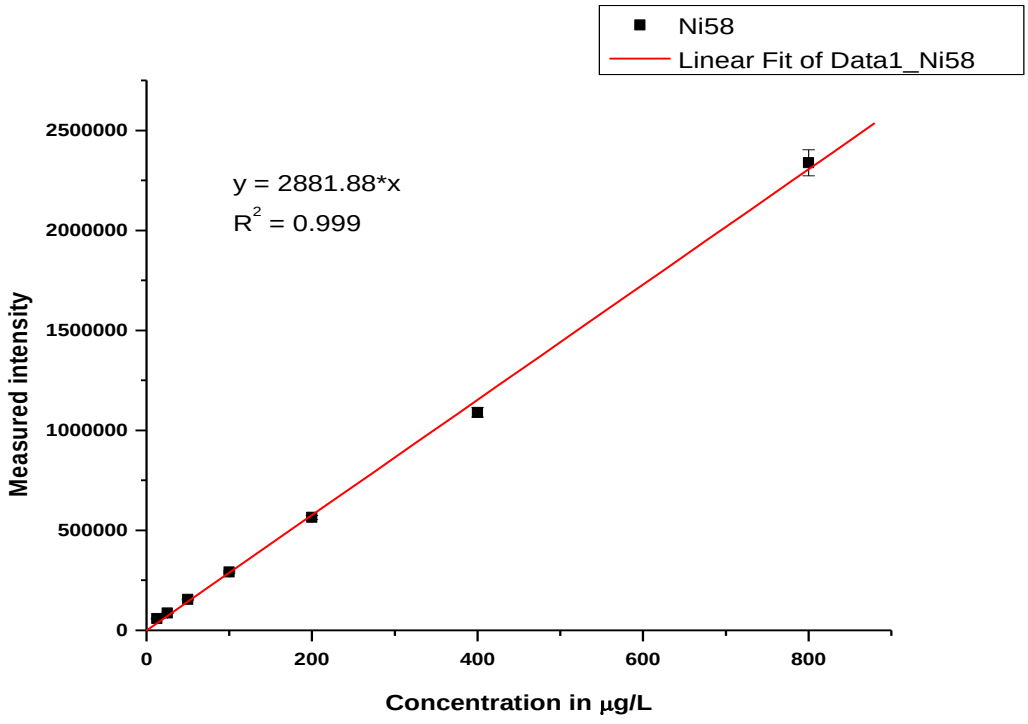

Fig. 74: Plot of mean intensity vs. concentration for Ni

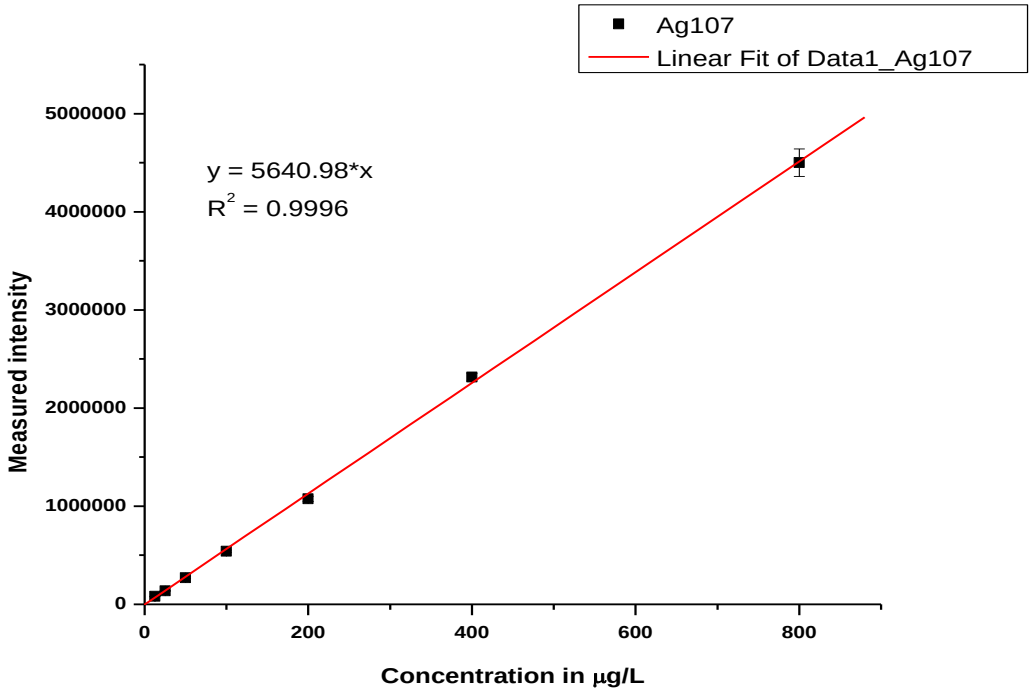

Fig. 75: Plot of mean intensity vs. concentration for Ag

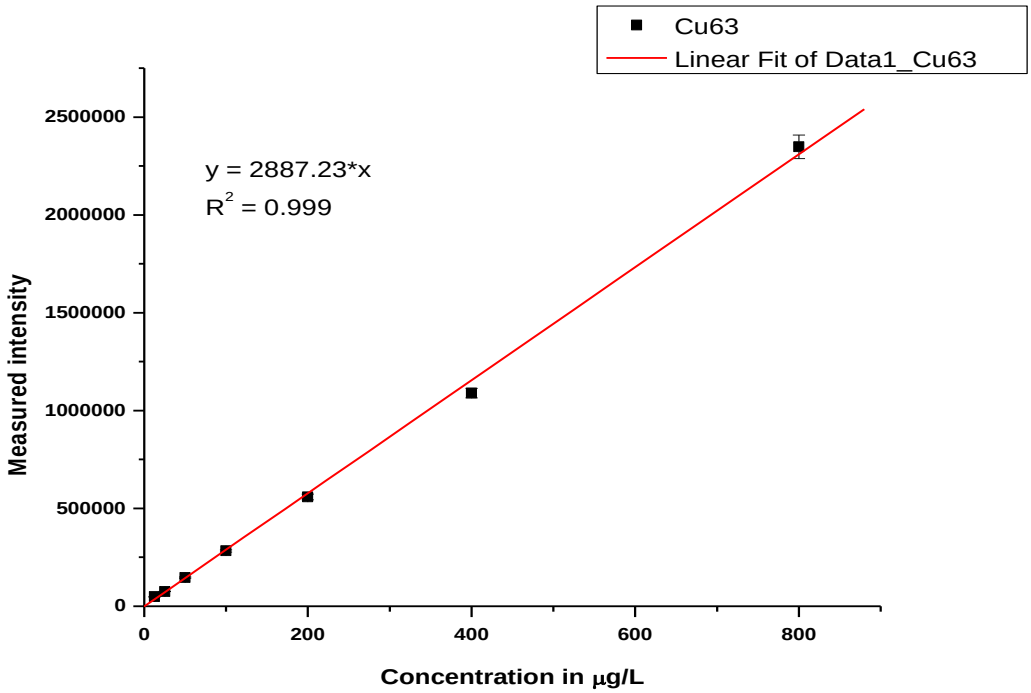

Fig. 76: Plot of mean intensity vs. concentration for Cu

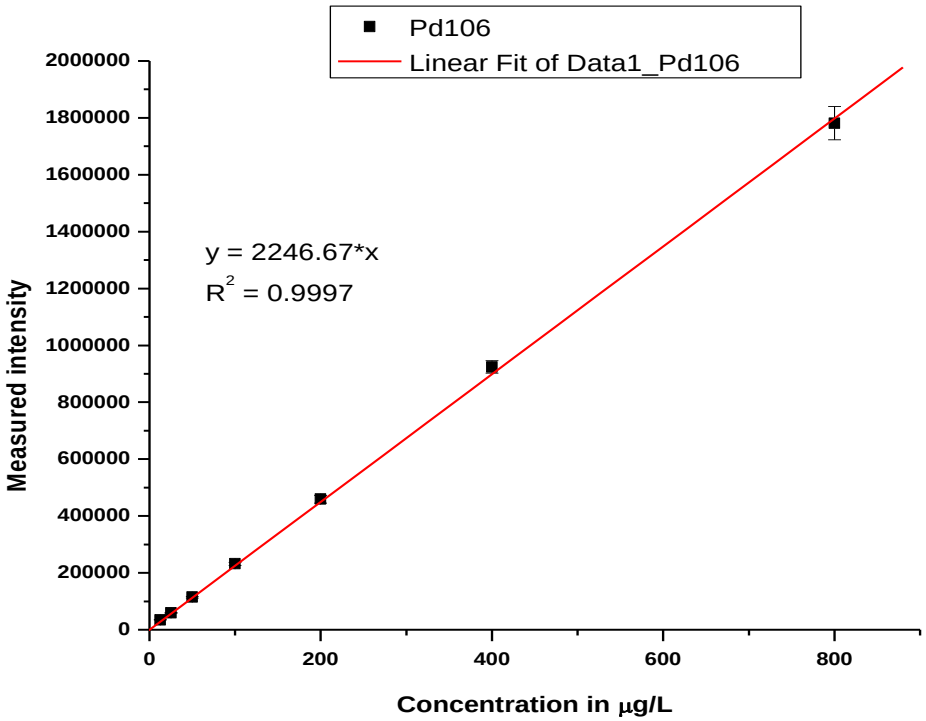

Fig. 77: Plot of mean intensity vs. concentration for Pd

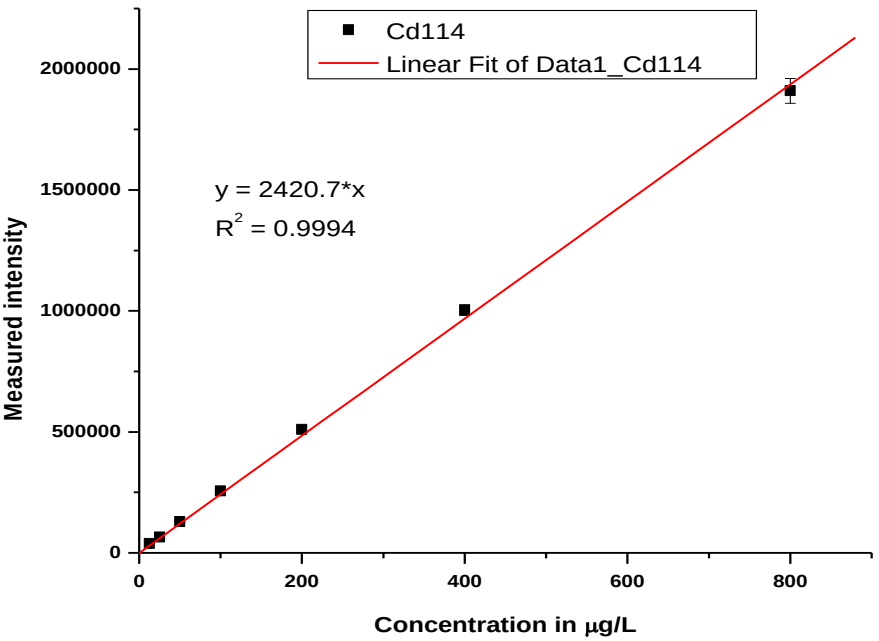

Fig. 78: Plot of mean intensity vs. concentration for Cd

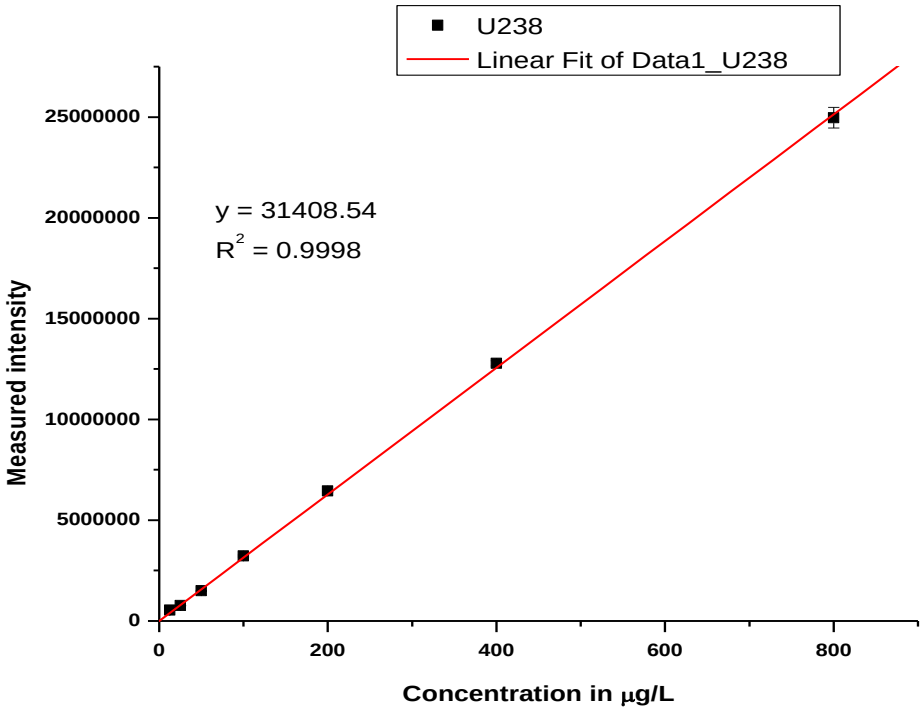

Fig. 79: Plot of mean intensity vs. concentration for Uranium

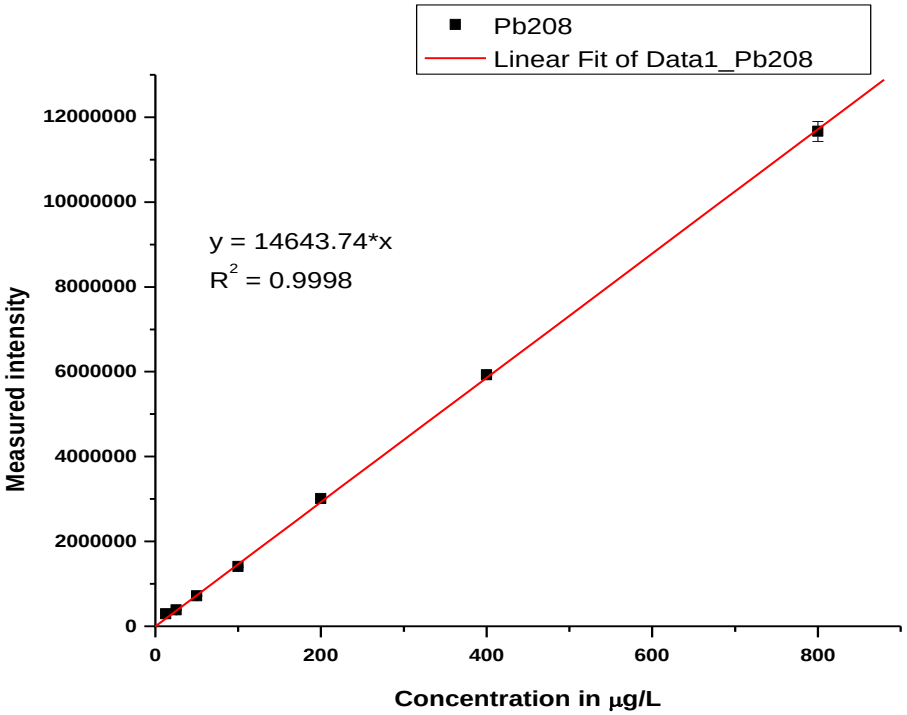

Fig. 80: Plot of mean intensity vs. concentration for Pb

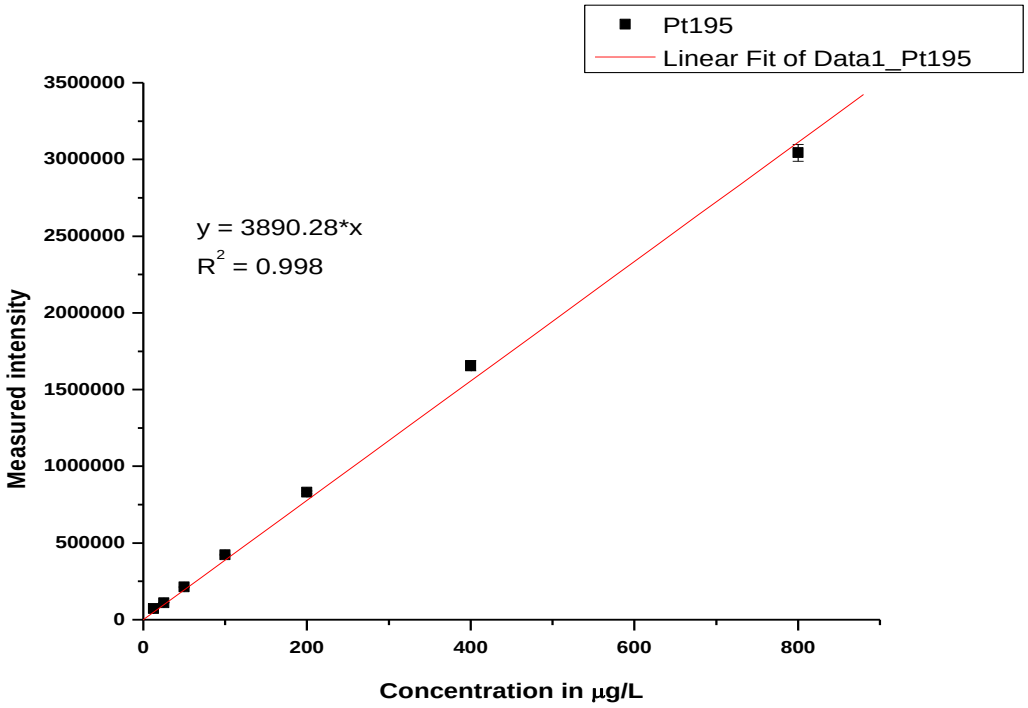

Fig. 81: Plot of mean intensity vs. concentration for Pt

From the results presented in Fig. 73 - Fig. 81 it can be derived that linearity of ICP-MS is given for all analyzed elements and a wide concentration range.

Linearity was evaluated by the correlation coefficient R^2. The criterion of acceptance was set to $R^2 \geq 0.995$ (section 2.4.3). The criterion is fulfilled for all measured elements.

Limit of detection and limit of quantification

Limits of detection and quantification were obtained by measuring a blank sample (3% HNO_3) ten times and calculating LOD and LOQ following eq. 17 (with k = 3 for LOD and 9 for LOQ).

Intensities were converted into concentrations by using equations given in Fig. 73 - Fig. 81. Results are summarized in Table 5.

Analyte	Mass	Mean Meas. Int.	SD	RSD %	LOD Intensity	LOD in µg/L	LOQ Intensity	LOQ in µg/L
Mn	55	2364.86	239.35	10.12	718.05	**0.09**	2154.16	**0.28**
Ni	58	36009.06	2340.91	6.50	7022.73	**2.44**	21068.18	**7.31**
Cu	63	890.1	34.39	3.86	103.18	**0.04**	309.55	**0.11**
Pd	106	154	9.50	6.17	28.50	**0.01**	85.49	**0.04**
Ag	107	337.62	22.25	6.59	66.74	**0.01**	200.22	**0.04**
Cd	114	190.8	10.90	5.71	32.70	**0.01**	98.11	**0.04**
Pt	195	420	48.05	11.44	144.15	**0.04**	432.46	**0.11**
Pb	208	3636.1	85.61	2.35	256.83	**0.02**	770.50	**0.05**
U	238	4136.1	236.75	5.72	710.25	**0.02**	2130.75	**0.07**

Table 5: Calculated LODs and LOQs of ICP-MS device for various analytes

4.2.1.3 Pd/Pt selectivity

The influence of potential interferences was examined by measuring a multielement solution containing 10 µg/ml Ca, Fe, Sr, Y, Cd, Ba, La, Ce, Nd, Sm Eu, Tb, Yb respectively. During the method development and optimization it was found that all interferences were eluted quantitatively already during the loading step, hence they will be found in the Pt fraction. Since none of these elements interfere with the measurement of Pt, it will be measured by ICP-MS with good precision even in the presence of these elements. However, it is important that the Pd fraction is clean with respect to interferences because these elements cause spectral interferences when analyzing Pd by ICP-MS. In order to quantify to which degree the Pd fraction is free of interferences decontamination factors (D_f) were calculated following eq. 10. Calculated D_f are summarized in Table 6.

The method shows selectivity for Pd since D_f values are greater than 100 (section 2.4.9). Only D_f value of calcium is marginal, but acceptable since it does not interfere when analyzing Pd by ICP-MS.

Analyte	**D_f**
Ca	>82
Fe	>125
Sr	>10370
Y	>2370
Cd	>220
Ba	>2920
La	>2630
Ce	>2434
Nd	>1300
Sm	>2013
Eu	>1074
Tb	>1973
Yb	>1835

Table 6: Decontamination factors of potential interferences in the Pd fraction

4.3 Method development for preconcentration and separation of ^{36}Cl and ^{129}I

Part of the results shown in this chapter were published in the Journal of Radioanalytical and Nuclear Chemistry [68].

In the characterization studies described in section 4.1 FClA resin show good properties towards silver uptake. The most important properties are summarized at this point.

FClA resin shows high selectivity only for Pd and Ag (Table 7). This is a very important feature of this resin because selectivity of the method is expected to be high (this will be discussed later).

Analyte	D_w, mL g^{-1}
Ag	650000
Cd	<1
Ce	4
Co	<1
Cu	<1
Fe	<1
Mn	<1
Ni	<1
Pd	87000
Zn	25

Table 7: Dw values of various elements on FClA resin in 1 M H_2SO_4

In sulphuric acid the D_w value for silver decreases with increasing pH value of sulphuric acid, but remains very high (Fig. 82).

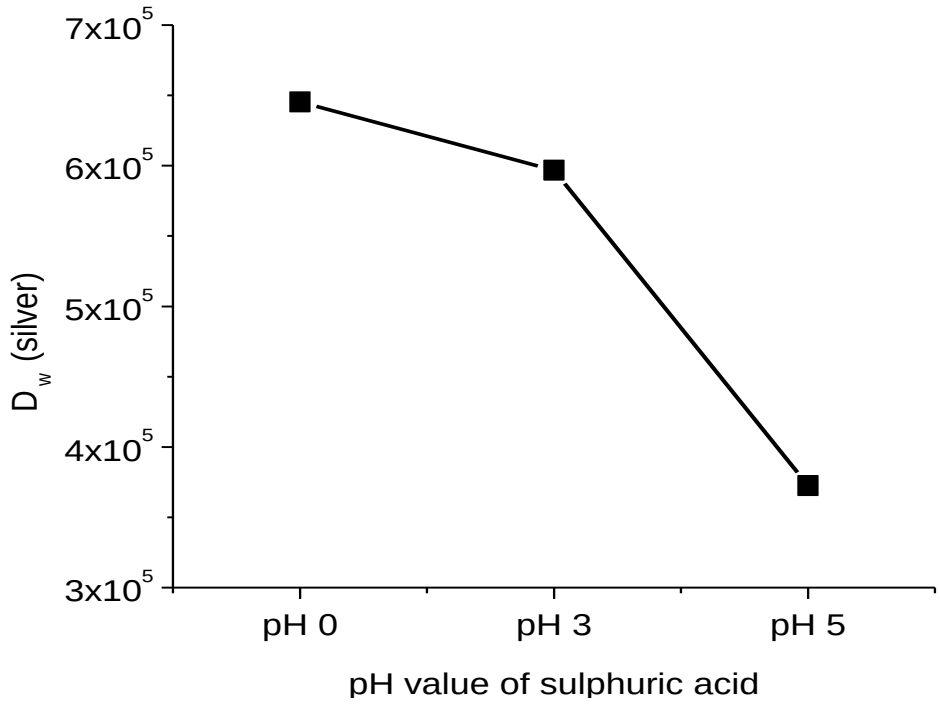

Fig. 82: Dependency of silver D_w value on the concentration of sulphuric acid

Furthermore the FClA resin showed a high maximum uptake for silver.

The maximum Ag^+ uptake was determined to be 38.5 ± 1.3 mg $Ag^+.g^{-1}$ resin under batch extraction conditions described in section 3.2.1.

4.3.1 Silver uptake

Additionally the silver uptake was also examined by column elution experiments. Several columns were prepared in order to allow estimating the influence of the contact time on the Ag^+ uptake. The columns used for the uptake studies were prepared by soaking 0.65 g of FClA resin in 10 mL 1M H_2SO_4 for 2 h under shaking; the resin was subsequently transferred into an empty 2 mL column. The packed columns were then loaded with a small volume (2 mL) of a 1M H_2SO_4 silver nitrate solution with a well known Ag^+ concentration (10 mg Ag^+ mL^{-1}) and allowed to stand for 0.5 h, 2.5 h, 10 h respectively. The columns were then rinsed three times with 10 mL 1M H_2SO_4, the rinsing solutions were collected in a volumetric flask, appropriately diluted and analyzed by ICP-MS for Ag content.

Ag^+ uptake in column geometry was found to be lower under the chosen conditions; additionally it was found that the uptake is time dependent: after 30 minutes 16.5 ± 0.8 mg Ag^+ g^{-1} resin were extracted, after 2.5 hours 19.5 ± 1.0 mg Ag^+ g^{-1} resin. Longer contact times did not result in a further increase of the Ag^+ uptake (Fig. 83).

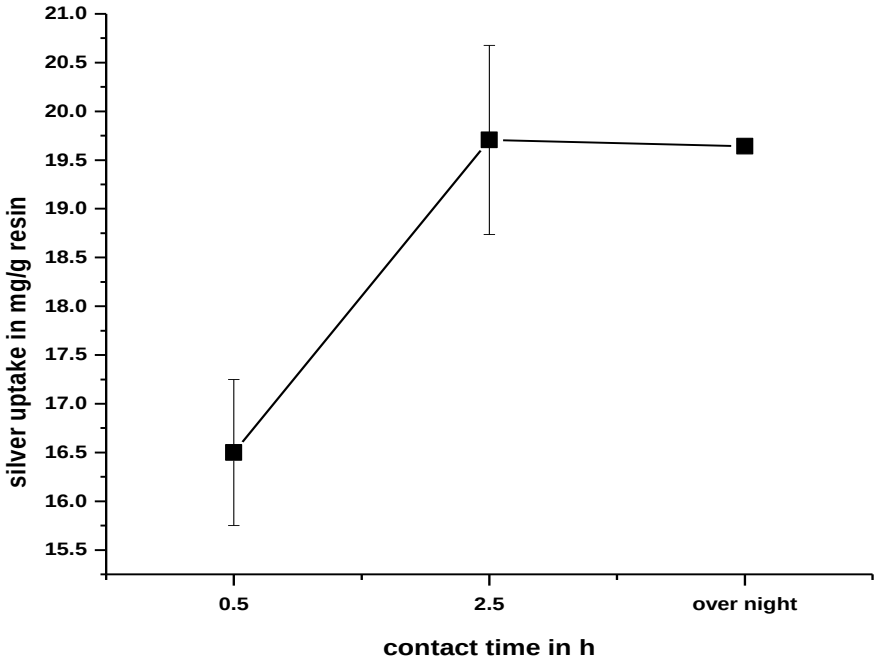

Fig. 83: Dependency of silver uptake on the contact time

From the results obtained it can be concluded that the resin's selectivity is overall suited for its designated purpose.

4.3.2 Preparation and characterization of silver loaded resin

Ag^+ loaded FClA resin was prepared by contacting 10 g of the FClA resin with 100 mL of a 1M H_2SO_4 solution containing 650 mg of $AgNO_3$ in a 250 mL PE flask on a vortex shaker over a period of 2 h. The resin was then filtered, rinsed with 1M H_2SO_4 (until absence of Ag^+ in the filtrate) and dried.

4.3.2.1 Maximum uptake of chloride and iodide

Chloride and iodide uptake behaviours were also examined via column experiments using FClA resin columns previously loaded with Ag^+. In case of chloride uptake, the columns were loaded with 5 mg of chloride, in case of iodide with 20 mg of iodide (both as sodium salts). Loaded columns were rinsed three times with 1M H_2SO_4, all rinsing solutions were collected, diluted and analyzed by ICP-MS. Calculations were

performed following eq. 27, obtained experimental results were compared to theoretical values (quantitative precipitation of iodide / chloride by 13 mg of Ag^+).

The chloride and iodide uptake of the FClA resin under the chosen conditions were found to be 4.3 ± 0.2 mg Cl^- g^{-1} resin and 16.3 ± 1.6 mg I^- g^{-1} resin, which agrees well with the theoretical values of 4.2 mg Cl^- g^{-1} resin and 14.9 mg I^- g^{-1} resin (Table 8).

Analyte	Theoretical value	Experimental value
iodide	14.9 mg	16.3 ± 1.6mg
chloride	4.2 mg	4.3 ± 0.2 mg

Table 8 Capacities of the silver loaded resin for chloride and iodide

4.3.2.2 Evaluation of chloride and iodide retention and elution conditions

D_w values were determined for chloride and iodide in 1M H_2SO_4, in 0.01, 0.05, 0.1 and 0.2M KSCN; in addition iodide D_w values were determined in 0.04, 0.09, 0.18 and 0.35M Na_2S [69]. Results are presented in Table 9 - Table 11.

Analyte	D_w retention
Chloride	1600
Iodide	1980

Table 9: retention of chloride and iodide in 1M H_2SO_4

It can be concluded that the silver loaded resin quantitatively retains both isotopes. Chloride can be quantitatively eluted at any SCN^- concentration whereas iodide remains on the resin; it can then be eluted at elevated Na_2S concentrations.

	Chloride	Iodide
KSCN conc.	**D_w elution**	**D_w elution**
0.01M	1.7	12000
0.05M	0.4	15000
0.1M	0.7	4000
0.2M	0.4	9000

Table 10: D_w values for chloride and iodide at different KSCN concentrations

Na_2S conc	Mean D_w
0.04M	40
0.09M	15
0.18M	0.7
0.35M	0.8

Table 11: D_w values for iodide at different Na_2S concentrations

4.3.2.3 Kinetics of the chloride and iodide retention on silver loaded resin

Retention kinetics for both halogenides were examined in batch experiments. Approx. 50 mg of the silver loaded FClA resin were weighted into a 2 ml Eppendorf tube. The resin was then preconditioned by shaking in 1M H_2SO_4 and 50 Bq of ^{36}Cl and ^{129}I, respectively, were added to the tube (both as chloride and iodide). The resin was then shaken for 5, 10, 15, 20, 30, 60, 90 and 120 minutes. Aliquots were withdrawn and analyzed by LSC.

It was found that uptake kinetics for both radioisotopes are fast on the silver loaded resin (Fig. 84). More than 95% of ^{36}Cl had been extracted after 20 minutes contact time; for ^{129}I this is the case after only 10 minutes contact time. Kinetics for ^{129}I is faster than for ^{36}Cl because the solubility product for AgI ($K_L = 1.5 * 10^{-16}$ [70]) is six orders of magnitude lower than for AgCl ($K_L = 1.5 * 10^{-10}$ [70]).

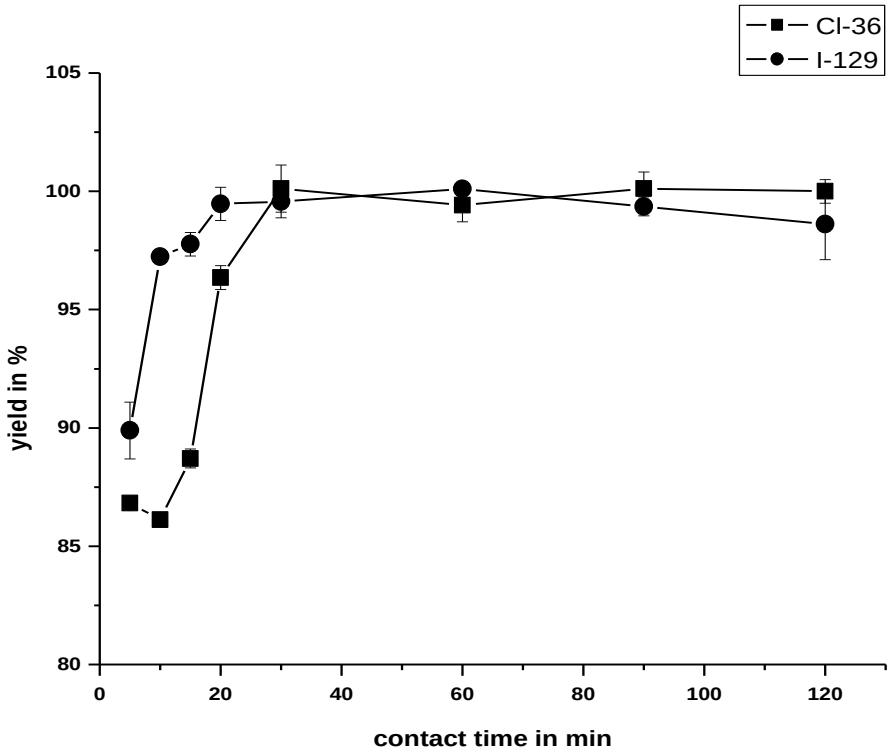

Fig. 84: Uptake kinetics for ^{36}Cl and ^{129}I in 1M H_2SO_4 on silver loaded FCIA resin

4.3.3 Method development

Results obtained during the characterization studies were very promising with respect to the use of the FCIA resin for the preconcentration and separation of ^{36}Cl and ^{129}I, and were thus tested and further optimized in column experiments.

The columns used during the elution studies were prepared similarly as described in section 3.2.2. The resin was soaked in 1M H_2SO_4 for 2 h and then transferred into the column. The columns were then loaded with 2 mL of 1M H_2SO_4 solution containing 13 mg of Ag^+ and allowed to stand for 2.5 h. The main aim of the elution study was to determine optimum volumes of the respective rinsing and elution steps. The loading solutions were collected directly, whereas rinsing and elution steps were collected in 5 mL fractions.

Elution studies on chloride and iodide were performed using sample load solutions that were 1M in H_2SO_4 and that contained either 50 Bq ^{36}Cl and 1 mg of chloride (as sodium chloride) or 50 Bq ^{129}I and 1 mg of iodide (as sodium iodide). The elution studies were first performed separately for chloride and iodide (Scheme 1). Elution conditions evaluated included 0.1M KSCN (for chloride elution) and 0.35M Na_2S (for iodide elution), both at pH 7, as well as several different rinsing steps upfront to the iodide elution with the focus of evaluating their influence on the iodide elution yield.

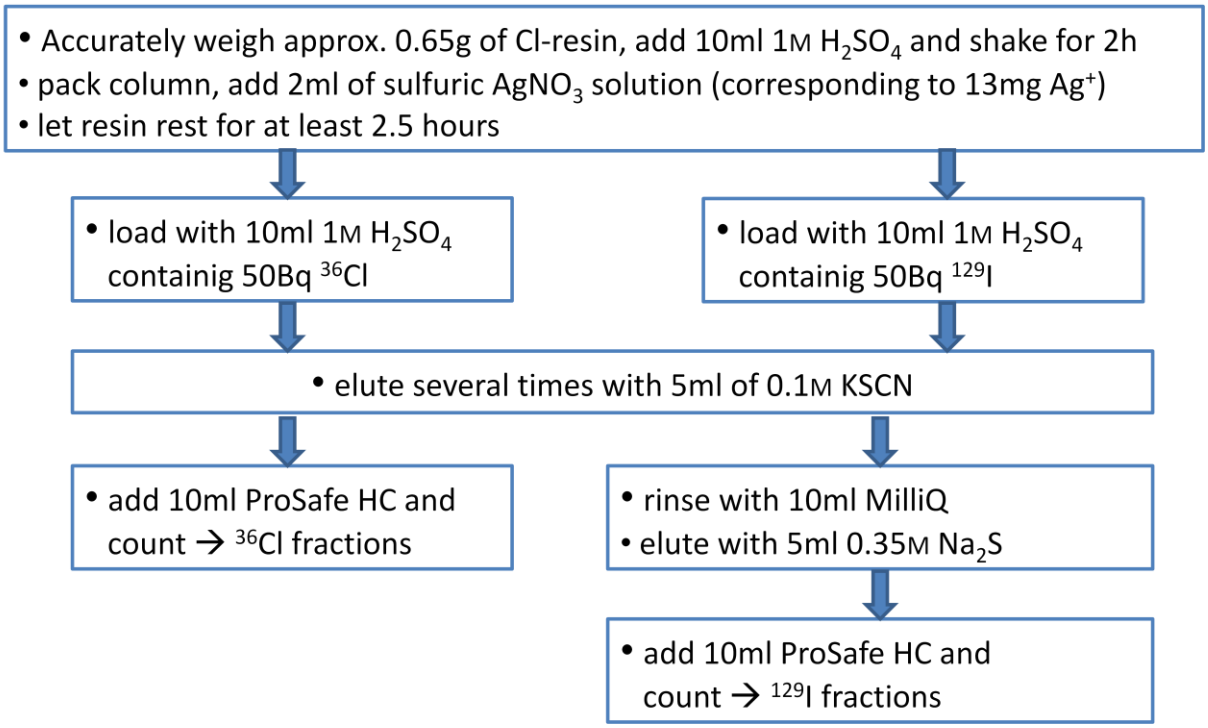

Scheme 1: Procedure for optimization elution volumes

Fig. 85 and Fig. 86 show the results of the initial elution studies; Fig. 85 shows that 5 mL 0.1M KSCN quantitatively remove chloride from the column, whereas, as Fig. 86 shows, no iodide is eluted; it further shows that iodide is mainly eluted in the first 5 mL of 0.35M Na_2S, almost none being eluted in the later fractions.

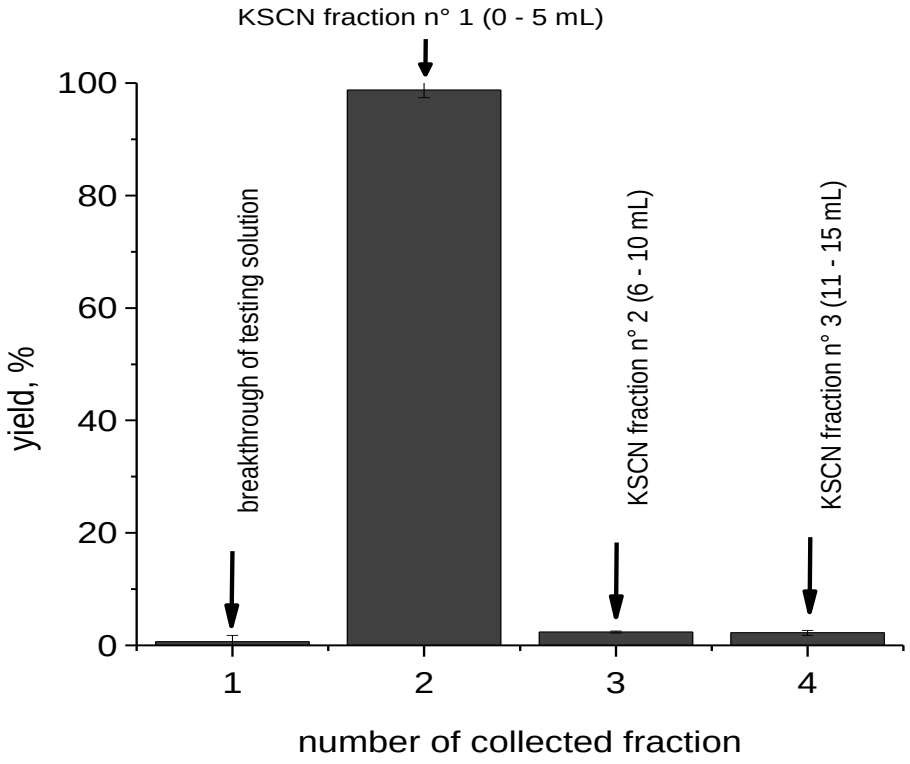

Fig. 85: Results of ^{36}Cl elution study, method optimization

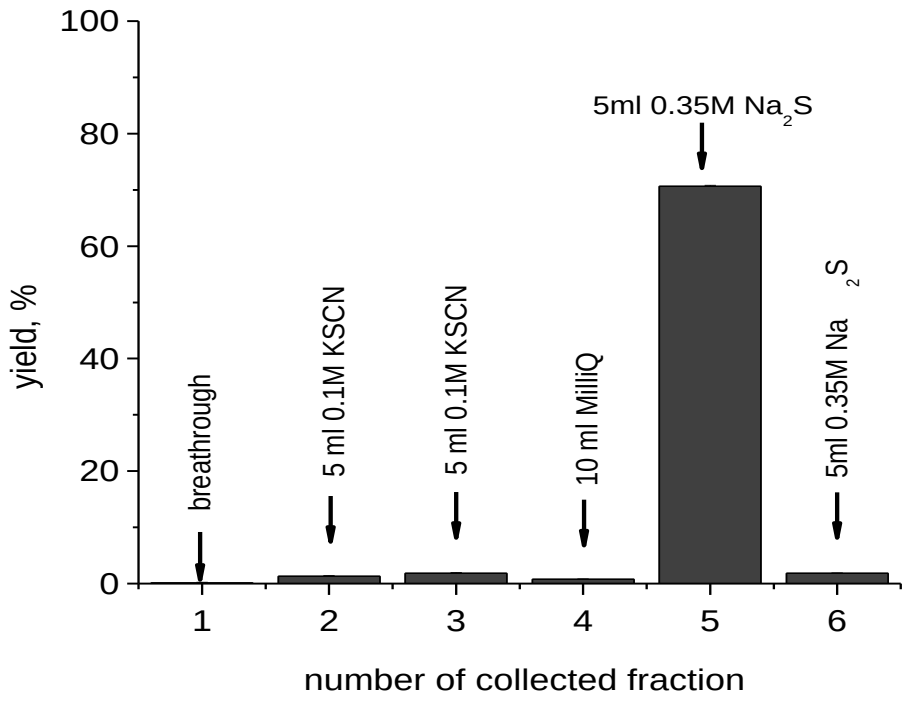

Fig. 86: Results of ^{129}I elution study, method optimization

Unfortunately the iodide yield was found to be only in the order of 70%. Follow up studies were performed applying various additional rinsing steps between the chloride and the iodide elution step including increasing amounts of deionized water, reducing and oxidizing agents and alkaline solutions. Fig. 87 shows the iodide yield in the iodide fraction in function of the rinsing step performed before the elution. 1% NH_3 and 1% NaOH solutions proved to be the best choice, resulting in near quantitative iodide elution. For practical reasons 1% NaOH was retained as additional rinsing step, since NH_3 complexed and eluted parts of the Ag^+ retained on the FClA resin column.

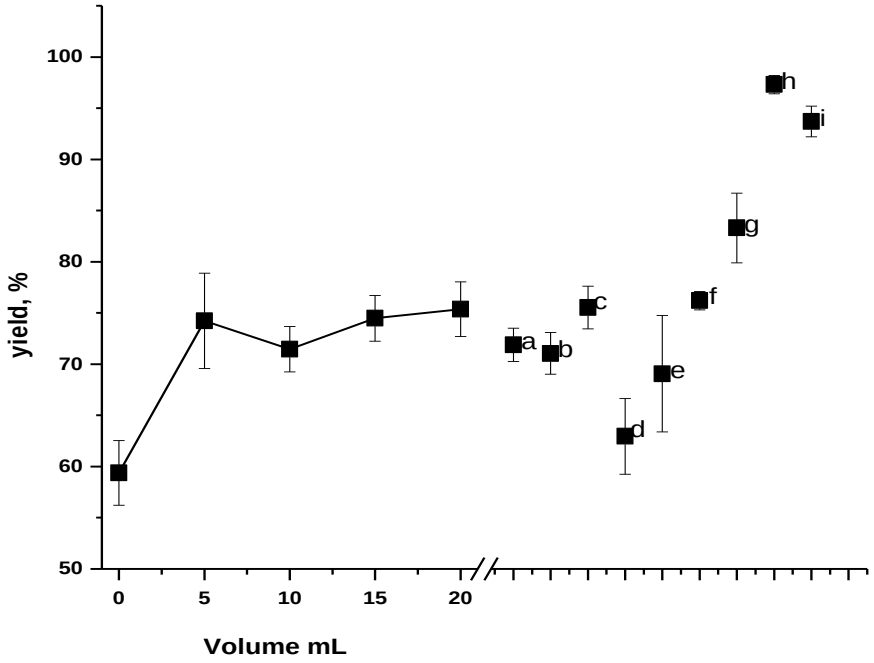

Fig. 87: Influence of the rinsing step upfront to the ^{129}I elution with Na_2S:

Rinsing with various volumes of deionized water; (a)10 mL 0.01M $NaHSO_3$, (b) 10 mL 0.1M $NaHSO_3$, (c) 10 mL 1M $NaHSO_3$, (d) 10 mL 1M $NaNO_2$, (e) 10 mL 30% H_2O_2, (f) 10 mL 1% NH_3 and (g) 10 mL 1% NaOH; 2 mL FCIA resin column (Ag^+ loaded)

In order to verify that the chloride / iodide separation is working sufficiently well for the foreseen use a solution containing ^{36}Cl and ^{129}I was separated using the described method, the observed separation is very clean, as Fig. 88 shows.

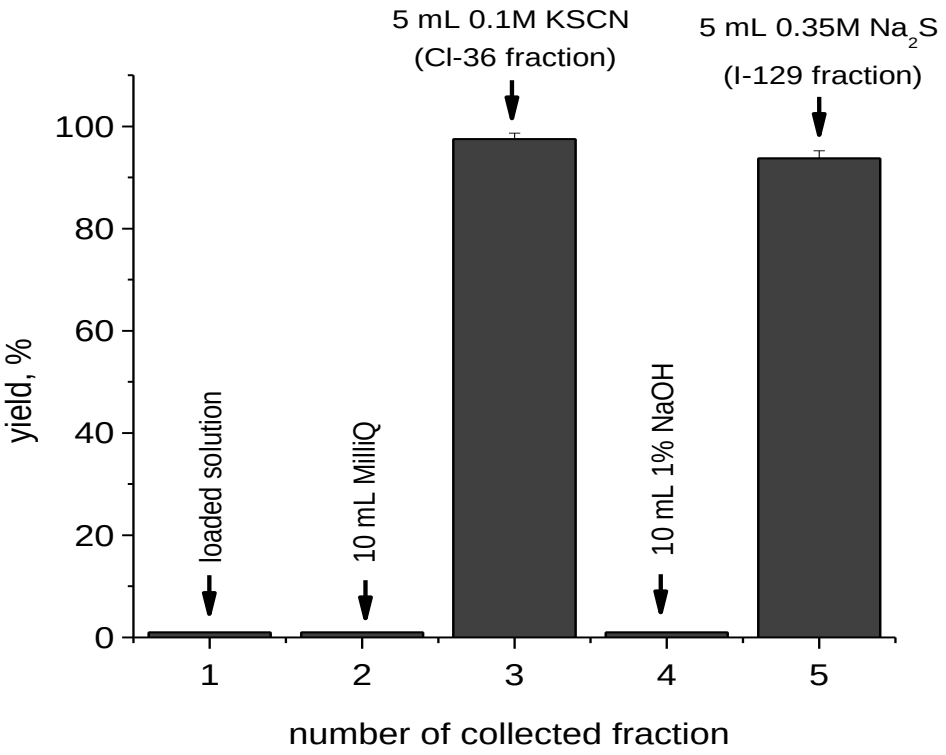

Fig. 88: Verification of the optimized method for the preconcentration and separation of ^{36}Cl and ^{129}I, separation of a ^{36}Cl and ^{129}I containing solution

The MilliQ wash step upfront to the KSCN step (Fig. 88) is a very important step with respect to the removal of potential interferences as can be seen from Fig. 89 and Fig. 90.

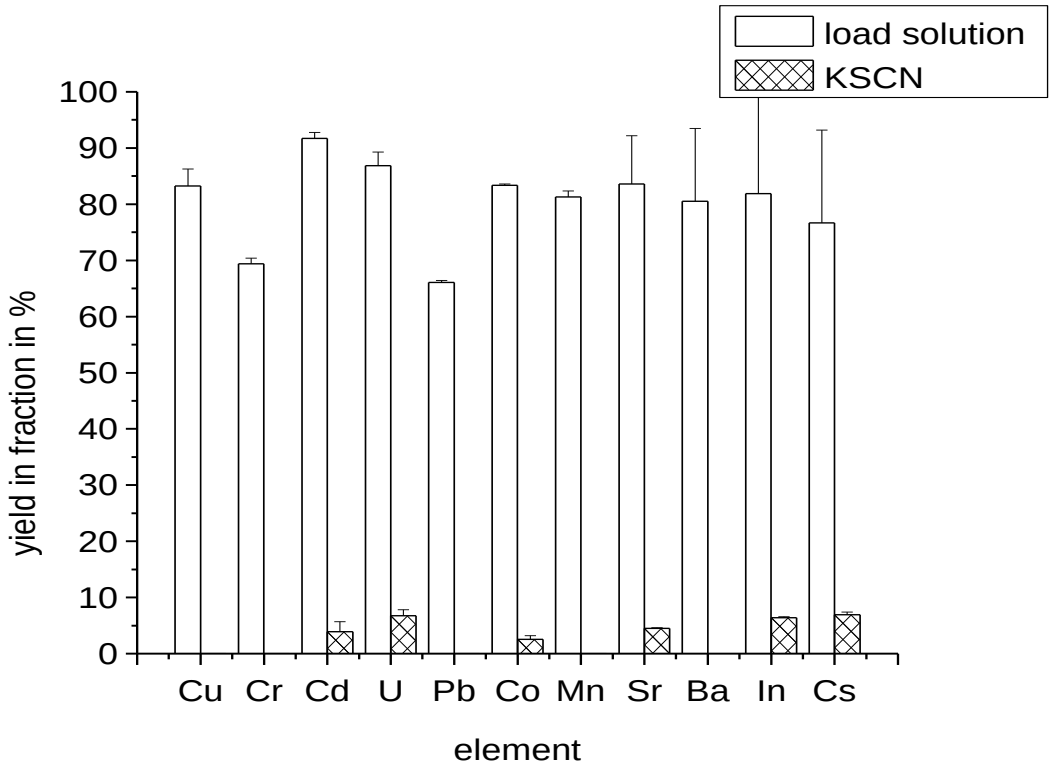

Fig. 89: Yield of various elements in KSCN fraction without additional MilliQ step before chloride elution

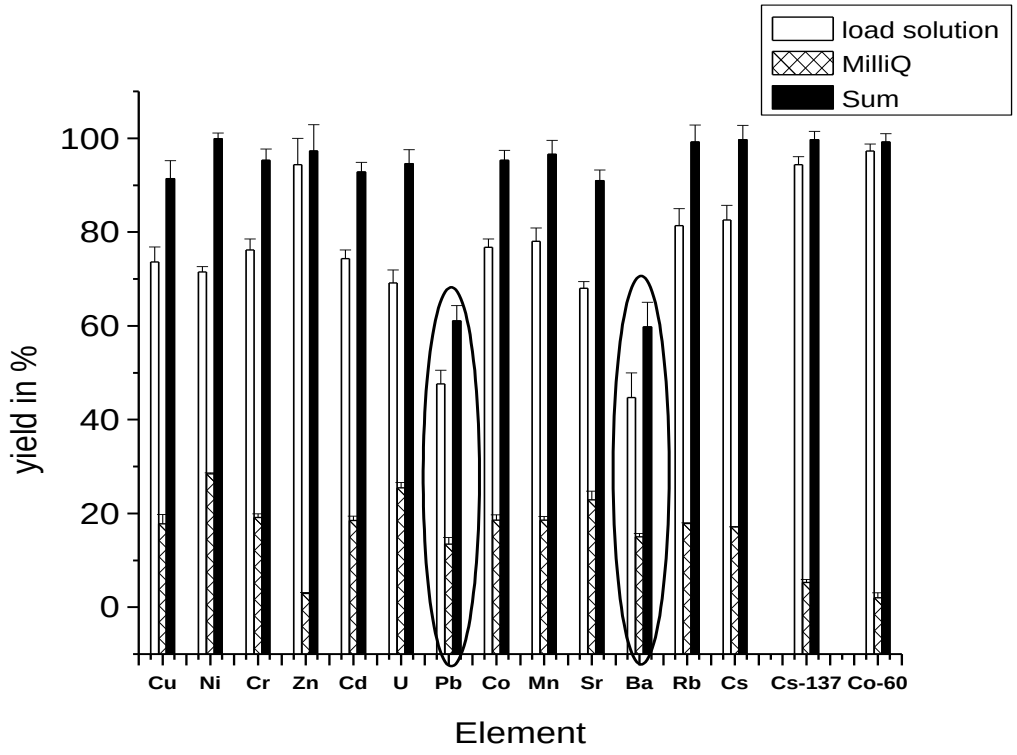

Fig. 90: Effect of the MilliQ wash step

Fig. 89 shows that without an additional wash step traces of potential interferences (Cd, U, Co, Sr, In, Cs) are found in the KSCN fraction. Thus elements in their radioactive form will fudge the Cl determination if present in the chloride fraction.

After the wash step KSCN fraction is expected to be clean (Fig. 90), since all interferences are removed quantitatively in the first two steps. Yields for Pb and Ba are about 60%. It is these elements form slightly soluble sulfates and remain partly on the column. To prove the cleanness of the chloride fraction decontamination factors were determined (see section 4.3.5.3).

The loading solution should preferably be adjusted to 1M H_2SO_4. Fig. 91 shows the results of a separation wherein the loading was performed from 1M NaOH. A large amount of chloride was eluted already during the loading and the rest is found in the MilliQ wash step. After adjusting the 1M NaOH solution to 1M H_2SO_4 and loading onto a column a clear separation of chloride and iodide was obtained (Fig. 92).

The separation was also performed with ClO_3^- and IO_3^- in two sets of experiments. In one set $SnSO_4$ was added to the loading solution (ClO_3^- and IO_3^-. in 1M H_2SO_4) as reducing agent, in the second set it was not added. In the case where $SnSO_4$ was not added a big amount of chlorate was eluted during the loading, the separation for iodate was not affected (Fig. 93). The result is not surprising since silver chlorate is water soluble [71] and iodate is precipitating on the column as silver iodate (K_{sp} = $3*10^{-8}$ [72]).

A clear separation of chlorate was then obtained after reducing with $SnSO_4$ (Fig. 94). Sn(II) is thus an efficient reducing agent for chlorate in 1M H_2SO_4. Iodine will be retained on the column as iodide as well as iodate.

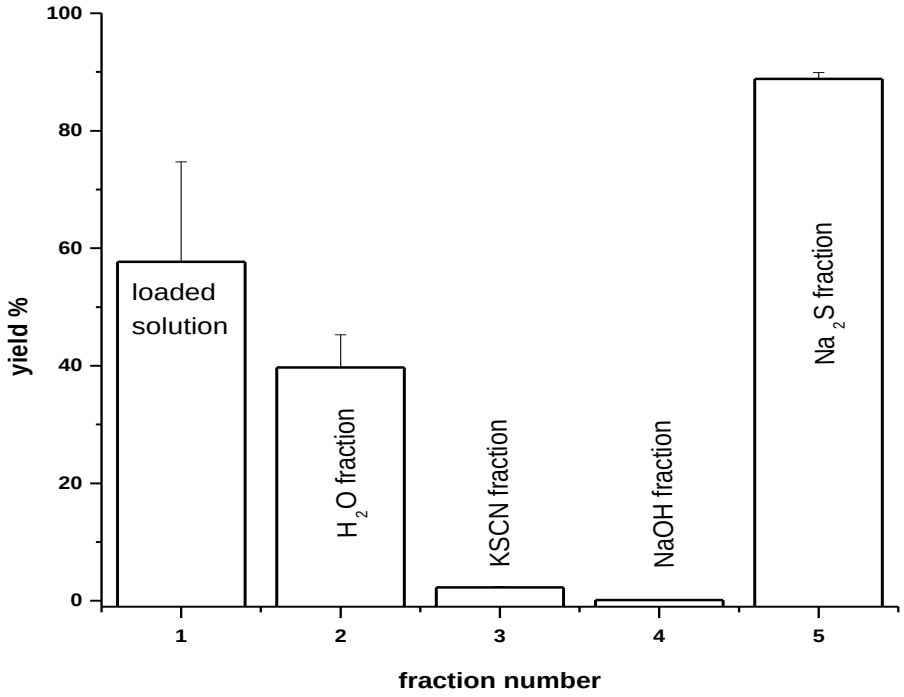

Fig. 91: Chloride and iodide separation from 1M NaOH as loading solution

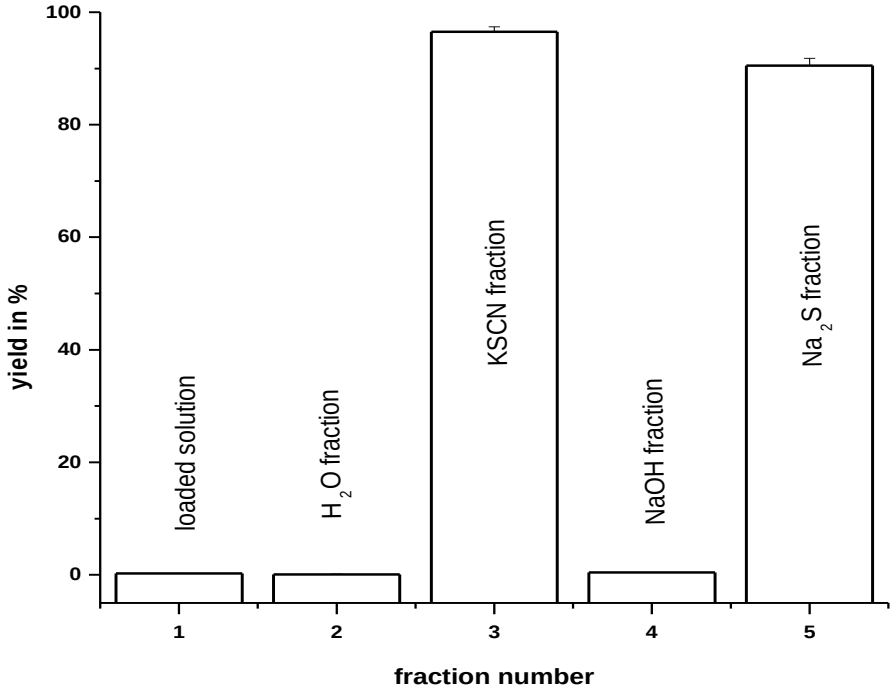

Fig. 92: Chloride and iodide separation from 1M NaOH adjusted to 1M H_2SO_4

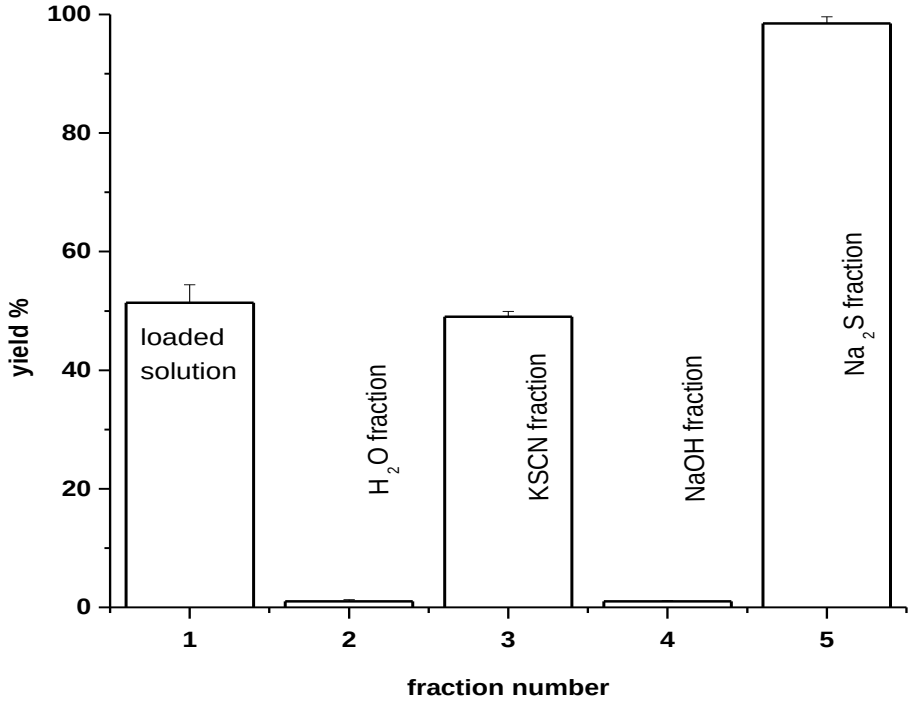

Fig. 93: Separation of chlorate and iodate from 1M H_2SO_4 as loading solution

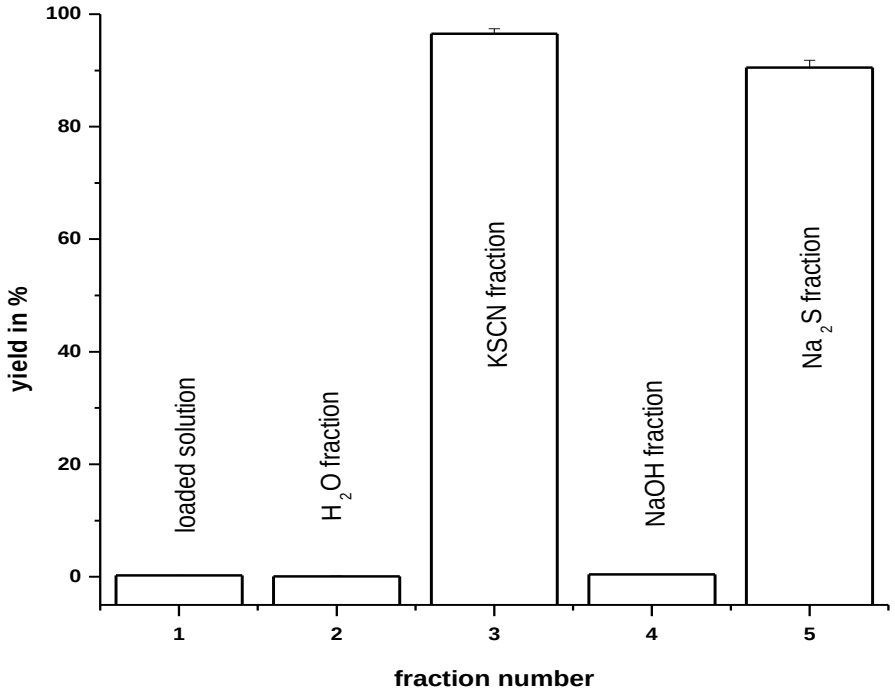

Fig. 94: Separation of chlorate and iodate from 1M H_2SO_4 after reduction with $SnSO_4$

4.3.4 Leaching experiments

There are several sample preparation methods for halogens, such as acid digestion [73-76], pyrohydrolysis [77-79], and tetramethyl ammonium hydroxide (TMAH) leaching [79-81] described in literature. When using acid digestion method losses of volatile halogen species, especially those of iodine, can occur; although no loss was observed for I determination when digestion vessels contained mineral acids and samples were treated under cool conditions. The pyrohydrolysis method is widely used because halogens show good volatility under high temperature conditions; therefore, it is possible to separate them from solid samples [79].

An increasingly popular alternative approach to acid digestion is alkaline extraction with TMAH. Alkaline solutions suppress the formation of volatile iodine species; however, incomplete extractions were observed for certain samples. The disadvantage of TMAH is that it contains considerable amounts of iodine as a contaminant [73].

In this study both alternatives, acidic and alkaline leaching, were tested. The procedure was adapted from [81] and modified:

Approximately 200 mg of soil, 300 mg of concrete and 170 mg of filter, respectively, were weight in a test-tube, spiked with 50 Bq ^{36}Cl or ^{129}I, filled with 5 ml of 1% NH_3, 1% NaOH, 1% HNO_3 or 1% H_2SO_4, respectively, capped and stored in a drying chamber for 4 hours at 70°C. After cooling to room temperature, all tubes were centrifuged and the matrices washed two times with 2 ml MilliQ. The combined solutions of each test-tube were collect in a LSC vial, filled with ProSafe and counted for 10 minutes. The results are summarized in Table 12.

The overall best yields, for all matrices as well as for both radioisotopes, were obtained with 1M NaOH.

		^{36}Cl			^{129}I		
		Mean yield / %	**SD**	**RSD / %**	**Mean yield / %**	**SD**	**RSD / %**
soil	1% NH_3	100.0	2.1	2.1	75.7	5.9	7.8
	1% HNO_3	98.4	1.4	1.4	60.7	2.3	3.8
	1% H_2SO_4	99.2	0.5	0.5	76.1	1.5	1.9
	1% NaOH	100.0	3.6	3.6	87.5	4.1	4.7
	1M NaOH	98.7	0.9	0.9	100.9	1.3	1.3
concrete	1% NH_3	60.1	6.0	9.9	62.7	4.2	6.8
	1% HNO_3	66.6	6.7	10.0	50.1	4.3	8.6
	1% H_2SO_4	61.5	4.5	7.4	62.8	9.1	14.5
	1% NaOH	79.3	3.6	4.6	84.7	2.6	3.1
	1M NaOH	84.7	2.6	3.1	93.0	3.5	3.8
filter	1% NH_3	101.2	2.0	2.0	82.5	2.5	3.0
	1% HNO_3	95.0	1.2	1.2	64.1	0.2	0.3
	1% H_2SO_4	96.2	0.8	0.9	93.3	0.8	0.9
	1% NaOH	92.6	0.1	0.1	94.0	0.4	0.4

Table 12: Results of leaching experiments; soil, concrete and filter matrices; chloride and iodide yields

4.3.5 Validation

4.3.5.1 Applicability

The best suited separation method can be summarized as follows:

The sample loading solutions are adjusted to 1M H_2SO_4 (in order to assure that iodine and chlorine are present as chloride and iodide Sn(II) might be added to the sample loading solution) and loaded onto the Ag^+ loaded FClA resin column. The column loading is followed by a first rinsing step with 10 mL deionized water in order to increase the pH on the column and to remove matrix elements and potential interferents. Chloride is eluted with 5 mL 0.1M KSCN. The column is then further rinsed with 10 mL 1% NaOH in order to optimize the iodide elution and finally iodide is eluted using 5 mL 0.35M Na_2S. Fig. 95 summarizes the method.

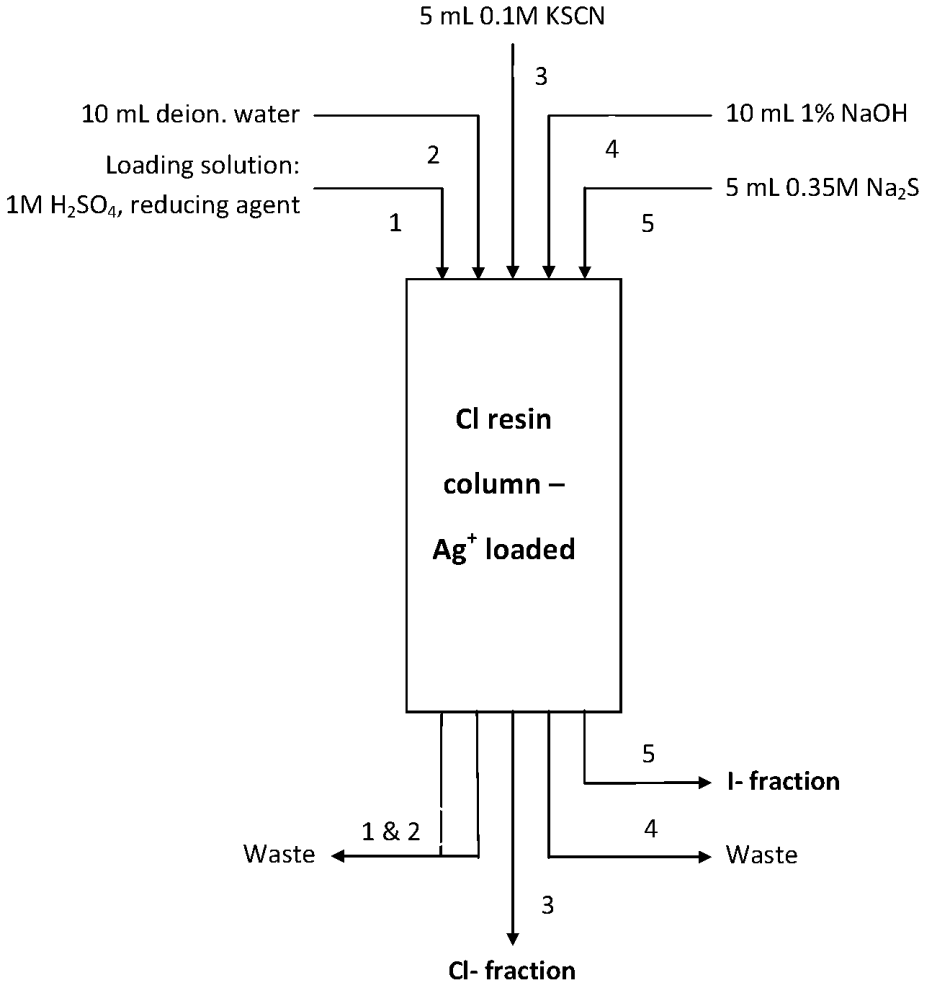

Fig. 95: Method to be validate

Spiked tap water, soil, concrete and filter samples were used for the validation.

The method was validated in the range of 1-90 Bq for ^{36}Cl and ^{129}I, respectively.

4.3.5.2 Sensitivity

Before validating the method sensitivity, the linearity of the counting device used during the validation process 1220 Quantulus, was controlled.

To check for linearity of the counting device standard samples of ^{36}Cl and ^{129}I in the range of 1 – 90 Bq were counted. Count rates were then plotted against spiked activities. Results are shown in Fig. 96 and Fig. 97.

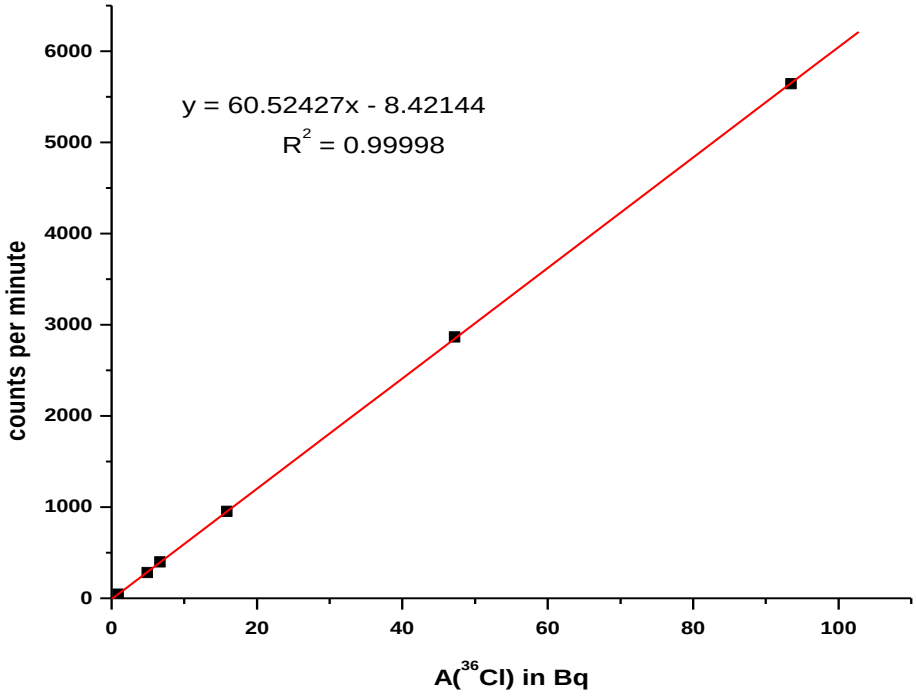

Fig. 96: Linearity for ^{36}Cl

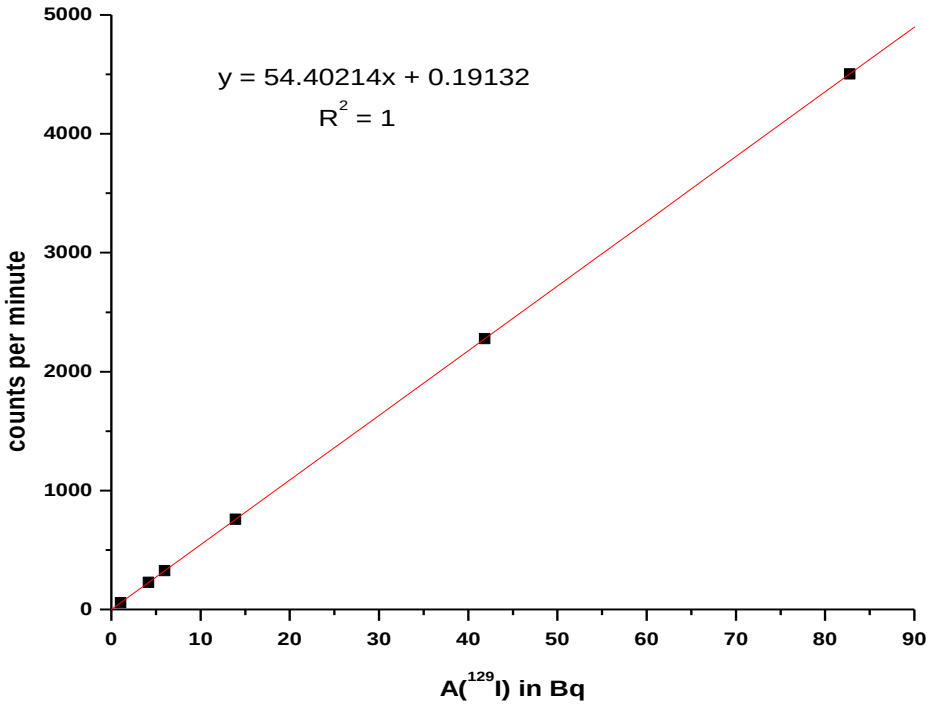

Fig. 97: Linearity for ^{129}I

Data obtained from linearity measurements were also used to calculate counting efficiencies of ^{36}Cl and ^{129}I. Actually, efficiency is depending on the so called quenching parameter SQP.

Table 13 shows the precision of the sample quench parameter (SQP), which is very good (for both isotopes < 1%).

SQP was measured for KSCN and Na_2S fractions, data were collected by measuring the samples for three day, 10 samples per day and calculated using eq. 13 - eq. 15.

Fraction	M_t	S_w	rel. S_w in%	S_b	rel. S_b in%	S_t	rel. S_t in%
KSCN	701.70	3.51	0.5	1.19	0.2	3.70	0.5
Na_2S	743.78	4.10	0.6	2.23	0.3	4.66	0.6

Table 13: precision of SQP; mean SQP (M_t), intra-day standard deviation (N = 10) s_b, inter day standard deviation (N=3) s_w, combined total standard deviation s_t

The results for precision of the SQP imply that when preparing the standard sample exactly the same way as the counting sample it is not necessary to consider the SQP. Efficiency is then calculated by

$$\varepsilon = \frac{R_{b,k} - R_0}{A_k} \qquad \textbf{eq. 28}$$

Where $R_{b,k}$ is the gross counting rate of the standard sample in seconds, R_0 is background counting rate in seconds and A_k the (certified) activity of the standard sample in Bq.

Relative standard deviation of the efficiency is then

$$\frac{s(\varepsilon)}{\varepsilon} = \sqrt{\frac{\frac{R_{b,k}}{t_m} + \frac{R_0}{t_0}}{(R_{b,k} - R_0)^2} + \left(\frac{s(A_k)}{A_k}\right)^2} \qquad \textbf{eq. 29}$$

Where $R_{b,k}$ is the gross counting rate of the standard sample in seconds, R_0 is background counting rate in seconds and A_k the (certified) activity of the standard sample in Bq, t_m and t_0 the counting time in seconds for the standard sample and background respectively, $s(A_k)$ is the uncertainty given for the (certified) activity.

Efficiencies for ^{36}Cl and ^{129}I were calculated from linearity measurement data and were found to be (1.00 ± 0.05) $s^{-1}\,Bq^{-1}$ and (0.900 ± 0.045) $s^{-1}\,Bq^{-1}$ respectively.

During the whole method validation standard samples were prepared in the same way as counting samples by running a blank sample in parallel and then spiking the respective fraction of the blank sample with either ^{36}Cl or ^{129}I.

For the calculation of the activity concentration c and its uncertainty following equations were used:

$$c = \frac{R_b - R_0}{\varepsilon \cdot Y} \qquad \textbf{eq. 30}$$

Where R_b is the gross counting rate of the sample in seconds, R_0 is background counting rate in seconds, ε the efficiency in $Bq^{-1}s^{-1}$ and Y the yield (for yields see Table 19).

$$\frac{s(c)}{c} = \sqrt{\frac{\frac{R_b}{t_m} + \frac{R_0}{t_0}}{(R_b - R_0)^2} + \left(\frac{s(\varepsilon)}{\varepsilon}\right)^2 + \left(\frac{s(Y)}{Y}\right)^2} \qquad \textbf{eq. 31}$$

Where R_b is the gross counting rate of the sample in seconds, R_0 is background counting rate in seconds, relative standard deviation for the efficiency is calculated by eq. 29, yields and uncertainty of the yield were determined experimentally during studies on precision in section 4.3.4.4.

4.3.5.3 Selectivity

The selectivity of the method was evaluated by determining of decontamination factors of various potential interferents in the chloride and the iodide fractions.

Data obtained during the chloride / iodide elution studies using the optimized method were also used to calculate decontamination factors (D_f) for chloride and iodide in the respective iodide and chloride fractions. These were calculated according to eq. 10.

In case the count rate in the respective fraction was lower than the limit of detection (LOD) of the used counting devise, N_A in eq. 10 was replaced by the LOD and the decontamination factor D_f was calculated according to eq. 32

$$D_f \geq \frac{N_{A0}}{LOD} \qquad \textbf{eq. 32}$$

where LOD is calculated for LSC measurements using eq. 18.

The method to be validated was further applied to loading solutions containing a number of different elements (Cr, Mn, Co, Ni, Cu, Zn, Rb, Sr, Cd, Cs, Ba, Pb, U; all 10 µg in 10 mL loading solution). Chloride and iodide fractions were collected and analyzed by ICP-MS; decontamination factors for these elements were calculated as indicated above, in case the concentration of an element was below the decision limit of the ICP-MS the decontamination factors were calculated according to eq. 32 with LOD being three times the standard deviation of the background count rate of the element in the blank sample.

Finally loading solutions containing known activities of $^{90}Sr/^{90}Y$, ^{60}Co or ^{137}Cs were prepared and separated on the Ag^+ loaded FClA columns, chloride and iodide fractions were collected and analyzed by LSC, decontamination factors were calculated as mentioned above.

The determined decontamination factors D_f are summarized in Table 14. In all cases the net count rates in the chloride and iodide fractions were below the respective limits of detection, accordingly all D_f values are given as being “greater than”. Overall the results indicate that the FClA resin and the chosen separation method show a suitable selectivity for the intended use.

Analyte	D_f in Cl^- fraction	D_f in I^- fraction
Ba	>1000	>600
Cd	>6900	>7700
Co	>170	>1500
Cr	>29	>430
Cs	>200	>6200
Cu	>210	>190
Mn	>210	>370
Ni	>170	>320
Pb	>300	>720
Rb	>16	>2300
Sr	>180	>17000
U	>1900	>200
Zn	>32	>11
^{60}Co	>320	>320
^{137}Cs	>150	>150
$^{90}Sr/^{90}Y$	>180	>160
^{36}Cl	NA	>160
^{129}I	>420	NA

Table 14: Decontamination factors D_f of various elements in chloride and iodide fractions

4.3.5.4 Precision

Precision experiments in column experiments were performed by spiking a 300 mL tap water sample with ^{36}Cl and ^{129}I (activity level of the final sample: each 0.5 $Bq.mL^{-1}$); homogenizing and dividing it into 30 subsamples. The samples were analyzed over three days, 10 samples per day. Standard deviations were calculated according to eq. 13 - eq. 15, wherein the total combined standard deviation s_t was calculated from the intra-day standard deviation s_b and the inter-day standard deviation s_w.

Table 15 shows the results of these precision experiments. The chloride elution shows very good precision with a $s_t < 3\%$. The precision of the iodide elution on the other hand is acceptable, but with a s_t in the order of 9% significantly lower than the chloride precision. In any case it is advisable to use stable chloride and iodide as internal standards.

Analyte	**M_t , %**	**s_w , %**	**s_b , %**	**s_t , %**
^{36}Cl	96.98	2.39	0.20	2.40
^{129}I	91.66	5.20	7.62	9.22

Table 15: Results of precision experiments for tap water: mean ^{36}Cl and ^{129}I yields (M_t), intra-day standard deviation (N = 10) s_b, inter day standard deviation (N=3) s_w, combined total standard deviation s_t

Further precision experiments were performed for the leaching procedure for spiked soil, concrete and filter samples. 250 mg of the respective matrix sample was spiked with 50 Bq ^{36}Cl and ^{129}I, respectively, and leached in 1M NaOH as described in section 4.3.3. The samples were analyzed over three days, three samples per day. Standard deviations were calculated according to eq. 13 - eq. 15, wherein the total combined standard deviation s_t was calculated from the intra-day standard deviation s_b and the inter-day standard deviation s_w.

Table 16 - Table 18 show the results of these precision experiments. The chloride and iodide leaching shows overall good precisions with a $s_t < 15\%$. In any case also in case ^{36}Cl and ^{129}I should be leached from matrix samples it is advisable to use stable chloride and iodide as internal standards.

Analyte	**M_t , %**	**s_w , %**	**s_b , %**	**s_t , %**
^{36}Cl	98.55	6.8	3.2	7.5
^{129}I	100.13	2.0	0.4	2.1

Table 16: Results of precision experiments for soil: mean ^{36}Cl and ^{129}I yields (M_t), intra-day standard deviation (N = 3) s_b, inter day standard deviation (N=3) s_w, combined total standard deviation s_t

Analyte	M_t , %	s_w , %	s_b , %	s_t , %
^{36}Cl	90.55	2.2	5.7	6.1
^{129}I	98.41	5.7	5.1	7.6

Table 17: Results of precision experiments for concrete: mean ^{36}Cl and ^{129}I yields (M_t), intra-day standard deviation (N = 3) s_b, inter day standard deviation (N=3) s_w, combined total standard deviation s_t

Analyte	M_t , %	s_w , %	s_b , %	s_t , %
^{36}Cl	93.51	3.5	4.0	5.3
^{129}I	103.91	9.2	11.4	14.6

Table 18: Results of precision experiments for filter: mean ^{36}Cl and ^{129}I yields (M_t), intra-day standard deviation (N = 3) s_b, inter day standard deviation (N=3) s_w, combined total standard deviation s_t

To obtain overall yields the yield of the column experiment was combined with the yield of the leaching experiment for the respective matrix by

$$M_{combined} = M_{column} \cdot M_{matrix} \qquad \textbf{eq. 33}$$

To obtain the overall precision common total standard deviations from column experiments and leaching experiments for the respective matrix were combined by

$$s_{t,comb} = \sqrt{s_{t,column}^2 + s_{t,matrix}^2} \qquad \textbf{eq. 34}$$

Results of the calculations are summarized in Table 19.

	^{36}Cl		^{129}I	
	M_t , %	**rel s_t , %**	**M_t , %**	**rel. s_t , %**
column	97.0	2.4	91.7	9.2
soil	98.6	7.5	100.1	2.1
concrete	90.6	6.1	98.4	7.6
filter	93.5	5.3	103.9	14.6
column combined with	^{36}Cl		^{129}I	
	M_t comb., %	**rel. s_t comb., %**	**M_t comb., %**	**rel. s_t comb., %**
soil	95.6	7.9	91.8	9.4
concrete	87.8	6.6	90.2	11.9
filter	90.7	5.8	95.2	17.3

Table 19: Combined yields and precisions

Table 19 shows the results of the calculations for combined precisions. The combined precision for chloride is overall good with a s_t comb < 15%. The combined precision for iodide is also good but in case of filter only acceptable (s_t > 15%). The overall yields are also good with ≥ 90% (exception for chloride from concrete, with 87.8% still acceptable).

4.3.5.5 Linearity

According to the German Radiation Protection Ordinance [82] limiting values for release are as follows:

- For sewage water > 10^5 m^3 a^{-1}: 10 Bq l^{-1} for ^{36}Cl and 4 Bq l^{-1} for ^{129}I
- For decommissioning waste and excavated soil > 1000 t a^{-1}: 1 Bq g^{-1} for ^{36}Cl and 0.1 Bq g^{-1} for ^{129}I
- For exhaust air in the range 10^4 m^3 h^{-1} – 10^5 m^3 h^{-1}: 0.1 Bq m^{-3} for ^{36}Cl and 0.03 Bq m^{-3} for ^{129}I. It is to mention that according to the “Measuring instructions for the supervision of the activity derivations of radioactive materials with the exhaust air from nuclear-technical arrangements” [83] samples should be taken at 20 m^3 h^{-1} – 150 m^3 h^{-1}

However, linearity was determined by preparing of five load solutions containing ^{36}Cl and ^{129}I in the range of 1-90 Bq respectively. Solutions were loaded onto five columns and these were eluted by the optimized method.

Appropriate fractions were counted by LSC, activity concentrations were calculated according to eq. 30 and then plotted against the spiked activities (Fig. 98 and Fig. 99).The criterion of acceptance is given by the correlation coefficient R^2. Since R^2 is greater than 0.995 in both cases the method is assumed to be linear for chloride and iodide.

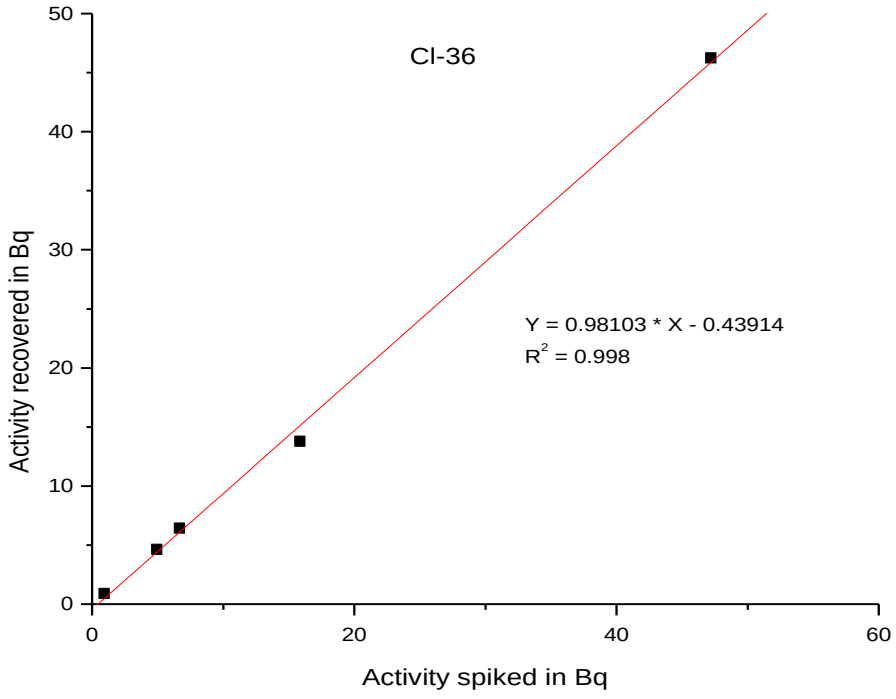

Fig. 98: Linearity for Cl-36

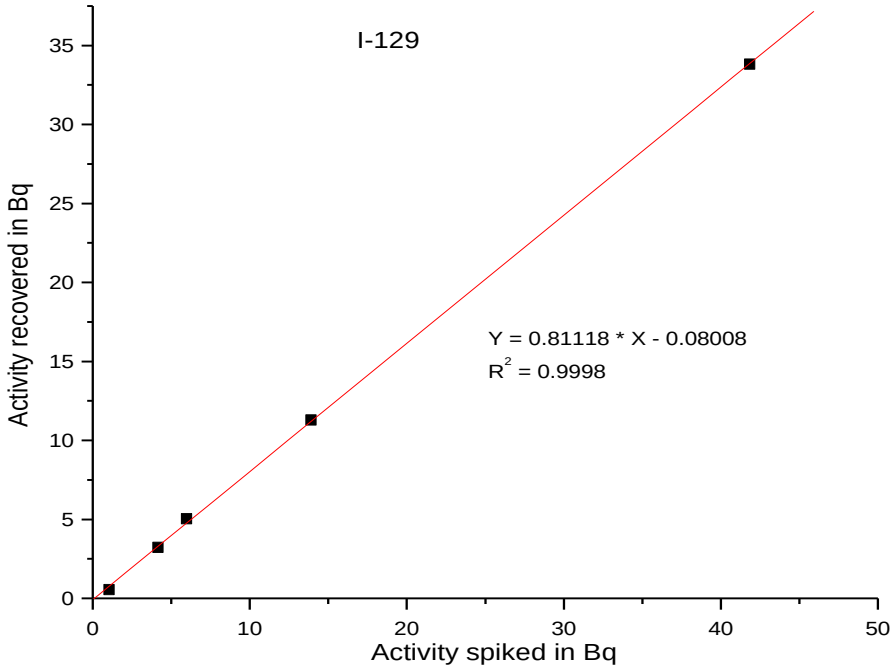

Fig. 99: Linearaty for I-129

4.3.5.6 Trueness

A simulated real sample was prepared by adding well known activities of ^{36}Cl (47.2 ± 2.4 Bq) and ^{129}I (41.1 ± 3.1 Bq), as well as known activity levels of ^{60}Co, $^{90}Sr/^{90}Y$ and ^{137}Cs (each 85 Bq) to 50 mL of a tap water sample previously adjusted to 1M H_2SO_4. 10 mL aliquots of this solution were analyzed in triplicate following the method to be validated, and the chloride and iodide fractions were analyzed by LSC.

Further simulated real samples were prepared by spiking soil, concrete and filter samples and allowing to dry. These were then leached, adjusted to 1M H_2SO_4 and filled to exactly 50 ml. 10 mL aliquots of these solutions were analyzed in triplicate following the optimized separation method, and the chloride and iodide fractions were analyzed by LSC.

Mean yields and contributions of the precision to the overall uncertainty were taken from the results of the precision experiments and used for activity and uncertainty calculation (eq. 30 and eq. 31). Results were evaluated according to eq. 11 and. eq. 12.

Table 20 - Table 23 compare the results obtained experimentally with the expected results. The determined and reference activities agree well, the E_n values are below 1. The determined results are thus not deviating significantly from the expected ones. The bias between determined and expected results is well below 15%, nevertheless some of the results show a slight negative bias, the use of an internal standard, for ^{36}Cl as well as for ^{129}I, is thus advisable.

	determined activities		reference activities			
^{129}I	A(^{129}I) ,	$U_{A(129I)}$,	A(^{129}I) ,	$U_{A(129I)}$,	Bias , %	E_n
Repl. 1	8.24	1.98	8.22	1.31	0.3	0.01
Repl. 2	8.17	1.97	8.22	1.31	-0.5	0.02
Repl. 3	7.86	1.89	8.22	1.31	-4.4	0.16
^{36}Cl	A(^{36}Cl) ,	$U_{A(36Cl)}$,	A(^{36}Cl) ,	$U_{A(36Cl)}$,	Bias , %	E_n
Repl. 1	8.97	1.05	9.44	0.94	-5.1	0.34
Repl. 2	9.11	1.06	9.44	0.94	-3.5	0.23
Repl. 3	9.12	1.06	9.44	0.94	-3.5	0.23

Table 20: tap water: Comparison of determined and reference activities, 3 replicates, bias and En, k=2

	determined activities		reference activities			
^{129}I	A(^{129}I) , Bq	$U_{A(129I)}$, Bq	A(^{129}I) , Bq	$U_{A(129I)}$, Bq	Bias , %	E_n
Repl. 1	7.89	2.82	8.22	1.31	-4.04	0.11
Repl. 2	8.28	2.96	8.22	1.31	0.78	0.02
Repl. 3	7.58	2.71	8.22	1.31	-7.79	0.21
^{36}Cl	A(^{36}Cl) , Bq	$U_{A(36Cl)}$, Bq	A(^{36}Cl) , Bq	$U_{A(36Cl)}$, Bq	Bias , %	E_n
Repl. 1	9.58	1.47	9.44	0.94	1.46	0.08
Repl. 2	9.20	1.41	9.44	0.94	-2.52	0.14
Repl. 3	9.70	1.48	9.44	0.94	2.71	0.15

Table 21: filter: Comparison of determined and reference activities, 3 replicates, bias and En, k=2

	determined activities		reference activities			
^{129}I	A(^{129}I) , Bq	$U_{A(129I)}$, Bq	A(^{129}I) , Bq	$U_{A(129I)}$, Bq	Bias , %	E_n
Repl. 1	7.71	1.96	8.22	1.31	-6.22	0.22
Repl. 2	7.74	1.97	8.22	1.31	-5.83	0.20
Repl. 3	7.61	1.94	8.22	1.31	-7.36	0.26
^{36}Cl	A(^{36}Cl) , Bq	$U_{A(36Cl)}$, Bq	A(^{36}Cl) , Bq	$U_{A(36Cl)}$, Bq	Bias , %	E_n
Repl. 1	9.40	1.56	9.44	0.94	-0.47	0.02
Repl. 2	9.32	1.54	9.44	0.94	-1.30	0.07
Repl. 3	9.35	1.55	9.44	0.94	-0.91	0.05

Table 22: concrete: Comparison of determined and reference activities, 3 replicates, bias and En, k=2

	determined activities		reference activities			
^{129}I	A(^{129}I) , Bq	$U_{A(129I)}$, Bq	A(^{129}I) , Bq	$U_{A(129I)}$, Bq	Bias , %	E_n
Repl. 1	7.65	1.59	8.22	1.31	-6.94	0.28
Repl. 2	7.60	1.58	8.22	1.31	-7.49	0.30
Repl. 3	7.47	1.56	8.22	1.31	-9.09	0.37
^{36}Cl	A(^{36}Cl) , Bq	$U_{A(36Cl)}$, Bq	A(^{36}Cl) , Bq	$U_{A(36Cl)}$, Bq	Bias , %	E_n
Repl. 1	9.39	1.76	9.44	0.94	-0.55	0.03
Repl. 2	9.59	1.79	9.44	0.94	1.60	0.07
Repl. 3	9.55	1.79	9.44	0.94	1.20	0.06

Table 23: soil: Comparison of determined and reference activities, 3 replicates, bias and En, k=2

4.3.5.7 Recoveries

Recoveries were calculated from data obtained for trueness by following equations:

$$\overline{R_m} = \frac{\overline{A_{obs}}}{A_{spike}} \quad \textbf{eq. 35}$$

Where $\overline{A_{obs}}$ is the mean of the calculated activity and A_{spike} is the spiked activity

$$\text{and } u(\overline{R}_m) = \overline{R}_m \times \sqrt{\left(\frac{s_{obs}^2}{n \times \overline{A}_{obs}^2}\right) + \left(\frac{u(A_{spike})}{A_{spike}}\right)^2} \quad \textbf{eq. 36}$$

where s_{obs} is the standard deviation of the replicate analysis of the spiked sample, n is the number of replicates and $u(A_{spike})$ is the standard uncertainty in the concentration of the spiked sample [84].

Results were evaluated by

$$t = \frac{|1-\overline{R}_m|}{u(\overline{R}_m)} \quad \textbf{eq. 37}$$

With a decision level $t_{krit} \leq 2$ [85]

Table 24 - Table 27 summarize the results on recovery for ^{36}Cl and ^{129}I determined in spiked tap water, filter, concrete and soil.

All recoveries were found to be not deviating significantly from 1 and the t-value is well below 2; calculated and determined recoveries thus match well.

	determined activities		reference activities							
^{129}I	**A(^{129}I) Bq**	**$u_{A(129I)}$ Bq**	**A(^{129}I) Bq**	**$u_{A(129I)}$ Bq**	**$\overline{A_{obs}}$, Bq**	**s_{obs}**	**$\overline{R_m}$**	**$u(R_m)$**	**$U(R_m)$**	**t-Test**
Repl. 1	8.24	0.99	8.22	0.65	8.09	0.20	0.93	0.07	0.15	0.94
Repl. 2	8.17	0.99	8.22	0.65						
Repl. 3	7.86	0.95	8.22	0.65						
^{36}Cl	**A(^{36}Cl) Bq**	**$u_{A(36Cl)}$ Bq**	**A(^{36}Cl) Bq**	**$u_{A(36Cl)}$ Bq**	**$\overline{A_{obs}}$. Bq**	**s_{obs}**	**$\overline{R_m}$**	**$u(R_m)$**	**$U(R_m)$**	**t-Test**
Repl. 1	8.97	0.53	9.44	0.47	9.07	0.08	0.96	0.05	0.10	0.82
Repl. 2	9.11	0.53	9.44	0.47						
Repl. 3	9.12	0.53	9.44	0.47						

Table 24: tap water: Calculation of the recoveries and t-test

	determined activities		reference activities							
^{129}I	**A(^{129}I) Bq**	**$u_{A(129I)}$ Bq**	**A(^{129}I) Bq**	**$u_{A(129I)}$ Bq**	**$\overline{A_{obs}}$, Bq**	**s_{obs}**	**$\overline{R_m}$**	**$u(R_m)$**	**$U(R_m)$**	**t-Test**
Repl. 1	7.89	1.41	8.22	0.65	7.92	0.35	0.96	0.08	0.16	0.46
Repl. 2	8.28	1.48	8.22	0.65						
Repl. 3	7.58	1.35	8.22	0.65						
^{36}Cl	**A(^{36}Cl) Bq**	**$u_{A(36Cl)}$ Bq**	**A(^{36}Cl) Bq**	**$u_{A(36Cl)}$ Bq**	**$\overline{A_{obs}}$, Bq**	**s_{obs}**	**$\overline{R_m}$**	**$u(R_m)$**	**$U(R_m)$**	**t-Test**
Repl. 1	9.58	0.73	9.44	0.47	9.49	0.26	1.005	0.05	0.10	0.10
Repl. 2	9.20	0.70	9.44	0.47						
Repl. 3	9.70	0.74	9.44	0.47						

Table 25: filter: Calculation of the recoveries and t-test

	determined activities		reference activities							
^{129}I	**A(^{129}I) Bq**	**$u_{A(129I)}$ Bq**	**A(^{129}I) Bq**	**$u_{A(129I)}$ Bq**	**$\overline{A_{obs}}$, Bq**	**s_{obs}**	**$\overline{R_m}$**	**u(R_m)**	**U(R_m)**	**t-Test**
Repl. 1	7.71	0.98	8.22	0.65	7.69	0.07	0.94	0.07	0.15	0.87
Repl. 2	7.74	0.98	8.22	0.65						
Repl. 3	7.61	0.97	8.22	0.65						
^{36}Cl	**A(^{36}Cl) Bq**	**$u_{A(36Cl)}$ Bq**	**A(^{36}Cl) Bq**	**$u_{A(36Cl)}$ Bq**	**$\overline{A_{obs}}$, Bq**	**s_{obs}**	**$\overline{R_m}$**	**u(R_m)**	**U(R_m)**	**t-Test**
Repl. 1	9.40	0.78	9.44	0.47	9.36	0.04	0.99	0.05	0.10	0.18
Repl. 2	9.32	0.77	9.44	0.47						
Repl. 3	9.35	0.77	9.44	0.47						

Table 26: concrete: Calculation of the recoveries and t-test

	determined activities		reference activities							
^{129}I	**A(^{129}I) Bq**	**$u_{A(129I)}$ Bq**	**A(^{129}I) Bq**	**$u_{A(129I)}$ Bq**	**$\overline{A_{obs}}$, Bq**	**s_{obs}**	**$\overline{R_m}$**	**u(R_m)**	**U(R_m)**	**t-Test**
Repl. 1	7.65	0.80	8.22	0.65	7.58	0.09	0.93	0.07	0.15	0.95
Repl. 2	7.60	0.79	8.22	0.65						
Repl. 3	7.47	0.78	8.22	0.65						
^{36}Cl	**A(^{36}Cl) Bq**	**$u_{A(36Cl)}$ Bq**	**A(^{36}Cl) Bq**	**$u_{A(36Cl)}$ Bq**	**$\overline{A_{obs}}$, Bq**	**s_{obs}**	**$\overline{R_m}$**	**u(R_m)**	**U(R_m)**	**t-Test**
Repl. 1	9.39	0.88	9.44	0.47	9.51	0.11	1.01	0.05	0.10	0.15
Repl. 2	9.59	0.90	9.44	0.47						
Repl. 3	9.55	0.89	9.44	0.47						

Table 27: soil: Calculation of the recoveries and t-test

4.3.5.8 Ruggedness

To study the ruggedness of the method it was performed by three more persons. The method is robust when intra-person standard deviation s_b, inter-person standard deviation s_w and the combined total standard deviation s_t are below 15%. Yields are expected to be greater than 90%. Values were calculated from eq. 13 - eq. 15.

Analyte	M_t %	s_w	rel. s_w %	s_b	rel. s_b %	s_t	rel. s_t %
Cl-36	94.96	4.85	5.1	4.79	5.0	6.81	7.2
I-129	97.34	5.51	5.7	3.72	3.8	6.65	6.8

Table 28: mean ^{36}Cl and ^{129}I yields (M_t), intra-person standard deviation (N = 3) s_b, inter person standard deviation (N=3) s_w, combined total standard deviation s_t

Table 28 confirms very well the ruggedness of the method since the yields are as expected and all standard deviations are below 15%. Furthermore there is no significant difference between the intra- and inter-person standard deviations.

4.3.5.9 Limit of detection

Throughout the whole validation process blank samples (for ^{36}Cl and ^{129}I) were prepared and measured to calculate net counting rates. In order to do so one additional column was loaded with 10 mL 1M H_2SO_4 without any analyte added. This blank sample is then separated in the same way as the sample to be analyzed. The chloride and iodide fractions obtained from the blank samples were counted via LSC (1220 Quantulus). The limit of detection for ^{36}Cl as well as for ^{129}I was then calculated from the counting rate of the blank samples according to eq. 18.

In both fractions, KSCN fraction for ^{36}Cl and Na_2S fraction for ^{129}I, N_0 is determined to be 0.133 cps (counts per second). For the calculation of the LOD the counting time of the sample was assumed to be equal to the counting time of the blank $t_m = t_0 = 86400$ seconds (= 24 hours) (for real environmental sample this counting time is quite realistic), as quintiles of the normal distribution $k_{1-\alpha} = 3$ and $k_{1-\beta} = 1.645$ were applied.

Under these considerations LOD is calculated to be 8.2 mBq.

However, LOD is mainly dependent on the counting time. Thus, a longer counting time of the sample as well as of the blank will result in a lower limit of detection.

4.3.5.10 Fitness for purpose

The validation study can be summarized as follows:

High decontamination factors for numerous elements and potential interferences were determined indicating for a good selectivity of the method. Precision and trueness were determined for water, soil, filter and concrete samples. For precision, combined standard deviations were determined, which were found to be < 15%. For trueness, determined activities were compared with reference activities and expressed as bias. Bias values were found to be small, but slight negative. Thus adding an internal standard is advisable. The recoveries were found to be ~1, the method shows linearity over a wide range of activities (1 – 90 Bq).

Ruggedness was evaluated by performing the method by three more persons. Intra-person and inter-person standard deviation were calculated and combined to a combined standard deviation. The combined standard deviation is <15%, inter- and intra-person standard deviations did not deviate significantly.

From the results of the method validation it can be concluded that the method is fit for its purpose, it is the preconcentration and separation of ^{36}Cl and ^{129}I from environmental and decommissioning samples.

However, it should be mentioned that the method is only suitable for chloride and iodide. It is partly suitable for other iodine species, e.g. IO^{3-}, which form slightly soluble compounds with silver ions. In all other cases chlorine and iodine species should be reduced to chloride and iodide using a reducing agent, e.g. $SnSO_4$.

5 Conclusions and Outlook

At this point some brief conclusions are drawn from the results of the work and also some suggestions are made for future works.

Batch experiments are suited for testing numerous parameters in a short time. But when comparing the results from the characterization studies (which were obtained from batch experiments) and those from method development (which were performed under column geometry), it can be concluded that results obtained from batch experiments, especially D_w values, can only give a hint for possible conditions for retention and elution. Those conditions cannot be transferred to column geometry directly; they should rather be tested in column geometry and further optimized. In most cases it was found that the concentration of a solution has to be optimized for use in column geometry.

For the method for the preconcentration, separation and determination of ^{36}Cl and ^{129}I it can be concluded that the method was developed successfully. The method validation showed that the method is fit for purpose. The method should now additionally be applied to the analysis of real samples. Currently, the interest in this method is high and test samples of the FClA resin are being sent to a number of institutions. First successful results from the analysis of real decommissioning samples already exist [86].

The method for the preconcentration, separation and determination of Pd and Pt was also successfully developed. Unfortunately, problems with new resin lots occurred and validation studies could not be finalized. It is suggested to analyze these resin lots, e.g. by GC-MS, NMR and related techniques, in order to identify the sources responsible for incoherent separation behavior of the resin lots. Once the sources are identified and eliminated the validation studies should be continued.

References

[1]. Palacios M., Gomez M. M., Moldovan M., Morrison G., Rauch S., McLeod C., Ma R., Laserna J., Lucena P., Caroli S., Alimonti A., Petrucci F., Bocca B., Schramel P., Lustig S., Zischka M., Wass U., Stenbom B., Luna M., Saenz J. C., Santamaria J.: Platinum-group elements: quantification in collected exhaust fumes and studies of catalyst surfaces, *Science of the Total Environment* **257** (2000) 1

[2]. Lippert B., Beck W.: Platinum Complexes in Cancer-Therapy, *Chemie in Unserer Zeit* **17** (1983) 190

[3]. Wataha J. C., Hanks C. T.: Biological effects of palladium and risk of using palladium in dental casting alloys, *Journal of Oral Rehabilitation* **23** (1996) 309

[4]. Kummerer K., Helmers E., Hubner P., Mascart G., Milandri M., Reinthaler F., Zwakenberg M.: European hospitals as a source for platinum in the environment in comparison with other sources, *Science of the Total Environment* **225** (1999) 155

[5]. http://www.buetzer.info/fileadmin/pb/pdf-Dateien/Autokatalysator.pdf, Accessed 04.08.2010

[6]. Palacios M. A., Gomez M., Moldovan M., Gomez B.: Assessment of environmental contamination risk by Pt, Rh and Pd from automobile catalyst, *Microchemical Journal* **67** (2000) 105

[7]. Gomez B., Palacios M. A., Gomez M., Sanchez J. L., Morrison G., Rauch S., McLeod C., Ma R., Caroli S., Alimonti A., Petrucci F., Bocca B., Schramel P., Zischka M., Petterson C., Wass U.: Levels and risk assessment for humans and ecosystems of platinum-group elements in the airborne particles and road dust of some European cities, *Science of the Total Environment* **299** (2002) 1

[8]. Zereini F., Skerstupp B., Alt F., Helmers E., Urban H.: Geochemical behaviour of platinum-group elements (PGE) in particulate emissions by automobile exhaust catalysts: experimental results and environmental investigations, *Science of the Total Environment* **206** (1997) 137

[9]. Moldovan M., Palacios M. A., Gómez M. M., Morrison G., Rauch S., McLeod C., Ma R., Caroli S., Alimonti A., Petrucci F., Bocca B., Schramel P., Zischka M., Pettersson C., Wass U., Luna M., Saenz J. C., Santamaría J.: Environmental risk of particulate and soluble platinum group elements released from gasoline and diesel engine catalytic converters, *The Science of The Total Environment* **296** (2002) 199

[10]. Hooda P. S., Miller A., Edwards A. C.: The distribution of automobile catalysts-cast platinum, palladium and rhodium in soils adjacent to roads and their uptake by grass, *Science of the Total Environment* **384** (2007) 384

[11]. Kalbitz K., Schwesig D., Wang W. X.: Effects of platinum from vehicle exhaust catalyst on carbon and nitrogen mineralization in soils, *Science of the Total Environment* **405** (2008) 239

[12]. Ravindra K., Bencs L., Van Grieken R.: Platinum group elements in the environment and their health risk, *Science of the Total Environment* **318** (2004) 1

[13]. http://www.nucleide.org/DDEP_WG/DDEPdata.htm, Accessed 04.08.2010

[14]. Rodriguez M., Pina G., Lara E.: Radiochemical Analysis of Chlorine-36, *Czechoslovak Journal of Physics* **56** (2006) D211

[15]. http://www.irsn.fr/FR/larecherche/Information_scientifique/Publications_Documentation/fiches-techniques-radionucleides/environnement/Documents/Iode_I129_v1.pdf, Accessed 04.08.2010

[16]. Cecil L. D., Welhan J. A., Green J. R., Grape S. K., Sudicky E. R.: Use of chlorine-36 to determine regional-scale aquifer dispersivity, eastern Snake River Plain aquifer, Idaho/USA, *Nuclear Instruments & Methods in Physics Research Section B-Beam Interactions with Materials and Atoms* **172** (2000) 679

[17]. Baxter M., Castle L., Crews H. M., Rose M., Garner C., Lappin G., Leong D.: A sensitive method for the determination of chlorine-36 in foods using accelerator mass spectrometry, *Food Additives and Contaminants Part a-Chemistry Analysis Control Exposure & Risk Assessment* **26** (2009) 139

[18]. Itoh M., Watanabe K., Hatakeyama M., Tachibana M.: Determination of Cl-36 in biological shield concrete using pyrohydrolysis and liquid scintillation counting, *Analyst* **127** (2002) 964

[19]. Hou X. L., Ostergaard L. F., Nielsen S. P.: Determination of Cl-36 in nuclear waste from reactor decommissioning, *Analytical Chemistry* **79** (2007) 3126

[20]. Muramatsu Y., Uchida S., Ohmomo Y.: Determination of I-129 and I-127 in Soil and Tracer Experiments on the Adsorption of Iodine on Soil, *Journal of Radioanalytical and Nuclear Chemistry-Articles* **138** (1990) 377

[21]. Schmidt A., Schnabel C., Handl J., Jakob D., Michel R., Synal H. A., Lopez J. M., Suter M.: On the analysis of iodine-129 and iodine-127 in environmental materials by accelerator mass spectrometry and ion chromatography, *Science of the Total Environment* **223** (1998) 131

[22]. Bienvenu P., Brochard E., Excoffier E., Piccione M.: Determination of iodine 129 by ICP-QMS in environmental samples, *Canadian Journal of Analytical Sciences and Spectroscopy* **49** (2004) 423

[23]. Yoshida S., Muramatsu Y., Katou S., Sekimoto H.: Determination of the chemical forms of iodine with IC-ICP-MS and its application to environmental samples, *Journal of Radioanalytical and Nuclear Chemistry* **273** (2007) 211

[24]. Kabai E., Vajda N., Gaca P.: Simultaneous determination of radioactive halogen isotopes and 99Tc, *Czechoslovak Journal of Physics* **53** (2003) A181

[25]. http://www.triskem-international.com/en/full_extraction_chromatographie.asp, Accessed 04.08.2010

[26]. Braun T., Ghersini G.: "Extraction Chromatography" (1975) Elsevier, Inc., Amsterdam-London-New York

[27]. Horwitz E. P., Dietz M. L., Fisher D. E.: Separation and Preconcentration of Strontium from Biological, Environmental, and Nuclear Waste Samples by Extraction Chromatography Using a Crown-Ether, *Analytical Chemistry* **63** (1991) 522

[28]. Mokhodoeva O. B., Myasoedova G. V., Kubrakova I. V., Nikulin A. V., Artyushin O. I., Odinets I. L.: New Solid Extractants for Preconcentrating Noble Metals, *Journal of Analytical Chemistry* **65** (2010) 12

[29]. Myasoedova G. V., Molochnikova N. P., Mokhodoeva O. B., Myasoedov B. F.: Application of Ionic Liquids for Solid-Phase Extraction of Trace Elements, *Analytical Sciences* **24** (2008) 1351

[30]. Anderson H. H., et al.: Solvent extraction process for plutonium, US Patent US2,924,506 19.02.1960,

[31]. http://en.wikipedia.org/wiki/Inductively_coupled_plasma_mass_spectrometry, Accessed 29.08.2010

[32]. Thomas R.: Spectroscopy tutorial - A beginner's guide to ICP-MS - Part II: The sample-introduction system, *Spectroscopy* **16** (2001) 56

[33]. Thomas R.: A beginner's guide to ICP-MS - Part III: The plasma source, *Spectroscopy* **16** (2001) 26

[34]. Thomas R.: A beginner's guide to ICP-MS - Part IV: The interface region, *Spectroscopy* **16** (2001) 26

[35]. Thomas R.: A beginner's guide to ICP-MS - Part V: The ion focusing system, *Spectroscopy* **16** (2001) 38

[36]. http://minerals.cr.usgs.gov/icpms/images/interface_region.jpg, Accessed 28.10.2010

[37]. Thomas R.: Beginner's guide to ICP-MS - Part VI - The mass analyzer, *Spectroscopy* **16** (2001) 44

[38]. Thomas R.: A beginner's guide to ICP-MS part X - Detectors, *Spectroscopy* **17** (2002) 34

[39]. Thomas R.: A beginner's guide to ICP-MS Part XII - A review of interferences, *Spectroscopy* **17** (2002) 24

[40]. Gerald O.: A young physicist at seventy: Hartmut Kallmann, *Physics Today* **19** (1966) 51

[41]. Kallmann H.: Scintillation Counting with Solutions, *Physical Review* **78** (1950) 621

[42]. Ageno M., Chiozzotto M., Querzoli R.: Scintillations in Liquids and Solutions, *Physical Review* **79** (1950) 720

[43]. Reynolds G. T., Harrison F. B., Salvini G.: Liquid Scintillation Counters, *Physical Review* **78** (1950) 488

[44]. Forster T.: Transfer Mechanisms of Electronic Excitation Energy, *Radiation Research Supplement* **2** (1960) 326

[45]. Horrocks D. L.: "Applications of Liquid Scintillation Counting" (1974) Academic Press, New York - London

[46]. Birks J. B., Kuchela K. N.: Energy Transfer in Organic Systems .2. Solute-Solute Transfer in Liquid Solutions, *Proceedings of the Physical Society of London* **77** (1961) 1083

[47]. Birks J. B., Conte J. M. D., Walker G.: Influence of Excimer Formation on Solvent-Solute Energy Transfer in Organic Liquid Scintillation, *Ieee Transactions on Nuclear Science* **NS13 (3)** (1966) 148

[48]. Happel S. A.: "Verfahrensoptimierung für die Bestimmung von alpha- und beta-strahlenden Nukliden in Wasser- und Bidenproben" (2003), PhD Thesis, Marburg

[49]. Voltz R., Laustriat G., Coche A.: Fluorescence - Mecanisme Du Transfert Denergie Dans Les Scintillateurs Liquides, *Comptes Rendus Hebdomadaires Des Seances De L Academie Des Sciences* **257** (1963) 1473

[50]. http://las.perkinelmer.com/Content/RelatedMaterials/Brochures/BRO_HighPerfLiquidScintAnalyzers.pdf, Accessed 04.08.2010

[51]. "Liquid scintillation systems ", Operation Manual (1984), Packard Instrument Co. I., USA

[52]. Fleming J., Albus H., Neidhardt B., Wegscheider W.: Glossary of Analytical Terms (II), *Accreditation and Quality Assurance: Journal for Quality, Comparability and Reliability in Chemical Measurement* **1** (1996) 87

[53]. http://www.eurachem.org/guides/pdf/valid.pdf, Accessed 04.08.2010

[54]. Thompson M., Ellison S. L. R., Wood R.: Harmonized guidelines for single-laboratory validation of methods of analysis - (IUPAC technical report), *Pure and Applied Chemistry* **74** (2002) 835

[55]. ISO/IEC 17043:2010(E), Conformity assessment - General requirements for proficiency testing,

[56]. Gonzalez A. G., Herrador M. A.: A practical guide to analytical method validation, including measurement uncertainty and accuracy profiles, *Trac-Trends in Analytical Chemistry* **26** (2007) 227

[57]. Fleming J., Albus H., Neidhart B., Wegscheider W.: Glossary of analytical terms (VII), *Accreditation and Quality Assurance: Journal for Quality, Comparability and Reliability in Chemical Measurement* **2** (1997) 51

[58]. http://www.bmu.de/files/pdfs/allgemein/application /pdf/strlsch_messungen_erk_nachweisgr.pdf, Accessed 31.08.2010

[59]. Fleming J., Neidhart B., Tausch C., Wegscheider W.: Glossary of analytical terms, *Accreditation and Quality Assurance: Journal for Quality, Comparability and Reliability in Chemical Measurement* **1** (1996) 41

[60]. http://www.measurementuncertainty.org/mu/QUAM2000-1.pdf, Accessed 17.08.2010

[61]. http://www.cytec.com/specialty-chemicals/PDFs/TransformationalSynthetic/CYANEX%20471X.pdf, Accessed 17.08.2010

[62]. Duche S. N., Dhadke P. M.: Extraction of palladium(II) with Cyanex-923 and Cyanex-471X from bromide media and its separation from Pt(IV), Rh(III) and Ir(III), *Journal of the Chinese Chemical Society* **48** (2001) 1115

[63]. Beamish F. B.: "The Analytical Chemistry of Noble Metals" (1966) Pergamon, Oxford

[64]. Ginzburg S.I., Ezerskaya N. A., Prokofyeva I. V., Fedorenko N. V., Shlenskaya V. I., Belsky N. K.: "Analiticheskaya Khimiya Platinovikh Metallov" (1972) Nauka, Moscow

[65]. Zolotov Y. A., Petrukhin O. M., Shevchenko V. N., Dunina V. V., Rukhadze E. G.: Solvent-Extraction of Noble-Metals with Derivatives of Thiourea, *Analytica Chimica Acta* **100** (1978) 613

[66]. Mojski M.: Extraction of Platinum Metals from Hydrochloric-Acid Medium with Triphenylphosphine Solution in 1,2-Dichloroethane, *Talanta* **27** (1980) 7

[67]. Duche S. N., Dhadke P. M.: Comparative study of the determination of platinum by extraction with Cyanex 923 and Cyanex 471X from bromide media, *Journal of Chemical Technology and Biotechnology* **76** (2001) 1227

[68]. Zulauf A., Happel S., Mokili B. M., Bombard A., Jungclas H.: Characterization of an extraction chromatographic resin for the separation and determination of 36Cl and 129I, *Journal of Radioanalytical and Nuclear Chemistry* **286** (2010) 539

[69]. Mondino A. V., Cols H. J., Cristini P. R., Furnari J. C.: Separation of iodine produced from fission with a porous metal silver column in Mo-99 production, *Journal of Radioanalytical and Nuclear Chemistry* **240** (1999) 731

[70]. CRC: "Handbook of Chemistry and Physics"

[71]. http://www.sciencelab.com/msds.php?msdsId=9924935, Accessed 25.09.2010

[72]. http://www.csudh.edu/oliver/chemdata/data-ksp.htm, Accessed 25.09.2010

[73]. Haldimann M., Eastgate A., Zimmerli B.: Improved measurement of iodine in food samples using inductively coupled plasma isotope dilution mass spectrometry, *Analyst* **125** (2000) 1977

[74]. Larsen E. H., Ludwigsen M. B.: Determination of iodine in food-related certified reference materials using wet ashing and detection by inductively coupled plasma mass spectrometry, *Journal of Analytical Atomic Spectrometry* **12** (1997) 435

[75]. Date A. R., Stuart M. E.: Application of Inductively Coupled Plasma Mass-Spectrometry to the Simultaneous Determination of Chlorine, Bromine and Iodine in the National-Bureau-of-Standards Standard Reference Material-1648 Urban Particulate, *Journal of Analytical Atomic Spectrometry* **3** (1988) 659

[76]. Tsukada H., Takeda A., Hasegawa H., Ueda S., Iyogi T.: Comparison of NAA and ICP-MS for the determination of major and trace elements in environmental sample, *Journal of Radioanalytical and Nuclear Chemistry* **263** (2005) 773

[77]. Bettinelli M., Spezia S., Minoia C., Ronchi A.: Determination of chlorine, fluorine, bromine, and iodine in coals with ICP-MS and IC, *Atomic Spectroscopy* **23** (2002) 105

[78]. Schnetger B., Muramatsu Y.: Determination of halogens, with special reference to, iodine, in geological and biological samples using pyrohydrolysis for preparation and inductively coupled plasma mass spectrometry and ion chromatography for measurement, *Analyst* **121** (1996) 1627

[79]. Tagami K., Uchida S., Hirai I., Tsukada H., Takeda H.: Determination of chlorine, bromine and iodine in plant samples by inductively coupled plasma-mass spectrometry after leaching with tetramethyl ammonium hydroxide under a mild temperature condition, *Analytica Chimica Acta* **570** (2006) 88

[80]. Rose M., Miller P., Baxter M., Appleton G., Crews H., Croasdale M.: Bromine and iodine in 1997 UK total diet study samples, *Journal of Environmental Monitoring* **3** (2001) 361

[81]. Yamada H., Kiriyama T., Yonebayashi K.: Determination of total iodine in soils by inductively coupled plasma mass spectrometry, *Soil Science and Plant Nutrition* **42** (1996) 859

[82]. http://www.umwelt-online.de/recht/energie/strahlen/ssv_ges.htm, Accessed 30.10.2010

[83]. http://www.bmu.de/files/pdfs/allgemein/application/pdf/srtlsch_messungen_j05.pdf, Accessed 25.09.2010

[84]. J. Barwick V., L. R. Ellison S.: Measurement uncertainty: Approaches to the evaluation of uncertainties associated with recovery, *Analyst* **124** (1999) 981

[85]. http://www.umweltdaten.de/publikationen/fpdf-l/2832.pdf,Accessed 05.09.2010

[86]. Presentation Dr. Phil Warwick: Determination of Cl-36 in decommissioning samples using a Pyrolyser furnace and extraction chromatographic separations. presented at the 11th International Symposium on Environmental Radiochemical Analysis. 15 - 17 September 2010,Chester (UK). ,

Appendix

Abbreviations

AMS	Accelerator Mass Spectrometry
CL	Chemiluminescence
EDTA	Ethylenediaminetatraacetic Acid
EEC	European Economic Comunity
EU	European Union
EXC	Extraction Chromatography
GC-MS	Gas Chromatography Mass Spectrometry
HETP	Heights of the Theoretical Plates
ICP-MS	Inductively Coupled Plasma Mass Spectrometry
LOD	Limit Of Detection
LOQ	Limit Of Quantification
LSC	Liquid Scintillation Counter
NAA	Neutron Activation Analysis
NMR	Nuclear Magnetic Resonance
PGE	Platinum Group Element
PMT	Photo Multiplier Tube
PTFE	Polytetrafluoroethylene
PUREX	Plutonium URanium EXtraction
RF	Radio Frequency
RSD	Relative Standard Deviation
SD	Standard Deviation
SQP	Sample Quench Parameter
TBP	Tributyl Phosphate
TOPO	Trioctylphosphine Oxide

List of figures

List of tables

Tables of weight distribution ratios

Weight distribution ratios for retention and elution conditions

$Pt(NO_3)_2$	FCIA			F49A		
HNO_3	D_w_Mean	D_w_SD	D_w_RSD / %	D_w_Mean	D_w_SD	D_w_RSD / %
3M	9.98	1.72	17.23	26.13	2.85	10.91
2M	16.97	0.57	3.36	23.26	0.98	4.21
pH 0	24.29	1.24	5.10	39.39	3.65	9.27
pH 1	34.51	8.76	25.38	92.34	0.72	0.78
pH 2	33.39	2.69	8.06	105.06	7.1	6.76
pH 3	73.35	3.01	4.10	105.87	13.46	12.71
pH 4	247	29.88	12.10	141.02	7.26	5.15
pH 5	269.6	20.43	7.58	118.31	8.91	7.53
$AgNO_3$	FCIA			F49A		
HNO_3	D_w_Mean	D_w_SD	D_w_RSD / %	D_w_Mean	D_w_SD	D_w_RSD / %
pH 0	924228.73	137446.87	14.87	1.04E+06	588119.39	56.35
pH 1	158724.47	6146.56	3.87	1.18E+06	57885.19	4.91
pH 2	398984.16	22942.63	5.75	417447.29	109799	26.30
pH 3	140775.27	15469.26	10.99	176436.37	33534.56	19.01
pH 4	43568.94	3317.22	7.61	47404.14	1186.3	2.50
pH 5	30283.29	7960.92	26.29	88763.77	8542.1	9.62

Appendix 1: Averaged values of measured D_w data for Pt, Ag, Pd and Hg in nitric acid

$Pd(NO_3)_2$	FCIA			F49A		
HNO_3	D_w_Mean	D_w_SD	D_w_RSD / %	D_w_Mean	D_w_SD	D_w_RSD / %
3M	62747.39	4399.62	7.01	79120.99	900.84	1.14
2M	130025.28	10023.37	7.71	70045.05	2142.07	3.06
pH 0	385744.52	56883.48	14.75	1.52E+05	28832.92	19.01
pH 1	186968.98	40056.77	21.42	2.55E+05	108486.15	42.57
pH 2	64806.7	5377.93	8.30	38241.46	3434.12	8.98
pH 3	895.2	47.43	5.30	2090.98	87.73	4.20
pH 4	454.5	35.6	7.83	512.81	31.81	6.20
pH 5	494.94	31.74	6.41	601.27	52.68	8.76
$Hg_2(NO_3)_2$	FCIA			F49A		
HNO_3	D_w_Mean	D_w_SD	D_w_RSD / %	D_w_Mean	D_w_SD	D_w_RSD / %
3M	38889.22	2418.33	6.22	96377.37	7700.89	7.99
2M	121409.34	11187.62	9.21	39391.35	4930.41	12.52
pH 0	2652.52	91.11	3.43	1.26E+03	19.35	1.54
pH 1	5934.61	146.51	2.47	3.28E+03	344.32	10.50
pH 2	5388.3	2306.35	42.80	2334.5	53.75	2.30
pH 3	2286.05	250.85	10.97	1149.38	26.71	2.32
pH 4	859.71	8.37	0.97	1292.16	175.44	13.58
pH 5	941.36	13.53	1.44	1059.62	21.04	1.99

Appendix 1 continued

$PtCl_4$	FClA			F49A		
HCl	D_w_Mean	D_w_SD	D_w_RSD / %	D_w_Mean	D_w_SD	D_w_RSD / %
3M	87.18	4.69	5.38	429.02	18.7	4.36
2M	120.44	6.35	5.27	564.56	57.64	10.21
pH 0	55.09	1.86	3.38	392.7	36.68	9.34
pH 1	104.61	28.9	27.63	170.12	7.01	4.12
pH 2	130.36	2.04	1.56	92.01	4.77	5.18
pH 3	95.63	10.97	11.47	54.53	3.91	7.17
pH 4	63.14	26.37	41.76	56.86	7.58	13.33
pH 5	56.12	14.4	25.66	60.52	11.5	19.00
$HAuCl_4$	FClA			F49A		
HCl	D_w_Mean	D_w_SD	D_w_RSD / %	D_w_Mean	D_w_SD	D_w_RSD / %
pH 0	56329.36	9314.39	16.54	4.84E+03	1133.98	23.45
pH 1	141306.26	23712.41	16.78	5.50E+04	3314.59	6.03
pH 2	7099.95	684.98	9.65	7270.27	970.09	13.34
pH 3	5877.46	2237.7	38.07	5471.95	181.41	3.32
pH 4	2796.88	368.2	13.16	1819.64	92.75	5.10
pH 5	1294.64	151.69	11.72	1429.95	0	0.00

Appendix 2: Averaged values of measured D_w data for Pt, Au, Pd and Hg in hydrochloric acid

$(NH_4)_2[PdCl_4]$	FClA			F49A		
HCl	D_w_Mean	D_w_SD	D_w_RSD / %	D_w_Mean	D_w_SD	D_w_RSD / %
3M	222497	#DIV/0!	#DIV/0!	266163.66	25238.68	9.48
2M	211411.28	34216.4	16.18	100513.02	954.83	0.95
pH 0	43748.69	1847.62	4.22	3.96E+04	1130.2	2.85
pH 1	106711.33	4239.92	3.97	8.46E+04	3375.06	3.99
pH 2	747.17	59.39	7.95	690.33	40.66	5.89
pH 3	1348.69	121.5	9.01	1338.13	76.01	5.68
pH 4	427.05	54.76	12.82	446.9	14.53	3.25
pH 5	313.07	41.64	13.30	340.61	41.52	12.19
$HgCl_2$	FClA			F49A		
HCl	D_w_Mean	D_w_SD	D_w_RSD / %	D_w_Mean	D_w_SD	D_w_RSD / %
3M	3098.84	214.18	6.91	4224.22	364.73	8.63
2M	7665.4	444.97	5.80	3343.19	199.58	5.97
pH 0	7797.3	1035.84	13.28	2.10E+03	369.99	17.64
pH 1	32427.63	2416.82	7.45	9.30E+03	1704.84	18.33
pH 2	42295.26	24722.2	58.45	15366.78	4973.93	32.37
pH 3	135490.16	10569.53	7.80	69550.95	41457.21	59.61
pH 4	184538.02	31012.18	16.81	50847.88	15136.19	29.77
pH 5	161636.01	5579.15	3.45	20782.02	227.23	1.09

Appendix 2 continued

PdSO4	C471X2			F49A		
H2SO4	D_w_Mean	D_w_SD	D_w_RSD / %	D_w_Mean	D_w_SD	D_w_RSD / %
pH 0	86682.57	18244.32	21.05	1.46E+05	18244.32	12.49
pH 1	67591.79	7331.52	10.85	8.65E+04	3523.21	4.08
pH 2	47442.07	4050.99	8.54	109440.38	12121.33	11.08
pH 3	35751.14	2031.9	5.68	84259.01	14670.46	17.41
pH 4	17397.15	48.68	0.28	63673.53	234.91	0.37
pH 5	13688.71	903.02	6.60	11603.24	900.37	7.76

Appendix 3: Averaged values of measured D_w data for Pd in sulphuric acid

Weight distribution ratios for Pd and Pt under influence of interferences

Cationic interferences

$NaNO_3$/ M	$Pd(NO_3)_2$					
	FClA			F49A		
	D_w_Mean	D_w_SD	D_w_RSD/%	D_w_Mean	D_w_SD	D_w_RSD%
0.01	557570.36	29125.4	5.22	951833.72	63197.92	6.64
0.1	691138.38	44368.98	6.42	525341.36	13624.27	2.59
0.2	720051.07	49200.79	6.83	445514.12	29763.15	6.68
0.5	785214.5	125536.68	15.99	501215.85	66566.08	13.28
1	621467.92	151883.37	24.44	437652.34	52297.86	11.95
$Ca(NO_3)_2$/ M	$Pd(NO_3)_2$					
	FClA			F49A		
	D_w_Mean	D_w_SD	D_w_RSD/%	D_w_Mean	D_w_SD	D_w_RSD%
0.01	470197.23	24961.79	5.31	1328336.45	140644.09	10.59
0.1	444656.4	52157.77	11.73	612494.82	493239.58	80.53
0.2	349557.51	53404.79	15.28	224639.34	21925.28	9.76
0.5	235150.82	26259.58	11.17	147881.53	66341.67	44.86
1	191237.62	26875.09	14.05	37236.69	22573.96	60.62
$Mg(NO_3)_2$/M	$Pd(NO_3)_2$					
	FClA			F49A		
	D_w_Mean	D_w_SD	D_w_RSD/%	D_w_Mean	D_w_SD	D_w_RSD%
0.01	771507.36	5491.44	0.71	540801.95	23568.71	4.36
0.1	524837.5	15258.58	2.91	317205.64	53074.84	16.73
0.2	408826.08	26813.16	6.56	176717.92	22684.35	12.84
0.5	228779.52	34235.49	14.96	119857.31	27424.28	22.88
1	73020.63	13237.45	18.13	68707.71	10393.52	15.13

Appendix 4: Mean D_w-values for Pd(II) on both resins for different interfering elements and concentrations in 1M HNO3

NH_4NO_3/M	$Pd(NO_3)_2$					
	FClA			F49A		
	D_w_Mean	D_w_SD	D_w_RSD / %	D_w_Mean	D_w_SD	D_w_RSD / %
0.01	2345633.3	72524.14	3.09	1512413.63	174535.9	11.54
0.1	2450224.81	13583.19	0.55	1596283.12	48574.04	3.04
0.2	2306389.61	268343.76	11.63	1504007.11	157391.15	10.46
0.5	2360610.67	64879.59	2.75	1575585.07	139142.95	8.83
1	2564850.38	244721.41	9.54	1720592.38	115443.88	6.71
$Fe(NO_3)_3$/M	$Pd(NO_3)_2$					
	FClA			F49A		
	D_w_Mean	D_w_SD	D_w_RSD / %	D_w_Mean	D_w_SD	D_w_RSD / %
0.01	722188.89	61523.34	8.52	54375.83	29782.05	54.77
0.1	620605.14	30817.49	4.97	155169.95	29087.07	18.75
0.2	590926.62	24843.91	4.20	144996.75	9240.48	6.37
0.5	187299.86	227.17	0.12	86353.3	456.53	0.53
1	306.24	11.82	3.86	268.75	36.64	13.63

Appendix 4 continued

NaCl/ M	FClA					
	$(NH_4)_2[PdCl_4]$			$PtCl_4$		
	D_w_Mean	D_w_SD	D_w_RSD / %	D_w_Mean	D_w_SD	D_w_RSD / %
0.01	48709.70	2228.12	4.57	209.66	12.45	5.94
0.1	44374.69	2900.45	6.54	176.78	27.04	15.29
0.2	31101.51	288.00	0.93	116.11	7.23	6.22
0.5	19974.15	2159.66	10.81	142.10	1.19	0.83
1	3471.86	574.37	16.54	29.34	0.67	2.29
$CaCl_2$/ M	FClA					
	$(NH_4)_2[PdCl_4]$			$PtCl_4$		
	D_w_Mean	D_w_SD	D_w_RSD / %	D_w_Mean	D_w_SD	D_w_RSD / %
0.01	226593.45	7468.85	3.30	242.79	20.97	8.64
0.1	180900.04	23924.39	13.23	154.71	14.41	9.31
0.2	126537.33	19875.63	15.71	150.25	43.19	28.75
0.5	62077.24	8918.68	14.37	52.7	2.22	4.21
1	10357.83	429.85	4.15	5.75	1.25	21.74
$MgCl_2$/M	FClA					
	$(NH_4)_2[PdCl_4]$			$PtCl_4$		
	D_w_Mean	D_w_SD	D_w_RSD/%	D_w_Mean	D_w_SD	D_w_RSD %
0.01	219729.5	3270.82	1.49	149.73	4.2	2.81
0.1	167749.7	5285.75	3.15	109.52	4.35	3.97
0.2	132919.02	6167.44	4.64	72.81	3.97	5.45
0.5	59012.39	5194.63	8.80	51.17	0.37	0.72
1	18987.5	1957.22	10.31	21	0.47	2.24

Appendix 5: FClA: Mean D_w-values for Pd(II) and Pt(IV) for different interfering elements and concentrations in 1M HCl

NH_4Cl/M	FClA					
	$(NH_4)_2[PdCl_4]$			$PtCl_4$		
	D_w_Mean	D_w_SD	D_w_RSD / %	D_w_Mean	D_w_SD	D_w_RSD / %
0.01	89086.25	6249.94	7.02	77.31	16.72	21.63
0.1	84009.95	6455.77	7.68	75.42	19.82	26.28
0.2	71988.35	1216.12	1.69	54.62	2.44	4.47
0.5	57154.1	1869.03	3.27	43.74	12.58	28.76
1	35169.5	6891.3	19.59	17	5.6	32.94
$FeCl_3$/M	FClA					
	$(NH_4)_2[PdCl_4]$			$PtCl_4$		
	D_w_Mean	D_w_SD	D_w_RSD / %	D_w_Mean	D_w_SD	D_w_RSD / %
0.01	193473.97	8185.23	4.23	79.88	12.03	15.06
0.1	200819.9	23093.8	11.50	4.25	0.01	0.24
0.2	247929.89	4062.13	1.64	0.55	0.03	5.45
0.5	284037.29	8742.36	3.08	7.87	0.65	8.26
1	101872.67	7140.22	7.01	25.96	1.46	5.62

Appendix 5 continued

NaCl/ M	F49A					
	$(NH_4)_2[PdCl_4]$			$PtCl_4$		
	D_w_Mean	D_w_SD	D_w_RSD/%	D_w_Mean	D_w_SD	D_w_RSD %
0.01	27340.96	324.3	1.19	509.9	1.63	0.32
0.1	24697.39	125.06	0.51	444.31	6.18	1.39
0.2	21945.4	662.23	3.02	466.81	2.9	0.62
0.5	17999.15	1103.45	6.13	308.75	25.43	8.24
1	15474.31	502.55	3.25	323.66	5.07	1.57
$CaCl_2$/ M	F49A					
	$(NH_4)_2[PdCl_4]$			$PtCl_4$		
	D_w_Mean	D_w_SD	D_w_RSD/%	D_w_Mean	D_w_SD	D_w_RSD %
0.01	75933.78	3001.73	3.95	586.82	16.7	2.85
0.1	77730.51	11518.19	14.82	490.25	57.29	11.69
0.2	70674.41	2772.28	3.92	379.99	5.07	1.33
0.5	54875.58	1057.74	1.93	396.59	25.12	6.33
1	35861.55	1700.66	4.74	546.03	30.95	5.67
$MgCl_2$/M	F49A					
	$(NH_4)_2[PdCl_4]$			$PtCl_4$		
	D_w_Mean	D_w_SD	D_w_RSD/%	D_w_Mean	D_w_SD	D_w_RSD %
0.01	89851.39	3293.72	3.67	447.06	36.91	8.26
0.1	69108.63	9376.6	13.57	451.48	22.44	4.97
0.2	49479.13	3022.58	6.11	377.04	13.55	3.59
0.5	37091.16	2030.59	5.47	383.45	13.42	3.50
1	33352.57	724.7	2.17	550.77	1.19	0.22

Appendix 6: F49A: Mean D_w-values for Pd(II) and Pt(IV) for different interfering elements and concentrations in 1M HCl

NH_4Cl/M	F49A					
	$(NH_4)_2[PdCl_4]$			$PtCl_4$		
	D_w_Mean	D_w_SD	D_w_RSD / %	D_w_Mean	D_w_SD	D_w_RSD / %
0.01	47229.75	2353.81	4.98	495.76	20.9	4.22
0.1	40048.56	2031.07	5.07	421.61	14.49	3.44
0.2	35738.36	3611.84	10.11	330.2	7.99	2.42
0.5	48260.95	2690.25	5.57	256.35	3.45	1.35
1	32868.61	2959.45	9.00	190.64	9.13	4.79
$FeCl_3$/M	F49A					
	$(NH_4)_2[PdCl_4]$			$PtCl_4$		
	D_w_Mean	D_w_SD	D_w_RSD / %	D_w_Mean	D_w_SD	D_w_RSD / %
0.01	105157.64	9255.18	8.80	78.11	5.26	6.73
0.1	70386.14	5587.04	7.94	3.42	0.37	10.82
0.2	65447.56	1058.83	1.62	3.3	0.16	4.85
0.5	1603	209.92	13.10	10.02	0.26	2.59
1	337.76	41.97	12.43	28.46	1.28	4.50

Appendix 6 continued

Na_2SO_4/ M	$PdSO_4$					
	FClA			F49A		
	D_w_Mean	D_w_SD	D_w_RSD / %	D_w_Mean	D_w_SD	D_w_RSD / %
0.01	274937.37	39149	14.24	149124.32	1721.96	1.15
0.1	273728.08	16656.41	6.09	263981.23	24560.17	9.30
0.2	341318.32	33577	9.84	361119.25	16909.91	4.68
0.5	349507.58	54865.07	15.70	362523.44	7142.17	1.97
1	366021.48	42833.67	11.70	309161.85	381.69	0.12
$MgSO_4$/M	$PdSO_4$					
	FClA			F49A		
	D_w_Mean	D_w_SD	D_w_RSD / %	D_w_Mean	D_w_SD	D_w_RSD / %
0.01	580434.26	19300.28	3.33	409601.54	14607.27	3.57
0.1	621508.68	22807.79	3.67	431496.87	42616.03	9.88
0.2	833282.85	43896.75	5.27	561383.13	61353.13	10.93
0.5	872534.63	131989.59	15.13	825290.08	30511.71	3.70
1	583714.07	32571.41	5.58	789872.47	78752.38	9.97
$(NH_4)_2SO_4$/M	$PdSO_4$					
	FClA			F49A		
	D_w_Mean	D_w_SD	D_w_RSD/%	D_w_Mean	D_w_SD	D_w_RSD%
0.01	363090.53	7204.86	1.98	94335.44	1923.59	2.04
0.1	467479.09	21338.53	4.56	132125.04	19980.47	15.12
0.2	603309.14	32451.75	5.38	197910.5	23943.96	12.10
0.5	759755.98	62382.71	8.21	387679.15	24589.68	6.34
1	1419262.74	250840.24	17.67	498882.22	13371.05	2.68

Appendix 7: Mean D_w-values for Pd(II) on both resins for different interfering elements and concentrations in 1M H_2SO_4

Anionic interferences

$PtCl_4$	FClA			F49A		
$(NH_4)_2C_2O_4*H_2O$	D_w_Mean	D_w_SD	D_w_RSD / %	D_w_Mean	D_w_SD	D_w_RSD / %
0.01	28.57	2.63	9.21	22.08	1.26	5.71
0.05	5.08	0.09	1.77	10.72	0.33	3.08
0.1	10.44	0.16	1.53	16.6	0.39	2.35
0.2	3.61	0.32	8.86	5.74	0.5	8.71
0.27	6.02	0.38	6.31	6.97	0.33	4.73
$(NH_4)_2[PdCl_4]$	FClA			F49A		
$(NH_4)_2C_2O_4*H_2O$	D_w_Mean	D_w_SD	D_w_RSD / %	D_w_Mean	D_w_SD	D_w_RSD / %
0.01	1250.84	8.12	0.65	477.03	13.36	2.80
0.05	52.91	6.8	12.85	38.04	2.38	6.26
0.1	34.24	4.37	12.76	27.01	2.63	9.74
0.2	17.76	0.52	2.93	19.93	0.27	1.35
0.27	12.22	0.86	7.04	15.34	3.18	20.73

Appendix 8: Oxalic interferences for Pd and Pt in their chloride form on FClA and F49A resins

$Pd(NO_3)_2$	FClA			F49A		
$(NH_4)_2C_2O_4*H_2O$	D_w_Mean	D_w_SD	D_w_RSD / %	D_w_Mean	D_w_SD	D_w_RSD / %
0.01	455.93	47.58	10.44	172.81	13.44	7.78
0.05	240.84	21.53	8.94	214	6.34	2.96
0.1	217.76	4.44	2.04	203.01	10.44	5.14
0.2	188.71	1.18	0.63	194.56	12.78	6.57
$PdSO_4$	FClA			F49A		
$(NH_4)_2C_2O_4*H_2O$	D_w_Mean	D_w_SD	D_w_RSD / %	D_w_Mean	D_w_SD	D_w_RSD / %
0.01	638.91	11.11	1.74	347.8	28.34	8.15
0.05	28.19	3.05	10.82	41.23	0.62	1.50
0.1	22.03	1.46	6.63	26.75	2.08	7.78
0.2	14.38	1.24	8.62	21.41	0.85	3.97

Appendix 9: Oxalic interferences for Pd in its nitrate and sulfate form on FClA and F49A resins

$PtCl_4$	FClA			F49A		
$(NH_4)_2HPO_4$	D_w_Mean	D_w_SD	D_w_RSD / %	D_w_Mean	D_w_SD	D_w_RSD / %
0.01	8.59	0.56	6.52	8.08	0.56	6.93
0.1	10.42	1.06	10.17	8.12	0.85	10.47
0.2	6.72	0.57	8.48	4.64	0.35	7.54
0.5	2.45	0.55	22.45	4.22	0.91	21.56
1	4.44	3.13	70.50	2.21	0.76	34.39
$(NH_4)_2[PdCl_4]$	FClA			F49A		
$(NH_4)_2HPO_4$	D_w_Mean	D_w_SD	D_w_RSD / %	D_w_Mean	D_w_SD	D_w_RSD / %
0.01	24.54	2.6	10.59	33.59	4.42	13.16
0.1	22.77	1.31	5.75	25.97	1.45	5.58
0.2	23.99	1.44	6.00	25.24	2.43	9.63
0.5	16.18	3.02	18.67	21.35	1.71	8.01
1	51.12	1.17	2.29	21.45	3.32	15.48

Appendix 10: Phosphatic interferences for Pd and Pt in their chloride form on FClA and F49A resins

$Pd(NO_3)_2$	FClA			F49A		
$(NH_4)_2HPO_4$	D_w_Mean	D_w_SD	D_w_RSD / %	D_w_Mean	D_w_SD	D_w_RSD / %
0.01	58	5.25	9.05	28.37	1.17	4.12
0.1	17.52	3.03	17.29	20.95	4.32	20.62
0.2	24.24	3.73	15.39	23.57	4.16	17.65
0.5	29.53	3.1	10.50	32.9	1.86	5.65
1	27.44	5.82	21.21	33.77	7.62	22.56
$PdSO_4$	FClA			F49A		
$(NH_4)_2HPO_4$	D_w_Mean	D_w_SD	D_w_RSD / %	D_w_Mean	D_w_SD	D_w_RSD / %
0.01	5.54	1.52	27.44	14.64	0.39	2.66
0.1	1.23	0.13	10.57	9.19	0.81	8.81
0.2	0.39	0.28	71.79	5.17	0.09	1.74
0.5	3.1	0.88	28.39	5.67	1.24	21.87
1	11.3	0.62	5.49	2.48	0	0.00

Appendix 11: Phosphatic interferences for Pd in its nitrate and sulfate form on FCIA and F49A resins

$Pd(NO_3)_2$	FClA		
NH_3	D_w_Mean	D_w_SD	D_w_RSD / %
0.1	157.11	2.47	1.57
0.2	128.99	5.44	4.22
0.5	129.5	8	6.18
1	131.03	7.3	5.57
$(NH_4)_2[PdCl_4]$	FClA		
NH_3	D_w_Mean	D_w_SD	D_w_RSD / %
0.1	21.98	0.36	1.64
0.2	22.29	2.6	11.66
0.5	18.7	0.5	2.67
1	20.39	1.57	7.70

Appendix 12: Evaluation of ammonia as elution agent for Pd

$Pd(NO_3)_2$	FCIA		
Na_2H_2EDTA	D_w_Mean	D_w_SD	D_w_RSD / %
0.01	74.64	2.39	3.20
0.02	55.57	3.68	6.62
0.05	43.13	3.02	7.00
0.1	98.3	4.44	4.52
$(NH_4)_2[PdCl_4]$	FCIA		
Na_2H_2EDTA	D_w_Mean	D_w_SD	D_w_RSD / %
0.01	2.62	0.25	9.54
0.02	3.21	0.01	0.31
0.05	2.4	0.18	7.50
0.1	3.32	0.19	5.72

Appendix 13: Evaluation of Na_2H_2EDTA as elution agent for Pd

Acknowledgements

I would like to thank everybody who contributed to this thesis by giving me their support, in particular

Prof. Dr. Jungclas for giving me the opportunity to accomplish this thesis in his group at Philipps-University of Marburg;

Dr. Happel for giving me the opportunity to work on a very interesting project, for his support, discussions and for proofreading. My special thanks are directed to you, I learned a lot from you;

TrisKem International for providing me with resin samples and other consumables;

Prof. Dr. Ensinger for acting as referee;

Prof. Dr. Tallarek and Prof. Dr. Sundermeyer for being members of the examination board;

C. Dirk, R. Streng and H. Thurn for performing experiments for the ruggedness studies;

M. Nau for her support concerning radiation protection and waste management;

T. Uderstadt for ordering all chemicals;

B. Beutel, K. Retzlaff, M. Kossatz and D. Wang for their support during their project works of the advanced nuclear chemistry course;

All actual and former members of the Nuclear Chemistry of Philipps-University of Marburg for the great time at the Institution;

My family, my parents and parents-in-law for their moral support and that they always believed in me;

And all those who I have forgotten to mention here.